TECHNICAL REPORT STANDARD TITLE PAGE

| 1. Report No. | 2. Government Accession No. | 3. Recipient's Catalog No. |
|---|---|---|
| | | |

| 4. Title and Subtitle | 5. Report Date |
|---|---|
| "The Behavior of an Axially Loaded Drilled Shaft Under Sustained Loading" | May 1974 |
| | 6. Performing Organization Code |
| 7. Author(s) | 8. Performing Organization Report No. |
| John A. Wooley and Lymon C. Reese | Research Report 176-2 |
| 9. Performing Organization Name and Address | 10. Work Unit No. |
| Center for Highway Research<br>The University of Texas at Austin<br>Austin, Texas 78712 | 11. Contract or Grant No.<br>Research Study 3-5-72-176 |
| | 13. Type of Report and Period Covered |
| 12. Sponsoring Agency Name and Address<br>Texas Highway Department<br>Planning & Research Division<br>P. O. Box 5051<br>Austin, Texas 78763 | Interim |
| | 14. Sponsoring Agency Code |

15. Supplementary Notes
Work done in cooperation with the Federal Highway Administration, Department of Transportation.
Research Study Title: "The Behavior of Drilled Shafts"

16. Abstract

This study pertains to the possible deleterious effects of sustained loading on the capacity of a drilled shaft. Long-term phenomena of creep and consolidation are considered. From a literary research it was found that creep can have the eventual effect of load shedding, a transfer of load to the lower regions of the shaft. This phenomenon, it is believed, can have the effect of increasing settlement.

From field observations and measurements taken during the course of loading, it was found that little load shedding had occurred. It is believed that this is a result of the relatively low stress levels in the soil compared to its capacity.

| 17. Key Words | 18. Distribution Statement |
|---|---|
| drilled shafts, loading, sand | |

| 19. Security Classif. (of this report) | 20. Security Classif. (of this page) | 21. No. of Pages | 22. Price |
|---|---|---|---|
| Unclassified | Unclassified | 165 | |

Form DOT F 1700.7 (8-69)

# THE BEHAVIOR OF AN AXIALLY LOADED DRILLED SHAFT UNDER SUSTAINED LOADING

by

John A. Wooley
Lymon C. Reese

Research Report Number 176-2

The Behavior of Drilled Shafts
Research Project 3-5-72-176

conducted for

The Texas Highway Department

in cooperation with the
U. S. Department of Transportation
Federal Highway Administration

by the

CENTER FOR HIGHWAY RESEARCH
THE UNIVERSITY OF TEXAS AT AUSTIN

May 1974

The contents of this report reflect the views of the authors, who are responsible for the facts and the accuracy of the data presented herein. The contents do not necessarily reflect the official views or policies of the Federal Highway Administration. This report does not constitute a standard, specification, or regulation.

# PREFACE

This report presents the results of the investigation of a drilled shaft under sustained loading. The test shaft was constructed by the slurry displacement procedure. Load was applied to the drilled shaft by the overhead bridge structure of which the drilled shaft was a part.

The authors wish to acknowledge the diligent work of a number of people. The field work was accomplished with the assistance of Mr. Harold Dalrymple, Mr. James Anagnos, Mr. Fred Koch, and Mr. Mark Toth. The planning and implementation of the test project was done with the cooperation of Mr. H. D. Butler, Horace Hoy, and Wayne Henneberger of the Texas Highway Department.

John A. Wooley
Lymon C. Reese

May 1974

## LIST OF REPORTS

Report No. 176-1, "The Behavior of Axially Loaded Drilled Shafts in Sand," by Fadlo T. Touma and Lymon C. Reese, presents the results of an investigation of the behavior of drilled shafts in sand.

Report No. 176-2, "The Behavior of an Axially Loaded Drilled Shaft Under Sustained Loading," by John A. Wooley and Lymon C. Reese, presents the results of an investigation of a drilled shaft under sustained loading.

ABSTRACT

This study pertains to the possible deleterious effects of sustained loading on the capacity of a drilled shaft. Long-term phenomena of creep and consolidation are considered. From a literary research it was found that creep can have the eventual effect of load shedding, a transfer of load to the lower regions of the shaft. This phenomenon, it is believed, can have the effect of increasing settlement.

From field observations and measurements taken during the course of loading, it was found that little load shedding had occurred. It is believed that this is a result of the relatively low stress levels in the soil compared to its capacity.

KEY WORDS: drilled shafts, loading, sand

# SUMMARY

This study can be divided into three major sections. The first section pertains to the possible detrimental effects of sustained loading on a drilled shaft. The second section pertains to the instrumentation employed in this study, and modifications of short-term testing procedure which were required to accomplish the testing. The final section pertains to the actual results of the test.

It was found that the load in a drilled shaft can be shed to lower portions of the shaft as a function of time. This is primarily due to the effect of creep of soils. It was felt that this load shedding could result in excessive settlements.

While some modification of the testing and data reducing processes used in short-term testing had to be made, it was believed that reasonably accurate data was acquired from the test instrumentation.

The main findings of this report suggest that the phenomenon of load shedding is practically non-existent for the shaft investigated. Furthermore, the design procedure employed is satisfactory for this particular shaft. Extrapolation of the behavior of this shaft to other shafts in different soils must be cautioned, however.

## IMPLEMENTATION STATEMENT

This study presents results which show that for the current design procedures, and for soils of the type tested, load shedding does not present a serious problem. It is believed that this is true because the design procedure used keeps the stress levels in the soil well below their actual capacity. Soils of significantly different characteristics should be approached with caution.

TABLE OF CONTENTS

PAGE

LIST OF TABLES

LIST OF FIGURES

# CHAPTER I

# INTRODUCTION

In 1965 studies were initiated at The University of Texas concerning the behavior of axially loaded drilled shafts, or drilled caissons. Now, in 1974, there have been a dozen load tests conducted of fully instrumented drilled shafts, with several more such tests scheduled for the future. A variety of soil conditions, shaft configurations, and construction techniques were studied, but all these tests had one thing in common: the installation and testing of these shafts took place in a relatively short span of time. In other words, there has been little, if any, data collected concerning the behavior of drilled shafts under a long-term (sustained) load. Because most structures will be subjected to a long-term load, it is, therefore, of interest to discern if any deviations exist between long-term and short-term behavior.

The concern about long-term behavior has led to the installation of a fully instrumented drilled shaft which has been incorporated in a full-scale structure. From studying the behavior of this shaft over an extended period of time, it is hoped that much can be learned concerning the similarities and differences of the behavior of drilled shafts under short-term and sustained loading.

## Discussion of Sustained Load Test

## Description

A sustained load test is one in which a load is placed on a structure, in this case, a drilled pier, and maintained for a prolonged period of time. Unlike the short-term load test, where the load is applied rapidly and increased incrementally to failure of the drilled shaft, the load for a sustained test is increased slowly and then maintained at a working level. The particular test pier described herein was incorporated into a highway structure, thereby linking the loading rate to the speed of construction. Readings of load in the test drilled shaft were then monitored and data were reduced in similar fashion as in a short-term test.

## Purpose

It is of interest to find out if there is any difference in the short-term and long-term behavior of a drilled shaft under load. Some researchers (Peck, 1965) feel that the effect of a sustained load will result in a phenomenom known as load shedding. This is simply the transfer of load from upper regions of the shaft to lower regions as a result of time-related phenomena. The mechanisms of these phenomena will be discussed later.

A problem related to load shedding is that of increased settlement with time. If a substantial amount of load is shifted to the base, the base pressure will subsequently increase. From previous research (Touma and Reese, 1972; O'Neill and Reese, 1970) it has been found that the settlement of a shaft has a definite relationship to the base pressure.

Therefore, the effect of load shedding could possibly be important with respect to accelerated settlement.

Another point of interest concerning long-term loading is the effect of seasonal variations in climatic factors on the overall load-carrying behavior of the shaft. By monitoring the distribution of load along a test shaft over several seasons, some insight should be gained concerning the possible detrimental effects of seasonal variations on the load-carrying behavior of the shaft.

The purpose of this report is to examine the sustained-load problem closely, to report on progress made to date, and to make recommendations regarding any desirable changes in design procedures. Another goal of the studies is to provide valuable information for future researchers concerning the design of such a test.

## Problems of Data Gathering

Because this study pertains to a long-term loading scheme, several basic problems were encountered in this study which were not present in the previous short-term studies.

The problems are of two general types. Some problems are time-related; that is, they originate because the test shaft is exposed to the load for a long period of time. The other problems are related to the fact that the test shaft in this experiment is actually a part of a full-scale public structure; therefore, some standard experimental practices cannot be allowed, because the integrity of the structure must be maintained.

The time-related problems are creep of concrete, attenuation of gages, and meteorological changes. Creep of concrete has a serious effect on the reduction of load data and will be discussed in a later chapter. Attenuation of gages and meteorological changes, while not as serious as creep, will have a definite effect on the final success of the measurements.

The other problems encountered in the study were caused as a result of the incorporation of the test into a public structure. While the use of an actual structure is helpful to research because it presents loading conditions similar to most drilled-shaft supported structures, it also presents serious problems. In most short-term load tests, the load is induced into the pier by means of a simple hydraulic system. By monitoring the hydraulic pressure, it is a simple matter to determine the load transferred into the shaft. For the long-term shaft there is no such simple calculation of the actual load in the pier; therefore, some problems will be encountered in the determination of the actual load. Also, for most short-term tests, large axial loads which took the shaft to plunging failure were induced. For the long-term test, however, the actual loads are in the range of 30 to 40 per cent of the failure load. Thus, the concrete strain is comparatively low, presenting difficulties in data acquisition.

# CHAPTER II

# EFFECTS OF SUSTAINED LOAD ON BEHAVIOR OF SOIL

In past load tests that have been conducted by The University of Texas, the load has been applied to the test shaft relatively quickly. This type of loading, by not approximating the actual field conditions for most structures, does not take into account some important factors which have an effect on the shear strength of a clay. The possibility exists that the soil will exhibit grossly different strength characteristics during testing than during service loading.

## Creep of Soils

Creep of soils is an important topic and has been the subject of much research. Creep, in general, is the continued time-dependent deformation of a continuum under stress. All engineering materials undergo this phenomenon to some degree, but it is of particular interest in soils because evidence shows that many soils undergo a loss of strength as a result of creep. Vyalov and Meschyan (1969) cite instances where the shear strength of clays was reduced by 60% over a period of 50 to 55 years. Goldstein and Ter-Stepian (1957) also reported similar findings for clay soils exposed to long-term loads. Casagrande and Wilson (1951), among other researchers, have found that, in general, when a load acts on a clay for a long period of time, the strength of the clay decreases.

To develop an understanding of creep and how it affects the shear strength of clays, it is helpful to develop a creep mechanism. A number of ideas are involved in the development of such a mechanism. Bjerrum (1973) presents a discussion of the structure of clay soon after it has been deposited. He states that most clays have a rather loose, flocculated arrangement as a result of their depositional processes. This structure undergoes very large compression as more overburden is built up. When the excess pore pressures set up by deposition have dissipated, the clay structure supports the overburden pressure. This pressure is transmitted from one grain to another by means of two different types of contact points. A mineral-to-mineral contact point exists where the transmitted stresses are relatively large and the adsorbed water surrounding the particles has been squeezed away. Viscous, non-mineral contact points will result when the load transmitted is relatively small and the adsorbed water remains in its original position.

A closer look at the mineral-to-mineral contact points will be valuable here. Bjerrum suggests that shear strength can best be defined by the use of the Hvorslev parameters. Hvorslev's theory contends that the mineral-to-mineral contact points resist shear through what is called "effective friction" (Hvorslev, 1937). This friction is a result of the atomic bonds in the area of contact of the two bodies. The number and magnitude of these bonds are governed by the effective normal stress transmitted through the contact area. Terzaghi (1925) discussed this frictional component in detail and suggested that the amount of shear which can be sustained is proportional to the normal force (Eq. 2.1).

$$s = \sigma' \tan \phi' \quad \ldots \ldots \ldots \ldots \ldots \quad (2.1)$$

where

$s$ = shear strength

$\sigma'$ = effective stress

$\phi'$ = effective angle of internal friction.

Friction, therefore, represents one component of shear strength; now, a discussion of the non-mineral contact points will be helpful. At each non-mineral contact point, the films of semi-rigid water merge so that an area of contact develops that can sustain the shear stress transmitted through it. The maximum shear stress which can be transmitted through this contact point is proportional to the area of the contact point and, thus, to the normal pressure transmitted through the contact. In regard to the effect of increasing pressure at the contacts, then, the mineral and non-mineral contacts behave in a similar manner. When the pressure is removed, however, the non-mineral contacts will remain unchanged, and their resistance to shearing will also remain unchanged. There is no elastic deformation of the water under load and, therefore, there is no mineral-like rebound during unloading. The contribution to the shearing resistance of the non-mineral contacts is termed "effective cohesion." Hvorslev suggested that the cohesive contribution increases with increasing consolidation pressure and remains unchanged for a constant water content. This relationship can be expressed in equation form as

$$c = Kp' \quad \ldots\ldots\ldots\ldots\ldots\ldots \quad (2.2)$$

where

$c$ = effective cohesion

$K$ = constant

$p'$ = equivalent consolidation pressure.

The addition of both of the parameters results in what is commonly known as Hvorslev's failure criterion:

$$s = Kp' + \sigma' \tan \phi' \quad \ldots\ldots\ldots\ldots \quad (2.3)$$

For drained triaxial tests of clays carried out at different confining pressures the shear strength can be expressed as

$$s = c_D' + \sigma' \tan \phi_D' \quad \ldots\ldots\ldots\ldots \quad (2.4)$$

where

$c_D'$ = apparent drained effective cohesion

$\sigma'$ = effective pressure

$\phi_D'$ = drained effective friction angle.

Equation 2.4 differs from Eq. 2.3 in the representation of the term "cohesion." Normally consolidated samples of clay have relatively small values of $c'_D$ . Such clays, however, do not resist shear only through the frictional component of strength, but also can exhibit appreciable cohesive components of shear strength. Recalling Eq. 2.3, involving Hvorslev's parameters, it should be remembered that $p'$ , the equivalent consolidation pressure, has a great effect on "effective cohesion." For drained triaxial tests conducted by increasing the stress level, $p'$ is of the same order of magnitude as $\sigma'$ . For samples consolidated at different pressures, $p'$ and $\sigma'$ increase linearly, which suggests that the effective cohesion and the effective friction increase linearly with the stress level. Therefore, what Hvorslev calls "effective cohesion" has an important role in the strength of a normally consolidated clay, even though $c'_D$ may be rather small.

Hvorslev showed that the effect of strain on clay is different for the two separate components of shear strength. With the aid of a curve-hopping technique developed by Schmertmann and Osterberg (1961), it was found that cohesion reaches a peak at a very small strain, and then decreases significantly with additional strain. On the other hand, the frictional component requires much larger strains for full mobilization. The above ideas expressed by Schmertmann and Osterberg are demonstrated by the two curves shown in Fig. 2.1.

Bjerrum (1973) presents the following logic to explain the effect of time on the shear strength of clay. It is evident from research that the time effect is primarily related to the cohesive element of shear

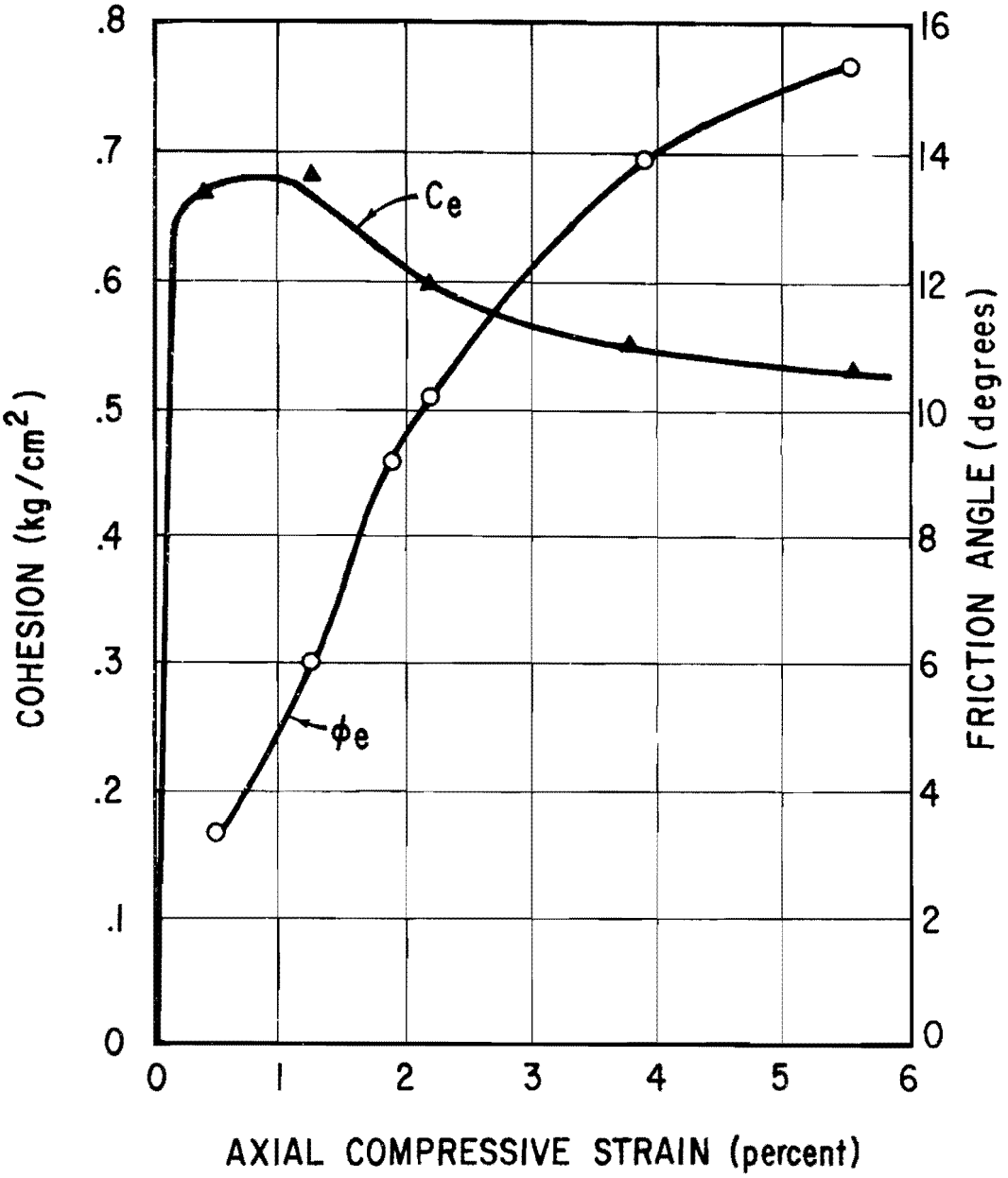


Fig. 2.1 Mobilization of Effective Cohesion and Friction with Increasing Strain for an Undisturbed Sample of Boston Blue Clay (after Schmertmann and Osterberg, 1961)

strength, while the frictional component is for the most part independent of time. In order to understand the time effect, a cohesive contact point between two clay particles should be considered. The negative charge of the clay particle will attract the positive ends of the water particles, therefore, making the adsorbed water maintain a definite molecular structure. Within this film of adsorbed water, the properties will vary from almost a solid next to the clay particle to a liquid far away from the clay particle. Under pressure two clay particles are forced together and their adsorbed water merges. If the pressure is not too high, the particles will remain separated by a fine film of adsorbed water which is very viscous. Due to thermal vibrations of the water atoms in the zone of contact, "interparticle creep" can occur (Bjerrum, 1973). This creep is defined as a relative movement at a constant rate in the direction of applied shear. An increase in shear stress or an increase in the interparticle water will result in an increased creep rate. For particles under greater pressures there is a mineral-to-mineral contact point established. This type of contact point will also creep under applied stress; however, the creep rate is much smaller than for a non-mineral contact.

Creep movement between particles will continue until a change in geometry takes place or until the contact point reaches the edge of one of the clay particles. At this time, the contact point fails. Under any given load, it will take a certain amount of time for such a contact point failure to occur. If the stresses are large, the time to failure is brief; while small stresses require a much longer time to achieve

failure. Thereby, it is seen that a load-carrying contact point can fail even if the shear stress applied is smaller than the shear strength of the contact point. So, a large mass of clay with many such contact points can undergo a constant rate of deformation due to the thermal vibrations of the interparticle water, and these deformations can in turn cause a reduced shear strength. These deformations are quite a separate phenomenon from the instantaneous elastic deformations.

Creep rates are highly dependent on the amount of stress applied. With time, and deformation, the tendency is for more and more of the stress to be transferred from the cohesive contact points to the frictional contact points. This is obvious from Fig. 2.1 where it can be seen that the cohesive component is mobilized quickly and then decays, while the frictional component steadily increases with strain. The reduction of the shear stress in the cohesive component of strength will result in a reduction in the creep rate, thereby causing fewer contact points to be destroyed per unit of time. If the shear stress applied is less than the frictional component of strength, all of the stress in the cohesive component will be relieved and transferred to the frictional component. A low level of shear stress will result in a slowed rate of creep with time until all the stress has been transferred to the frictional component; then the creep will cease completely, except for the small amount of creep that will occur in the frictional contact points. If the shear stress applied is greater than the frictional component of shear strength, the cohesive component will have to carry the balance of the stress. The creep rate will decrease with time until all the friction is mobilized,

then the creep rate will remain constant. Figure 2.2 shows the relation between shear stress, axial strain ($\varepsilon_a$), and rate of shear strain as obtained by Berre and Bjerrum (1973). The figure was derived from undrained tests, but the authors disclosed that drained conditions yielded similar results. The figure suggests that at a sustained stress level, the strain rate will decrease with additional axial strain. The data presented by the figure verify the mechanism of creep, which suggests a decaying creep rate with time as more stress is transferred from cohesive to frictional contacts.

Now, it will be of interest to see what effect creep will have on the bearing capacity of a drilled shaft. The application of load to a shaft will cause shear stresses in the supporting soil, with the shear stresses being maximum at the interface of the shaft and soil. If the soil is clay, some of the stress will be carried by the frictional component and some will be carried by the cohesive component. The cohesive component will tend to transfer some of its stress to the frictional component; but, before or during this phenomenon, the amount of stress in the cohesive component will cause a creep in the soil. This creep will in turn cause a reduction in the shear strength of the soil as discussed before. The loss of strength will cause a shift of the load in the shaft and a settlement of the shaft. The magnitude of the shift in load and settlement are matters of considerable interest.

Most of the preceding discussion of creep pertained to clay soils. It should be mentioned, however, that although creep of sands is

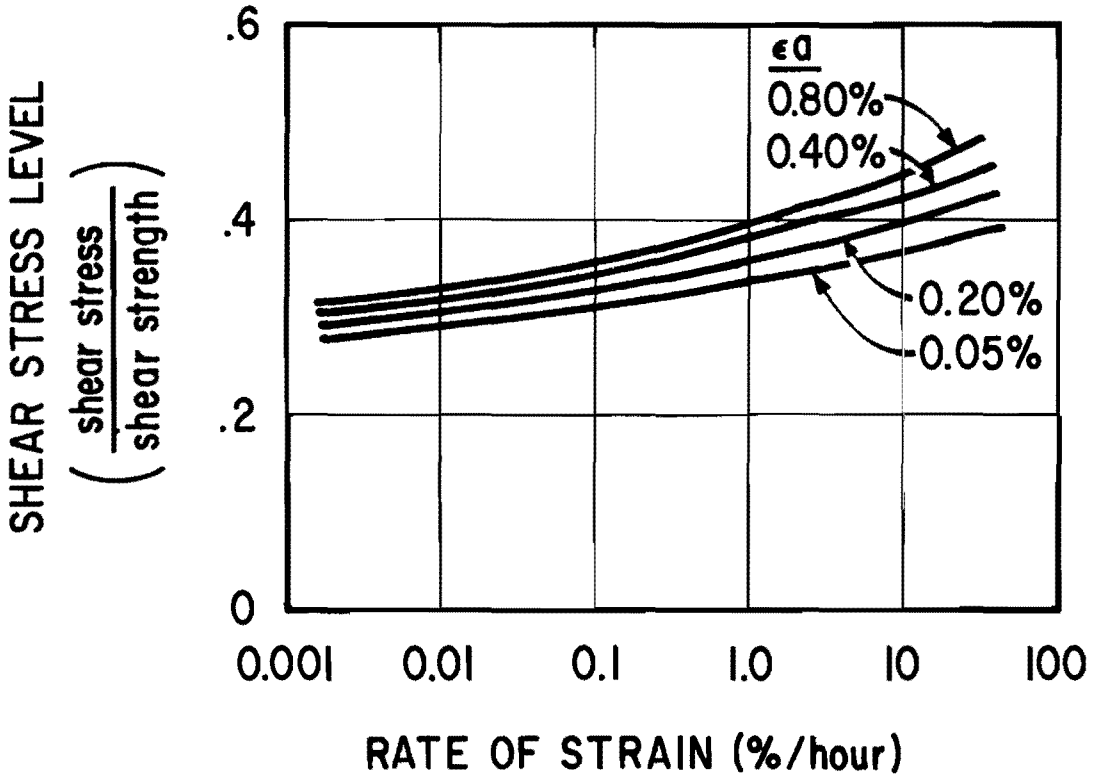


Fig. 2.2 Correlation Between Shear Stress, Rate of Strain, and Axial Strain for Samples of Drammen Clay (after Berre and Bjerrum, 1973)

not a well-researched topic, the possibility of creep deformation occurring in sands should at least be considered.

While sand will probably not creep as much as the more "viscous" clay, there will probably be some creep. Since the sand has a more rigid structure, with more well defined mineral-to-mineral contact points between sand particles, and fewer viscous contact points, the resulting creep is not as large as for clay. However, as the percentage of clay particles in a sand increases, it would seem evident that the number of viscous contacts would increase, thereby causing increased creep rates.

Rate of Loading

Another important time-related factor, like creep, is the rate of loading. The rate of loading is related directly to the time to failure. The importance of the rate effect was explained by Bjerrum (1973). Bjerrum examined several load tests of driven piles conducted by other authors (Eide, et. al., 1972; Marsal and Mazari, 1969; Torstensson, 1973) and concluded that the bearing capacity in any one loading test is not the absolute bearing capacity of a pile. The capacity of a pile decreases significantly with reduced rates of loading. He also concluded that this rate effect seems to affect clays having highly variable plasticity indices in much the same manner. This fact suggests that the rate phenomenon is separate from the creep phenomenon which seemed to be related to the plasticity index of the clay.

The three tests cited involved loading of piles to failure in tension. This loading scheme insured that all the load was being carried

in side shear or adhesion as Bjerrum refers to it. Figure 2.3 shows Bjerrum's results. For any of the three tests, it can be seen that the adhesion decreases as the rate of deformation decreases. There seems to be no relation between plasticity index and the adhesion.

Figure 2.4 also shows the relationship of time to failure and shear stress level. Once again the figure is for undrained tests but the authors (Berre and Bjerrum, 1973) relate that drained tests yield similar results. Tests were run on samples of Drammen clay in which different loading rates and, thus, different times to failure were employed. The results show a significant loss of strength with time to failure. Figure 2.4 shows clearly the effect of time to failure on the shear strength of clays.

The fact that the rate of loading influences the shear strength for a driven pile could be of importance for a sustained load test on a drilled shaft. The load applied to the test shaft was applied very gradually and was dependent on the construction sequence of the fabrication of the structure. It seems possible, therefore, that some of the deleterious effects of slow rates of loading on the shear strength of clays will be felt by the sustained load test shaft.

Drained Conditions, Consolidation

The discussions presented above present evidence concerning the detrimental effect of time on the shear strength of clays under sustained loading. However, sustained loading can cause the opposite effect, that is, the increase in shear strength with time due to consolidation. It is well

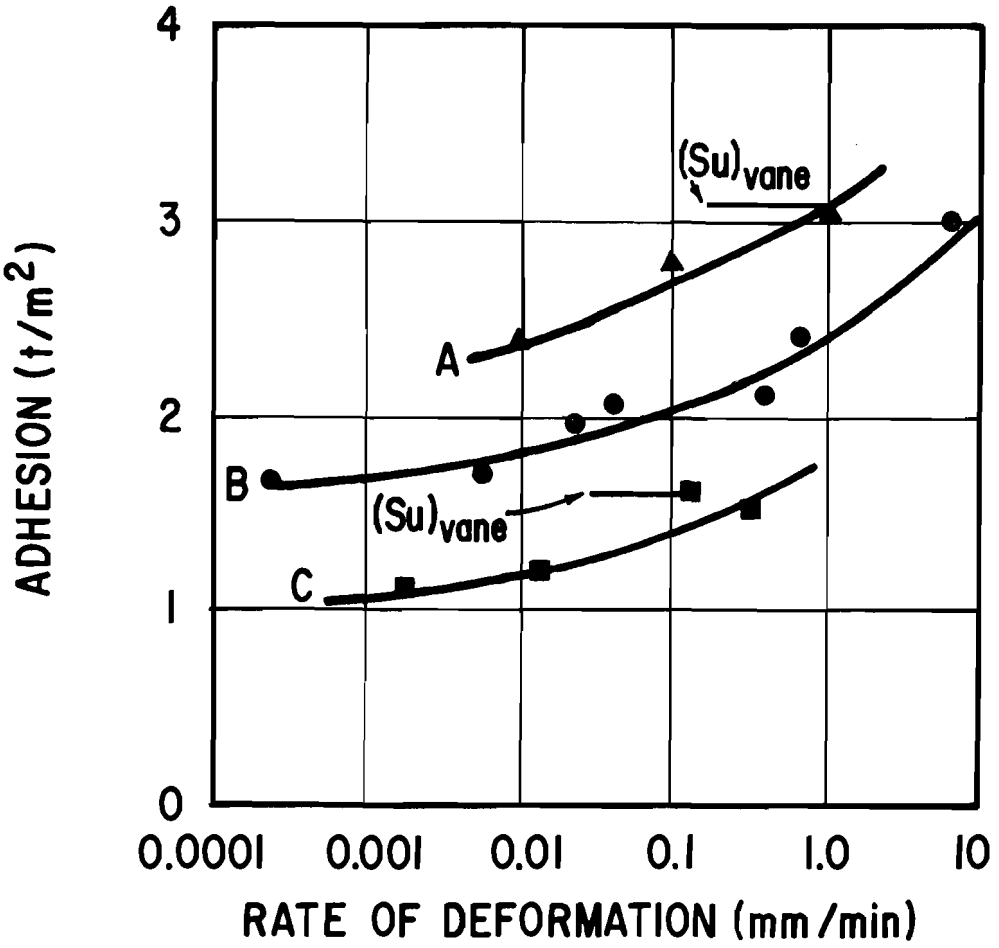


| SYMBOL | SITE | PLASTICITY INDEX OF CLAY | TYPE OF PILE | LENGTH OF PILE |
|---|---|---|---|---|
| A | Oslo | 20% | Concrete Cast in-situ | 6m |
| B | Mexico City | 250% | Timber | 5m |
| C | Gothenburg | 92% | Concrete Precast | 1m |

Fig. 2.3 Relationship Between Adhesion and Rate of Deformation for Tension Test of Piles (after Bjerrum, 1973)

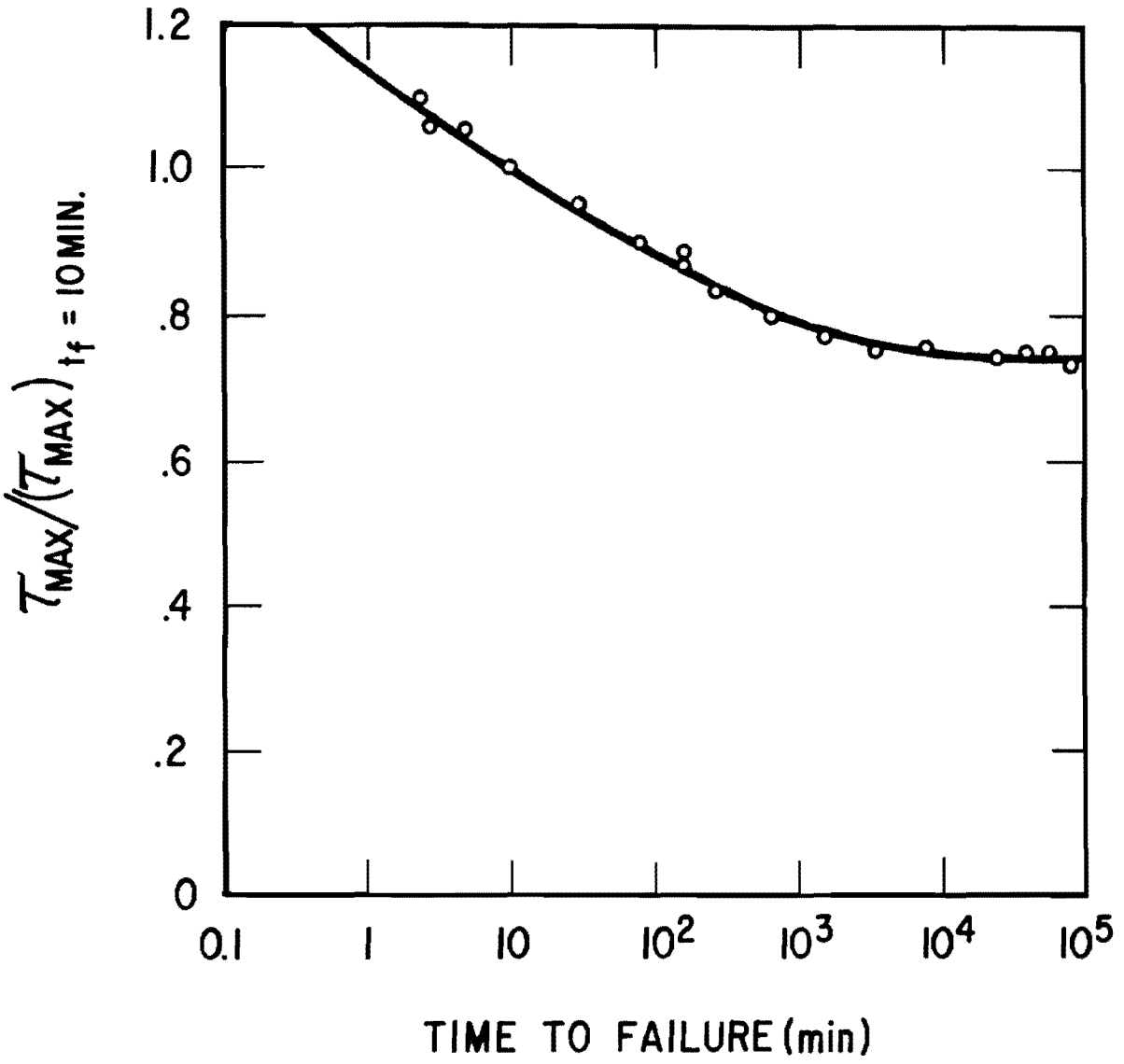


Fig. 2.4 Relationship Between Shear Stress Level and Time to Failure for a Drammen Clay (after Berre and Bjerrum, 1973)

known that the consolidation of clay causes an increase in shear strength. Bishop and Lovenbury (1969) found that for a controlled strain-rate, drained triaxial test the strength of a normally consolidated clay was independent of the time of loading. It was suggested that the decrease in the rheological component of strength due to the breaking of viscous contact bonds was balanced by an increase in strength caused by a decrease in the void ratio and by secondary consolidation.

On a simplified basis, the effect of consolidation can be explained rather easily. Referring to Eq. 2.3, it can be seen that the frictional component of strength can be expressed as $\sigma' \tan \phi'$ . The effect of consolidation on $\sigma'$ , the effective stress, will be considered. As consolidation occurs, the excess pore water pressure dissipates with time. Terzaghi's equation for effective stress,

$$\sigma' = \sigma - u \quad \ldots\ldots\ldots\ldots\ldots\ldots \quad (2.5)$$

where

$\sigma'$ = effective stress

$\sigma$ = total stress

$u$ = pore water pressures,

shows the effect that the reduction of pore water pressure has on the shear strength. As the pore water pressure decreases, the effective stress gets larger and larger. This increase in effective stress will thereby result in an increase in the frictional component of strength

assuming $\phi'$ remains constant. Bjerrum (1973) also suggests that there will be an increase in the cohesive component of shear strength due to an increase in $p'$. As shown by Eq. 2.3, an increase in $p'$, the equivalent consolidation pressure, will also result in an increase in shear strength.

So, it is seen that during long-term loading, the phenomena of consolidation tends to cancel out the effects of creep and rate of loading. If the soil undergoes a large volume change, it is likely that the consolidation will be the predominant phenomenon and, therefore, the strength will probably remain about constant. On the other hand, if there is little volume change, or if the soil is over-consolidated already, it is probable that the creep effect of reduced strength will be felt.

The preceding discussion has been limited to a clay soil. Nevertheless, the phenomenon of consolidation must also be recognized for a sand. Consolidation of sands will occur as the interparticle water is compressed from the sand structure. The effect of consolidation on sand, therefore, will be similar to that for clays.

## Previous Data From Sustained Load Tests

A literature search reveals only scant information concerning previous sustained load tests. Eide, Hutchinson, and Landva (1961) of the Norwegian Geotechnical Institute carried out a series of long-term and short-term tests on single, driven, wooden piles. Four short-term loadings were carried out on the piles before two long-term tests were initiated. Each long-term test lasted for about a year. After the two

long-term tests were completed, a final short-term test was conducted. Each short-term test showed an increase in bearing capacity over the previous test, with the long-term tests yielding a similar capacity (See Fig. 2.5). It can be seen that the values for the long-term bearing capacity are slightly lower than those for the short-term bearing capacity, but the values are too close to allow any definite conclusions to be drawn. The primary differences in the load tests was the fact that the pile exhibited considerably more settlement for the sustained load tests than for the short-term loading. The average settlement for the short-term loadings was around 25 mm, while for the long-term test it was around 70 mm. It was felt by the three authors that the long-period loading enabled the soil to consolidate, and this consolidation in turn led to the greater settlement.

Calculations were made for the ultimate bearing capacity using theory and the data from soil explorations. The calculations predicted a bearing capacity from undrained shear tests of about 17 tons while the actual capacity under sustained load was about 30 tons. Because the soil exploration data indicated a soft, silty clay in the region of the tip of the pile it is doubtful that the additional capacity was derived from any additional tip capacity. It seems therefore, that the additional capacity must have been derived from the increase in the shaft adhesion component of capacity. This tends to suggest that the consolidation effect was more predominant than the deleterious effects of creep and rate of loading. The consolidation probably caused the increase in adhesion. There is some question, however, as to what effect the series of

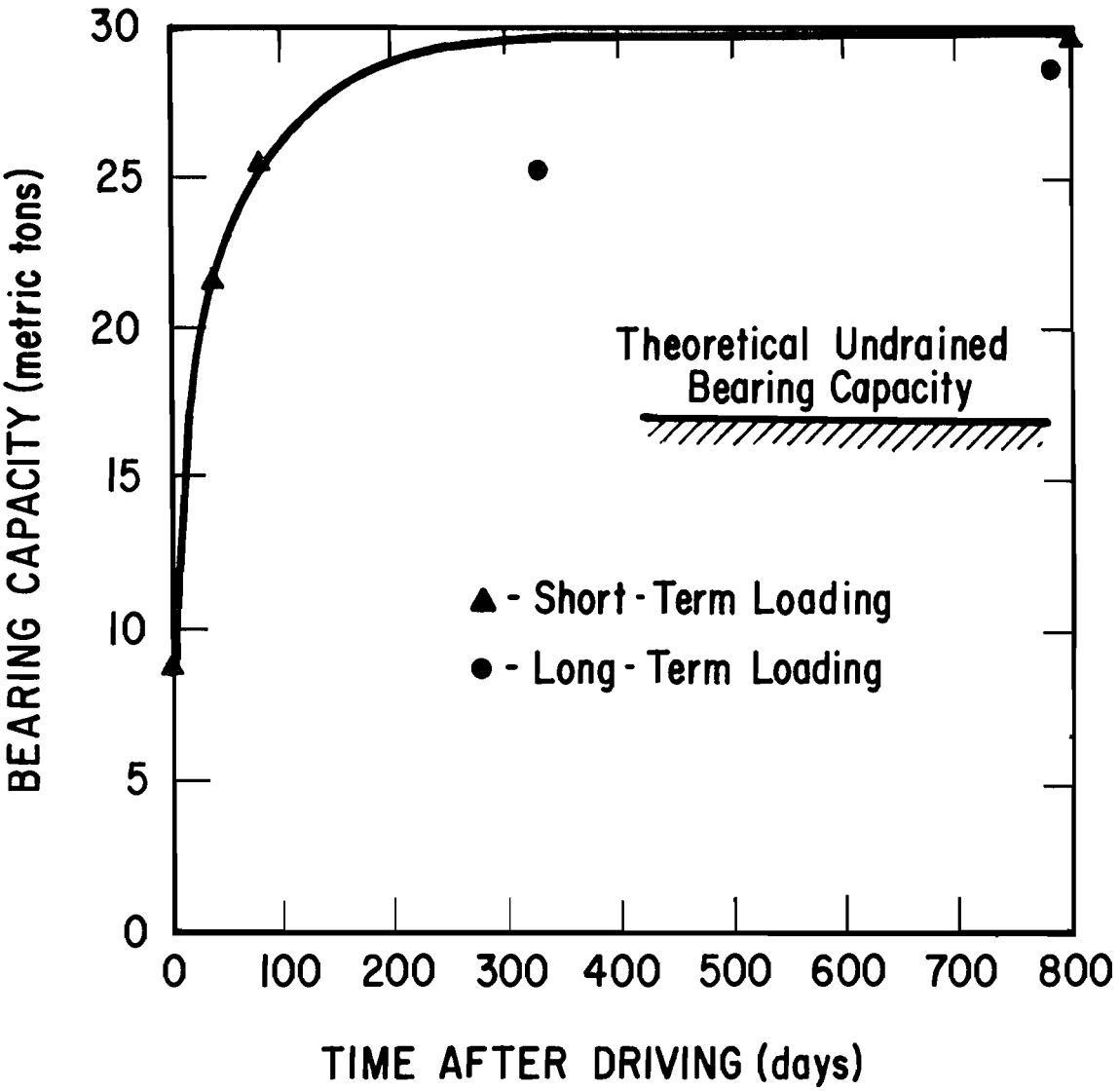


Fig. 2.5 Relationship Between Bearing Capacity and Time for a Driven Pile (after Eide, Et. Al., 1961)

repetitive loadings had on the load-carrying ability of the clay. It does seem that for this case the reduction in shear strength due to slow rates of loading and creep was counterbalanced by the apparent gain in adhesion due to consolidation during the period of sustained loading.

## Implications for a Sustained Load Test

As shown by the preceding discussions, the effects of a sustained load on the behavior of a drilled shaft or a driven pile involve a number of factors that are not well understood. It is difficult to predict how all of the contradicting sustained-load-related factors are going to affect the load-carrying behavior of a shaft. One thing is certain, however; the magnitude of the effect of each phenomenon is a function of many things: soil characteristics, magnitude of load, rate of application of load, and creep rate of the soil.

To examine what possible effect creep of soils could have on a drilled shaft, it is necessary to consider a theoretical load-distribution curve. Figure 2.6 shows such a curve. In Fig. 2.6 the slope of the load-distribution curve at some depths is shown to decrease as a result of load shedding. This decrease in slope can result in an eventual increase in the base pressure of the shaft as shown in Fig. 2.6. From relationships derived by Touma and Reese (1972), and O'Neill and Reese (1970), it is likely that the increase in base pressure would cause an acceleration of settlement, whether the tip is founded in clay or sand. Settlement can also be caused by the consolidation of the clay as a result of dissipation of excess pore water pressure under a sustained load. These arguments tend

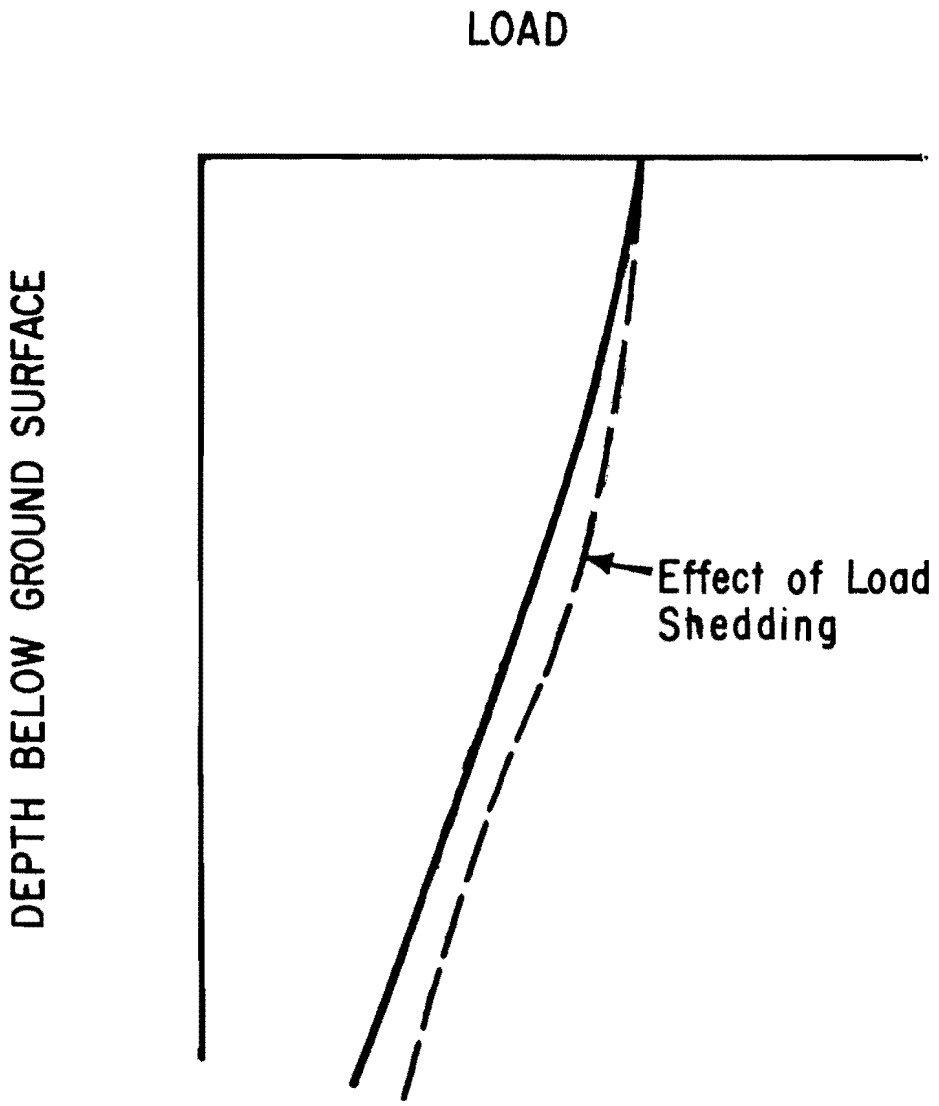


Fig. 2.6 Effect of Load Shedding

to agree with the results of the load test which were discussed in the previous section (Eide, et. al., 1961). Regardless of the cause of the settlement, the fact that it occurs may have an impact on design considerations.

# CHAPTER III

# TEST SITE AND SOIL CONDITIONS

## Location

The long-term test shaft was incorporated into a highway overpass structure. For short-term testing, this arrangement permitted the reaction shafts to become a part of the final structure, thereby retrieving some of the expense of the load test. For the sustained-load test, however, the test shaft itself becomes part of the final structure.

The instrumented shaft is shaft No. 45, in Bent 11, at the I-45 and I-610 interchange in Houston, Texas. Another test shaft, that one referred to as "G-1" by Touma and Reese (1972), was located in Bent 12 about 75 feet east of the sustained-load shaft. Therefore, due to the proximity of these two shafts, the soil data obtained for G-1 will be used in the analyses of the results of the sustained-load test. In addition to the data from the soil tests run on samples taken by the Center for Highway Research at the exact location of the G-1 test shaft, soil data were obtained from the Texas Highway Department, Houston, Urban Expressways Division, from soil investigations in the area of the test shaft. The two most pertinent borings are 125 and 126; both borings are about 95 to 100 feet away from the instrumented shaft. Details of location of test shafts and borings are shown in Fig. 3.1.

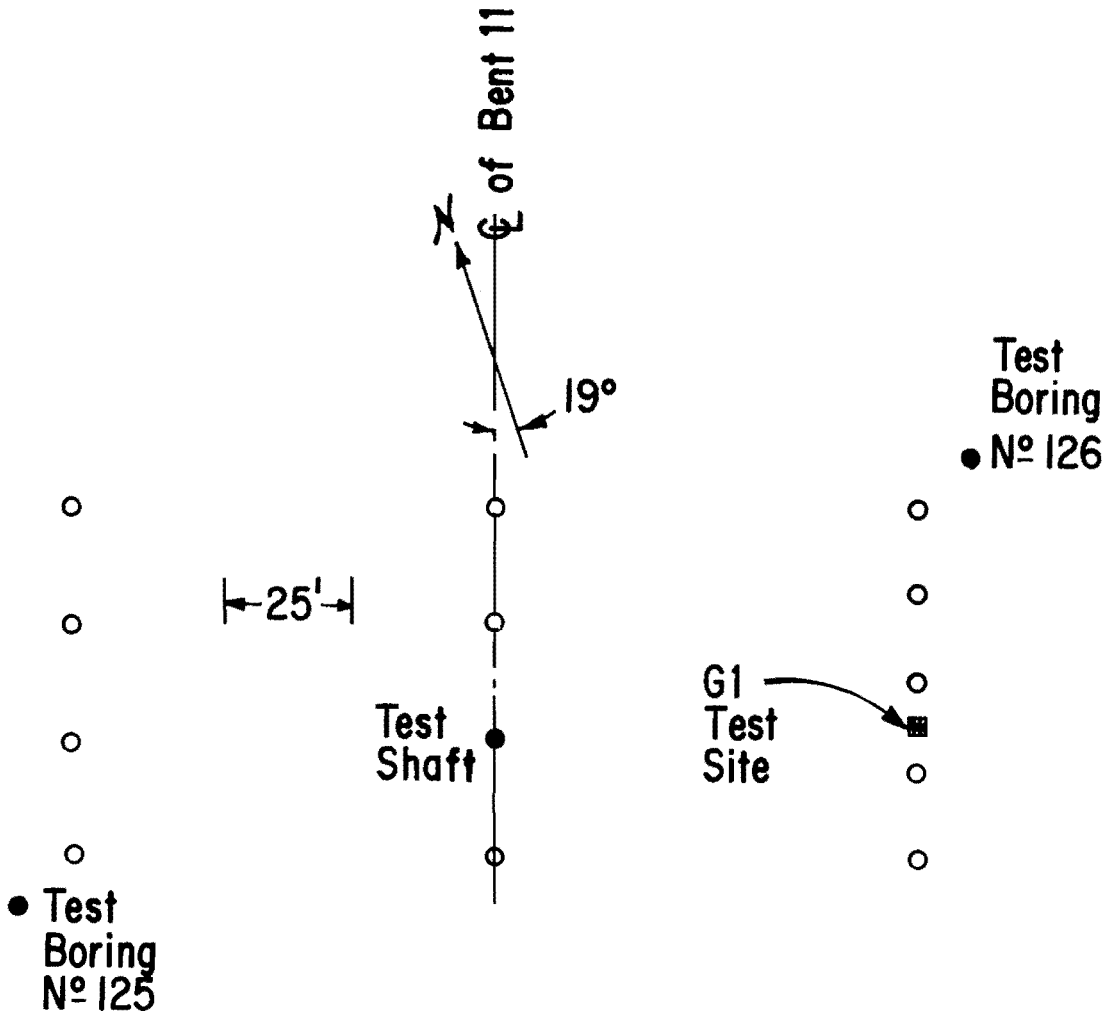


Fig. 3.1 Location of Long-Term Test Shaft, G-1 Test Shaft, and Test Borings 125 and 126

Soil Investigation Program

An intensive battery of tests was performed by Touma and others at the G-1 site. The tests performed included the Texas Highway Department penetration test (THDP), the standard penetration test (SPT), the transmatic triaxial test, the U. T. triaxial test, and granulometric analysis (for explicit details of these tests see Touma and Reese, 1972). Results of these tests are shown in Appendix A.

The soil profile at the site consists of a layer of over-consolidated clay, about 32 feet deep, overlying a layer of sand. An extensive discussion of the evaluation of the properties of the soils was presented by Touma and Reese (1972). For further details concerning the tests, that reference should be consulted. The final estimate of shear strength as projected by Touma and Reese is shown in Fig. 3.2. Touma's representation of shear strength will be used for calculations in this report.

Concerning the possible behavior of a drilled shaft in this soil formation, the phenomena discussed in Chapter II should be remembered. It is likely that the over-consolidated clay in the upper regions of the shaft will show little if any gain in strength due to consolidation. Therefore, it seems likely that the deleterious effects of creep and slow rate of loading will be felt more than the strengthening effect of consolidation. Because the bottom half of the shaft is founded in a sand, it is questionable how the time-related phenomena will affect that portion of the shaft.

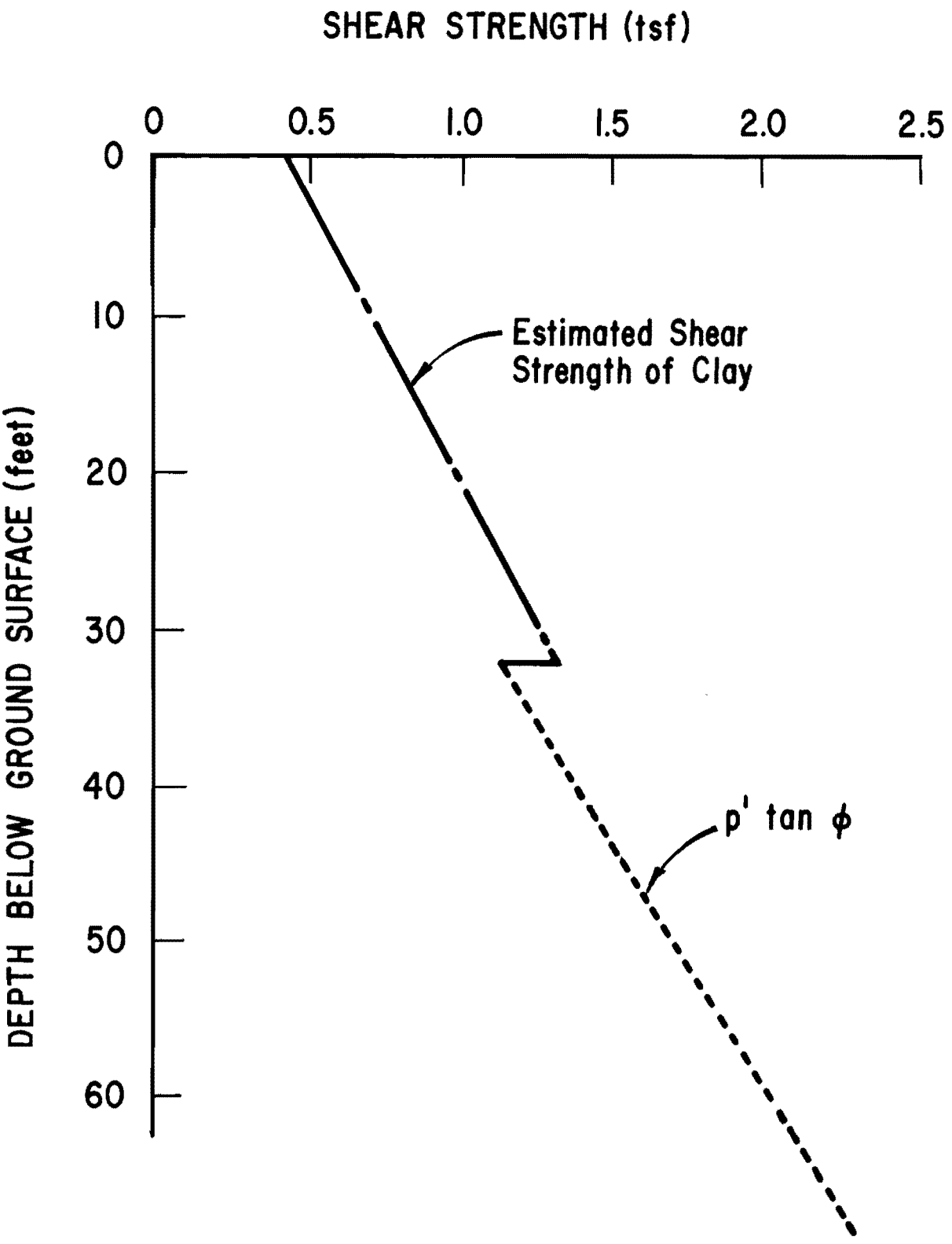


Fig. 3.2 Shear Strength Vs. Depth - G1 Site (after Touma and Reese, 1972)

# CHAPTER IV

# FIELD TEST SYSTEM

## Reaction System

Because of the expense of constructing an appropriate long-term loading system, the sustained load test was incorporated into a full-scale structure. The particular shaft which is being tested has a "calculated load" of 273 tons, the largest axial load on any of the drilled piers in the I-610 eastbound structure.

## Construction of Test Shaft

The long-term test shaft was constructed using the technique known as the slurry displacement method. This technique has found its way into extensive use in the Houston area and is discussed in detail by Touma and Reese (1972). The method consists basically of utilizing a slurry to maintain an open hole, and then displacing the slurry with an equal volume of concrete. The method has been found to give acceptable values for side load transfer.

Tests conducted on eight concrete specimens taken at the site showed the concrete in the shaft to have an average compressive strength ($f'_c$) of 6026 pounds per square inch (psi), and an average Young's Modulus (E) of $5.6 \times 10^6$ psi. These values are not significantly different from those that have been obtained for the other drilled shafts tested by The University of Texas. The test shaft was installed on December 6, 1972,

and was allowed to cure about two months before the column was constructed. The bent cap was installed on March 15, 1973, the girders were placed during the summer, and the decking was placed in the fall.

As of December, 1973, the overhead structure was essentially complete, with the guard rails and markings remaining to be installed.

## Instrumentation

### Mustran Cell

The Mustran cell is the instrumental mainstay of much of the drilled shaft research carried out by The University of Texas. The device was developed by the Center for Highway Research and has been discussed extensively by Barker and Reese (1969). The gage is designed specifically to measure the axial load in a test shaft. The device simply measures the deformation between two points in the shaft by use of a strained bar on which electrical resistance gages are attached. The Mustran cell used for the long-term test has a reduced section at the strain gages in order to magnify output. A view of the cell is shown in Fig. 4.1. The ends of the bar are machined to fit end caps which assist in the bonding of concrete to the cell. A rubber hose is also attached to the end caps, which enables a desiccant to be contained around the electrical strain gages. Since the device employs electrical circuits, it is very susceptible to damage as a result of ambient moisture. In addition to the placement of the desiccant, another safeguard against moisture has been provided. The lead wires are brought through the top of the cell through

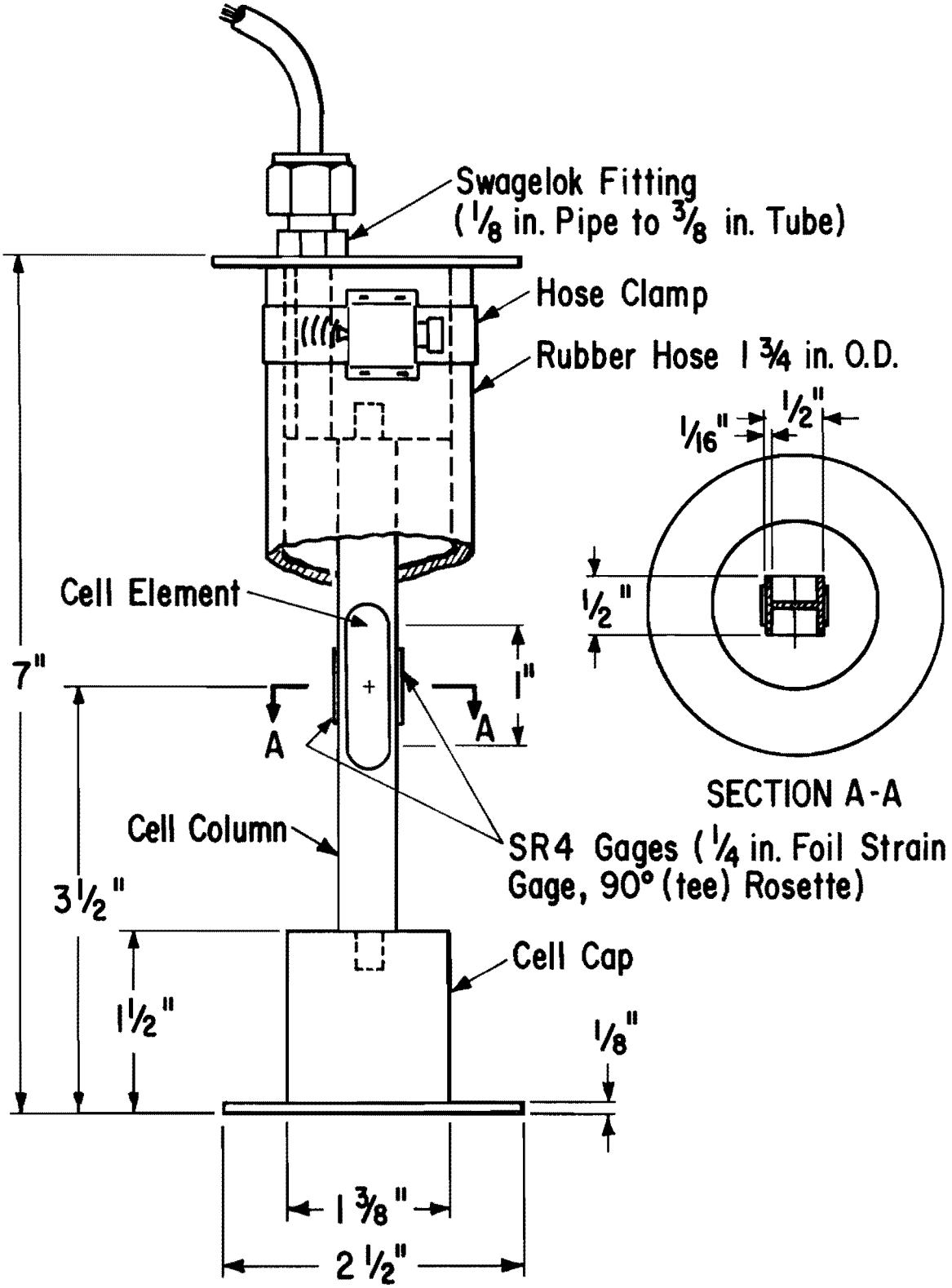


Fig. 4.1 Mustran Cell (after Barker and Reese, 1969)

a fitting. The opposite ends of the lead wires can be collected in a pressurized manifold. The pressure in the manifold acts through the insulated cable and, therefore, pressurizes the Mustran cells and drives out any moisture. The design of the cell is such that the stiffness of the cell is about equal to that of the displaced concrete. A lengthy discussion of this aspect of the design is presented by Barker and Reese (1969). The final product is shown in the photograph in Fig. 4.2.

Due to its previous use exclusively for short-term tests, it was not known whether or not the Mustran cell was stable over a prolonged period of time. Since it is an electrical gage, it was feared that the infiltration of water into the gage would cause severe difficulties, even if the gage had performed satisfactorily at the beginning of its life. Simple immersion tests, in which concrete blocks containing Mustran cells were kept under 30 feet of water, yielded data concerning stability for a period of about 1 1/2 years. The gages seemed to perform reliably, with the only drift coming from the temperature variations in the uncontrolled environment. Even though these results seemed promising, the reliability of the gage was still in question in regard to its proposed use in a sustained load test. In order to get the best possible data from the Mustran gages, the utmost care was employed in the preparation of the gages; furthermore, an alternate instrumentation system was employed as a reserve.

2 Mustran Cell Ready for Installation

Vibrating Wire Gage

The reserve system for the Mustran cell was the vibrating wire gage system. Unlike the Mustran cell, the vibrating wire gage is basically a mechanical gage. The gage consists of two end caps, a tensioned wire, and an electromagnetic coil by which the tensioned wire can be plucked. The tensioned wire can be vibrated at will by the plucking device. If the tension in the wire is high, the frequency will also be high. The relationship between the frequency of vibration and the applied strain can be derived by use of physical principles. The simple relationship between strain and vibrating frequency is given in Eq. 4.1.

$$\varepsilon = K (f_2^2 - f_1^2) \quad (4.1)$$

where

$f_1$ = original frequency

$f_2$ = loaded frequency

$\varepsilon$ = microstrain

K = constant for each type of gage.

The electromagnetic plucking coil is specially calibrated to double as a resistance temperature element. The element can cover a range of temperatures from -20°C to +100°C. The relationship which relates temperature to resistance over this range is assumed to be linear, and can be expressed as:

$$R_t = R_{20} [1 + \alpha (t - 20)] \quad (4.2)$$

where

$R_t$ = Resistance at t°C

$R_{20}$ = Resistance at 20°C

$\alpha$ = Temperature coefficient in ohms per °C

$t$ = Temperature in °C.

With the use of the vibrating wire strain gages, there is no need for the addition of thermocouples in the test shaft to monitor temperature.

The long-term stability of the vibrating wire gage is claimed by the manufacturer to be one microinch per inch per year. Temperature compensation is unnecessary for the range of temperatures encountered in civil engineering problems. In short, it appeared that the vibrating wire gage would be satisfactory for use in a sustained load test.

For the full-scale drilled shaft, the Perivale Company PC 657 NA vibrating wire strain gage was chosen. The Perivale gage has a reputation as a reliable and stable instrument over a prolonged period of stress. This gage is equipped with two electromagnetic coils to act as pluckers. The gage is 5 7/8 inches long and 2 1/32 inches in diameter. A sketch of the gage is shown in Fig. 4.3. For the creep studies, which will be discussed later, a smaller vibrating wire gage was used. It is the Perivale PC 641 gage. It works with the same principle as the PC 657 NA, but has only one electromagnetic coil. It is 4 1/16 inches in length and 7/8 inch in diameter. A cross-section of this gage is shown in Fig. 4.4.

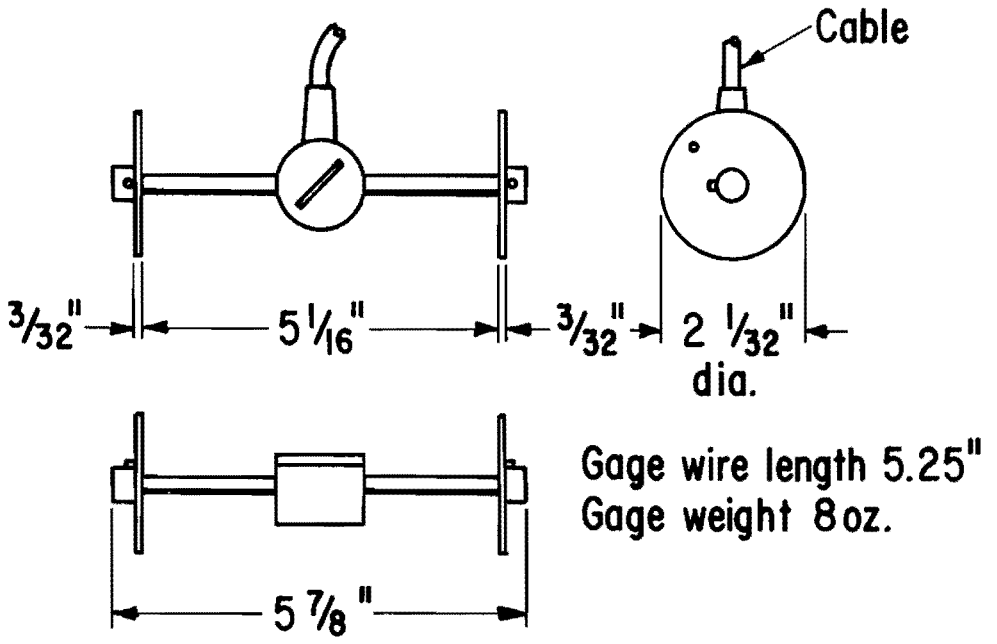


Fig. 4.3 Sketch of PC 657 NA Vibrating Wire Strain Gage (after Perivale Instruments, Inc.)

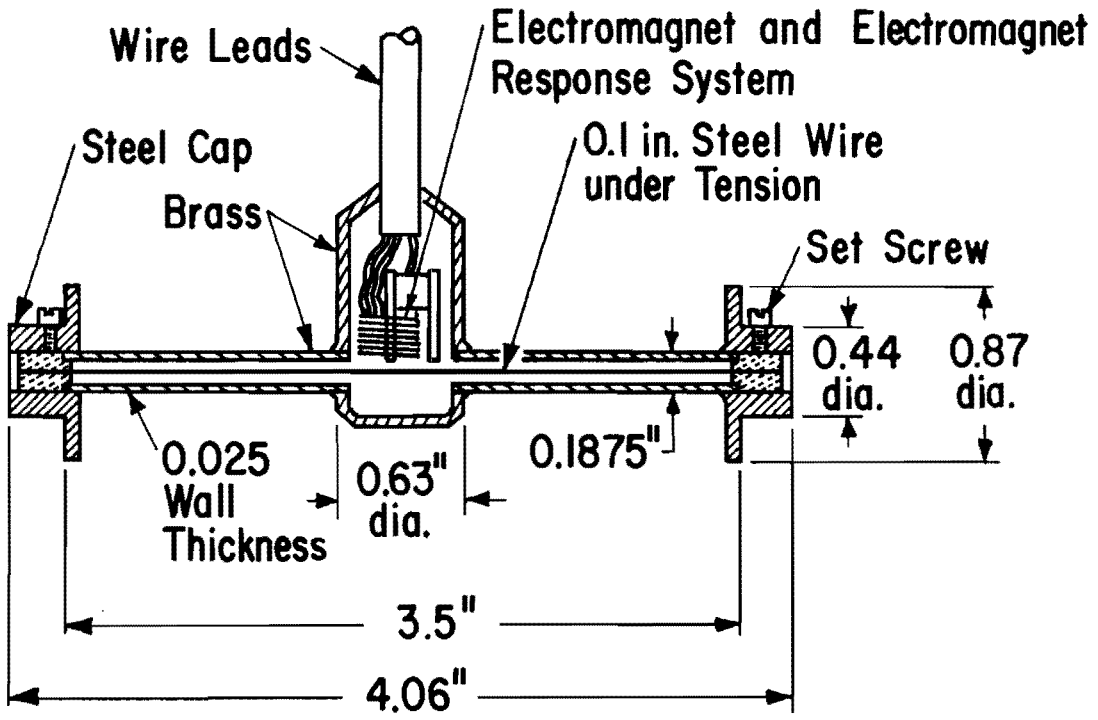


Fig. 4.4 Cross Section of PC 641 Vibrating Wire Strain Gage (after York, Et. Al., 1970)

Because of its small size the PC 641 gage is particularly useful for research models. The gages are pictured in Fig. 4.5 ready for installation.

Placement of Strain-Sensing Devices

In all, 38 strain-sensing devices were installed inside the test shaft itself. Twenty-six of these were Mustran cells, while 12 were vibrating wire gages. The gages were attached to the steel reinforcing cage by means of steel brackets, that were fabricated specifically for that purpose. The Mustran cells were installed at 12 different levels, and the vibrating wire gages were installed at five of those levels. The upper gaging levels were of critical importance because the magnitude of the actual applied load was to be determined from the output at the upper gages. For this reason, there were four Mustran cells installed at the highest level at three feet below ground level; while at all other levels, only two Mustran cells were used. The second level of Mustran cells was placed at five feet below ground level with the rest of the levels coming at six-foot spacings, except for a concentration of gages near the tip of the shaft and a shift of levels from 35 to 32 feet in depth. Pairs of vibrating wire gages were placed at levels of five feet, 23 feet, 41 feet, and 57 feet. Four vibrating wire gages were placed at the three-foot level. A diagram of gage placement is presented in Fig. 4.6.

The Mustran cells were affixed at each level to opposite reinforcing bars in order to eliminate the effect of any bending. Likewise, the vibrating wire gages were installed on opposite reinforcing bars, and their reference plane was rotated 90° from that of the Mustran cells. All

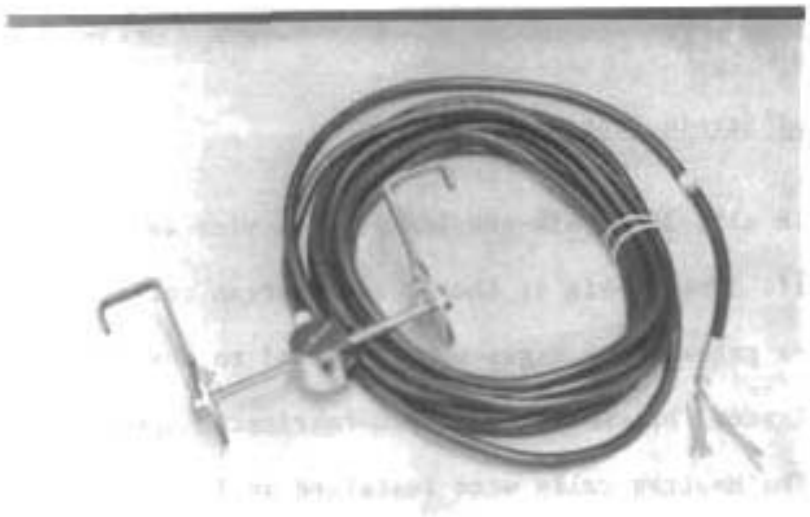

Fig. 4.5a Photograph of PC 657 NA Vibrating Wire Strain Gage

Fig. 4.5b Photograph of PC 641 Vibrating Wire Strain Gage

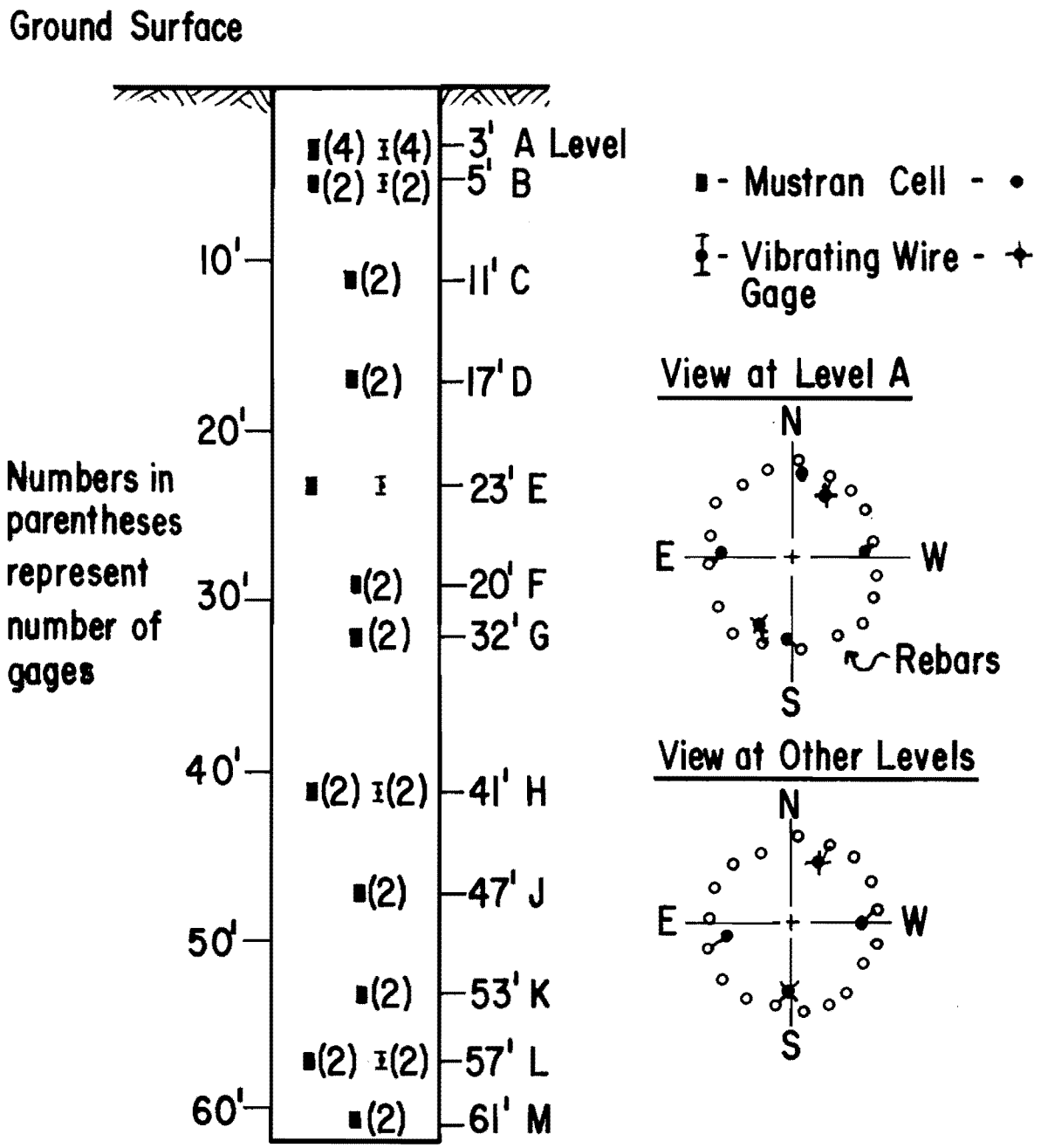


Fig. 4.6 Placement of Strain Gages

of the gages were affixed near enough to the reinforcing bars that it was felt that there would be no danger of damage resulting from impact from the tremie. Another precaution was taken with regard to the tremie. Tremie guides were installed on the reinforcing cage at three points along the cage in order to insure no contact between the tremie and the gages.

Nuclear Moisture/Density Probe

In an attempt to monitor any changes in the water content of the soil due to seasonal moisture variations, the Troxler Nuclear Moisture/Density apparatus was employed at the long-term test site. Two probe tubes were placed on either side of the test shaft near Bent 11. Locations of the probes are shown in Fig. 4.7. The system consists of a probe and an embedded aluminum tube, 30 feet deep, in which the probe is placed. The probe is extended to the bottom of the hole and then extracted incrementally with readings being taken at each level of extraction.

The probe is actually a neutron source and it emits high energy or fast neutrons in all directions; upon collision with atomic nuclei the neutrons are back-scattered at a slower speed and counted by a detector inside the probe. Hydrogen nuclei have a large scattering cross-section relative to most other nuclei, therefore, the concentration of slow neutrons near the probe can be related by calibration charts to the actual moisture content.

A similar method is employed to obtain measurements of density. An error of about 4% is the maximum expected for both of the measurements.

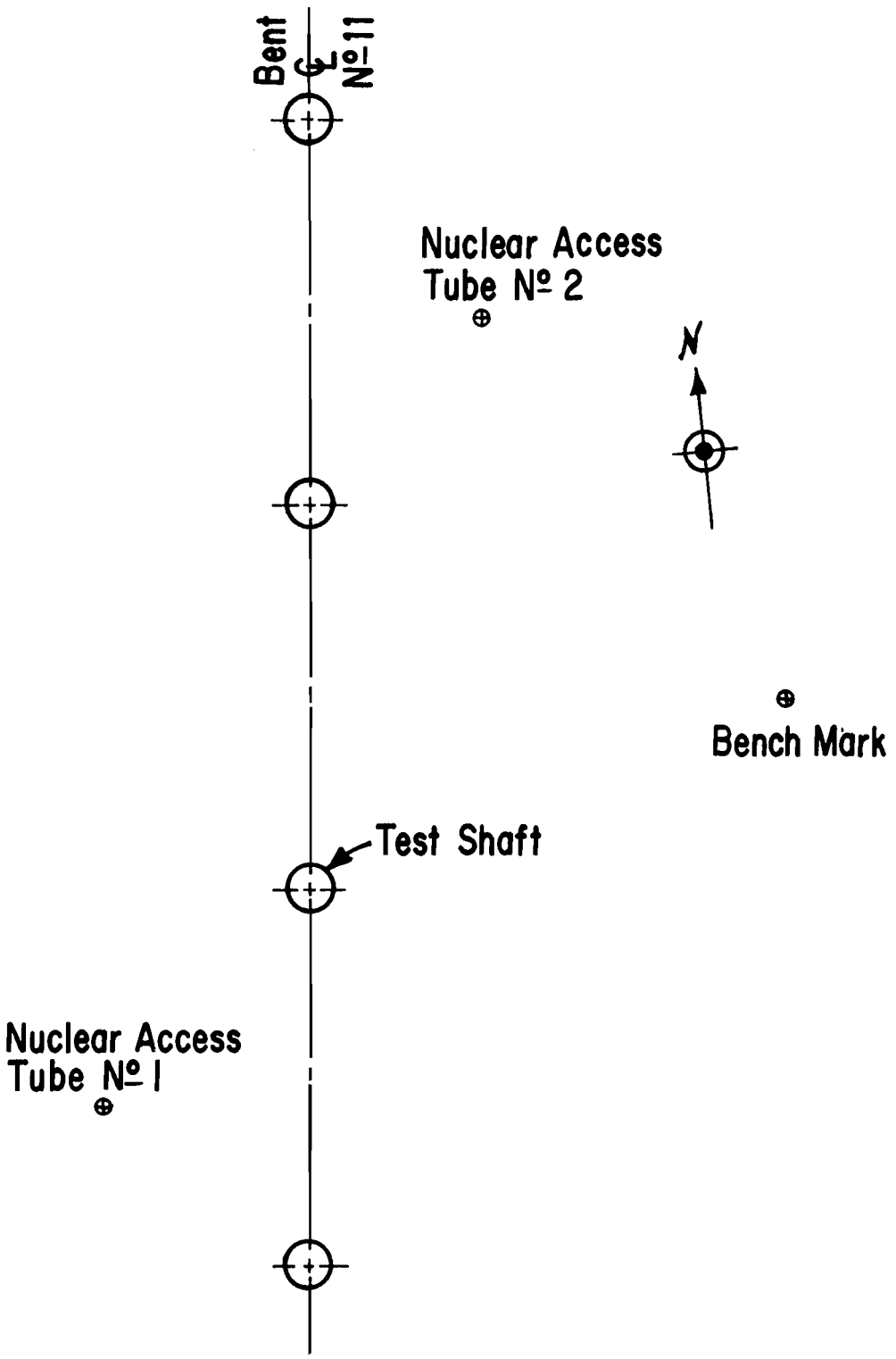


Fig. 4.7 Location of Nuclear Probes and Bench Mark

Settlement Measurements

A simple method was selected for measurement of settlement in that ordinary surveying techniques were used. A special bench mark (shown in Fig. 4.8) was placed about 30 feet from the test shaft, with the tip of the bench mark support extending to sand. It was felt that this design would offer a suitably stable reference for measurements. Precision machinist's scales were affixed to each of the four shafts in the test bent. It is believed that these scales can be read by an automatic level with an accuracy of 0.001 inches for close sightings. The surveyor's rod can easily be read with an accuracy of 0.005 feet which establishes the accuracy of the entire system at about 0.005 feet. The procedure for reading the system is to set up the instrument between the bench mark and the test shaft. Then, a reading of the height of instrument is taken from the rod, followed by readings of the machinist's scales affixed to the shafts.

Readout System

Because the test site was exposed continuously to a hostile environment, it was impractical to leave any readout system in the field permanently. For this reason, portable readout systems were employed to read the gages.

Before any permanent accommodations could be made for the accumulated lead wires, construction had to be completed and the site cleared of construction equipment. Until that time, the lead wires were housed in a

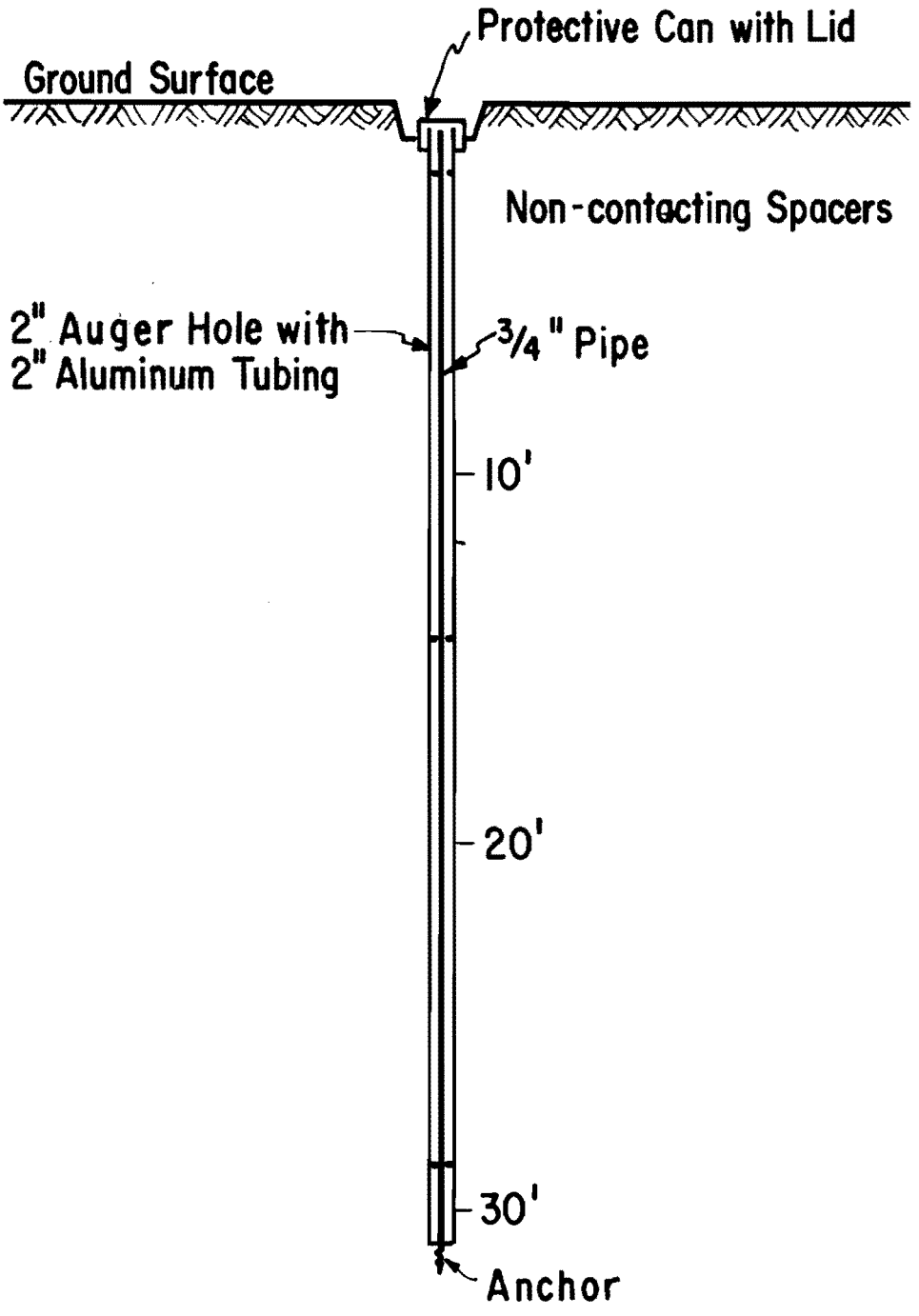


Fig. 4.8 Schematic Diagram of Bench Mark

small shack near the test shaft. To read the gages, the lead wires were taken out of the shack and attached to the readout equipment. The Mustran cells were read by means of a strain indicator manufactured by the Budd Instruments Division. Individual gages were checked for integrity by means of an ohmmeter. The vibrating wire gages were read by means of a comparator provided by the Perivale Controls Company. This device has a built-in frequency which is compared to the frequency of the gage. By changing the frequency in the comparator, the frequency, and therefore, the strain, in the gage can be detected.

The readout system for the Nuclear Moisture/Density apparatus was the standard unit employed by the Troxler Company. It correlates the amount of radiation refracted by the soil to calibration curves which give values for moisture content and density.

# CHAPTER V

# EFFECT OF CREEP OF CONCRETE ON DATA REDUCTION

## Effect of Creep of Concrete

The effect of creep on the load-carrying characteristics of the soil has already been discussed, but creep of concrete has an equally important effect on the acquisition of test data. The values for the load in a shaft are obtained from devices that measure strain. Strain is converted to load by using the properties (modulus of elasticity and cross-sectional area) of the material concerned (concrete and reinforcing steel). In all of the tests conducted by The University of Texas, including the sustained test, devices that measure strain have been used. The use of such instruments commits the accuracy of the test results to the accuracy of determining the composite modulus of elasticity, the cross-sectional area, and the strain of the concrete and steel in the shaft.

This indirect method of determining load presents no particular problem for a short-term test; readings of strain are taken and converted directly to load using a calibration level of gages at which the load is known. For the long-term test, however, the values obtained from strain-reading instruments in the shaft are affected by the creep strain which is induced in the concrete. Any engineering material will creep under load as a function of time. Creep shows up on any strain-sensitive instrument simply as strain. Therefore, it is important to know how much gage output is being caused by strain from load, and how much is being

caused by strain due to creep of the concrete. If the creep effect were neglected, the load in the shaft would appear to be increasing with time to a greater extent than the actual load on the shaft increases during the construction period.

Another property of concrete which is related to creep, in the sense that it can produce deformation without any change in load, is shrinkage. Shrinkage does not affect the long-term test appreciably, because the loading cycle was begun after most of the shrinkage had occurred in both the structure and the creep specimens. Chuang, Kennedy, and Perry (1970) showed that most shrinkage had taken place 90 days after curing had begun. For the shaft used in the sustained load test, more than 90 days had elapsed before any substantial loads were applied to the structure, thereby rendering shrinkage considerations of minimal importance.

## Creep Apparatus

In order to determine what part of the strain output from the test shaft was a result of the applied stress, it was necessary to eliminate the strain created by creep of the concrete under load. Separating the components of strain has been attempted before. York, et. al. (1970), and Kennedy and Perry (1970) carried out such studies at The University of Texas. The hypothetical relationship of the components of deformation, based upon their findings, is shown in Fig. 5.1.

Following the example set by the above named researchers, an attempt was made in this study to approximate the effect of creep on gage

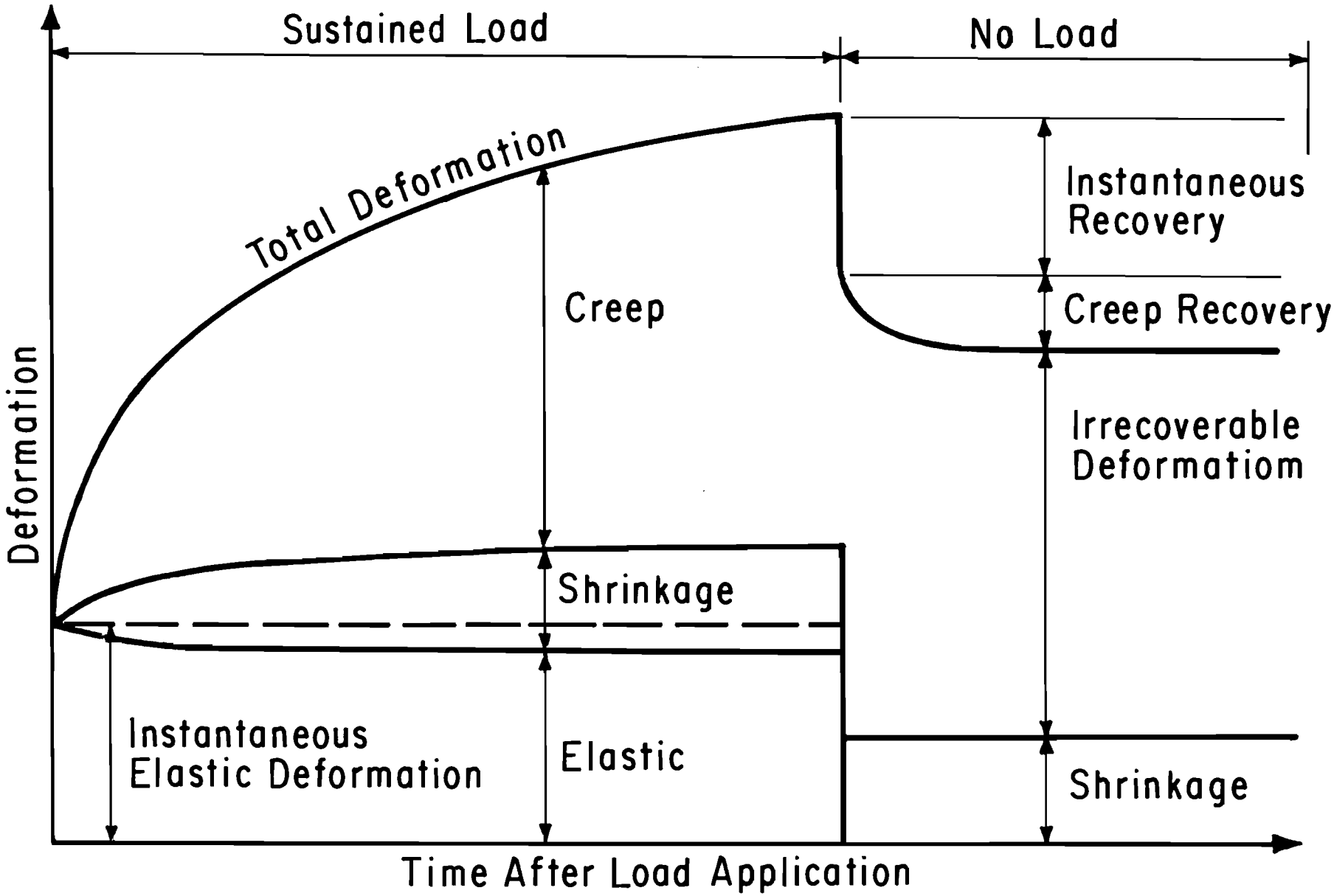


Fig. 5.1 Typical Deformation Vs. Time Curve for Concrete Under a Sustained Load Which is Later Removed (after York, Kennedy, and Perry, 1970)

output. To accomplish this task a loading apparatus to study creep was devised. A diagram of the creep apparatus which was used is shown in Fig. 5.2. The apparatus consists of two heavy plates connected by three tension rods. Between the end plates, a concrete specimen may be loaded in compression by means of two heavy, helical springs. The quantity of load induced into the specimen was derived by measuring the deflection of the helical springs, and then relating this displacement to calibration curves for the springs. The calibration curves are approximately linear until the separate coils of the springs begin to "bottom out"; at that time, the curve begins to break over. The calibration curves are shown in Appendix B. The deflection of the spring was measured by means of two dial gages affixed to the head of the loading device (See Fig. 5.2). Four separate creep apparatuses were employed and each applied different stress levels to the specimens, with the highest level being about the same magnitude as the maximum stress in the drilled pier.

Cast inside each of the concrete specimens were one Mustran cell and one vibrating wire gage. The Mustran cells are of the same design as those in the shaft; while the vibrating wire gages are of the PC 641 type, not the same as those installed in the shaft, but working on the same principle. The concrete specimens themselves are eight inches in diameter, 29 inches in height, and were formed from the concrete batches from which the shaft was constructed.

Since there are four specimens loaded at four different stress levels, each specimen will creep at a different rate. The rate of creep is generally proportional to the stress level if the stresses are not

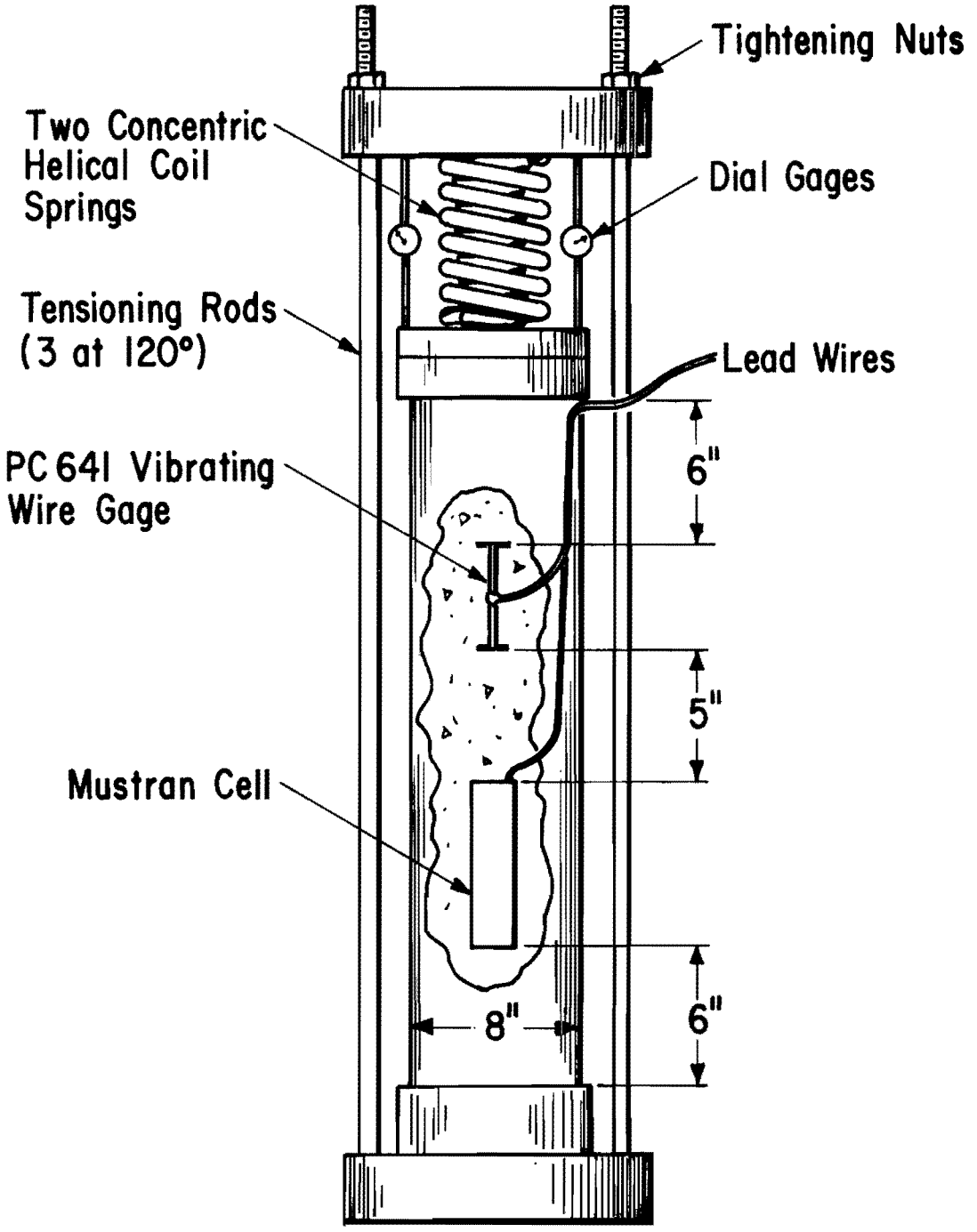


Fig. 5.2 Schematic Diagram of Creep Loading Apparatus (Not to Scale)

more than one-third of the ultimate strength of the concrete (York, Kennedy, and Perry, 1970). Because the specimen with the greatest load was stressed to only about 1/30th of the strength of the concrete, the results of the creep tests of the four specimens can be displayed in a single figure such as Fig. 5.3. As a result of creep, the amount of concrete strain will be increasing; this will cause the stress-strain diagram to decrease in slope. As can be seen from Fig. 5.3, the value of the modulus of elasticity (E) will decrease for increasing values of time. Therefore, the effect of creep can be taken into account when analyzing test data by simply reducing values of the modulus of elasticity for the concrete at different times.

## Approximation of Various Moduli of Elasticity

Although the overall effect of creep is understood, the exact magnitude of creep strain for any concrete and load is difficult to predict. Creep strain is a complex function of a number of parameters. Some of these parameters are: the properties of the concrete, curing history, temperature, and percentage of reinforcing steel. York, Kennedy, and Perry (1970) found that elevated temperatures resulted in increased creep of concrete. Likewise, test specimens allowed to cure in an "air-dried" environment showed accelerated creep while those cured "as cast" showed less creep. Increasing the confining pressure and longer curing time affected the specimens by decreasing the creep strain.

According to the results of the research by York et. al., it is apparent that the prediction of exact values of creep strain is a difficult

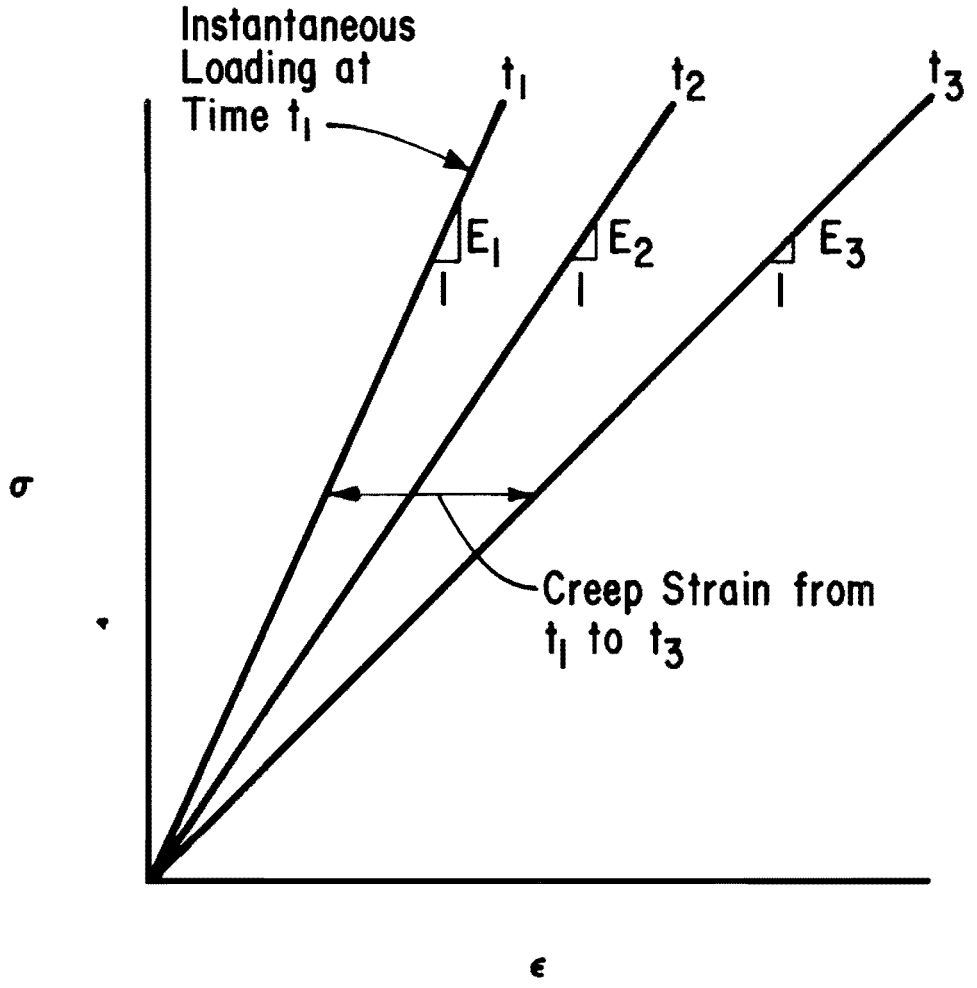


Fig. 5.3 Theoretical Decay of the Modulus of Elasticity with Time

task. To get a better estimate of how closely the creep specimens can predict the creep strains in the test shaft, a consideration of some of the influencing factors affecting creep and of the creep-testing procedure which was employed will be helpful.

The concrete mix design is an important variable. Because the four creep specimens came from the four concrete trucks which were employed to cast the shaft, the creep specimens should all exhibit approximately the same creep properties and the same properties as the concrete in the test shaft, if all other variables remain the same.

The temperature of concrete is also an important variable affecting creep behavior. The temperature in the test shaft has remained about constant since the initial temperature changes due to the curing of the concrete. The temperature has remained about 70 to 77°F, with some minor deviations coming near the ground surface. These temperatures were obtained by the temperature-sensing devices incorporated into the vibrating wire gages. The same type of device was incorporated into each of the four creep specimens. The temperature indicated for the test specimens was approximately the same as that in the test shaft (70 to 72°F). The creep specimens are presently occupying a controlled-temperature vault in which the temperature has been kept at about 72°F. Therefore, it seems evident that there will be no major discrepancies due to the effect of temperature on the creep of the specimens or of the test shaft itself.

The curing history before loading is a variable which will have a significant effect on creep strain. The test shaft and the creep specimens underwent significantly different methods of curing. The test shaft was cured in place; that is, there was plenty of available moisture at the

site, and this condition most nearly approximates a 100% humidity situation. The load was applied incrementally with the first major loads coming at least four to five months after the shaft's placement. The creep specimens were cast at the same time as the test shaft, and underwent eight weeks in a 100% humidity curing situation. After that initial curing period, the specimens were dormant for six months in a non-humid atmosphere until the load was applied. All four specimens were loaded to different stress levels, but the loads were applied almost instantaneously compared to the procedure for the test shaft. This curing and loading procedure induces three effects into the analysis. First, the creep specimens should creep more than the test shaft due to the fact that they approximated more nearly an "air-dried" condition defined by Kennedy (1972), while the test shaft is actually an "as cast" situation. Secondly, and conversely, the creep specimens should creep less than the test shaft since they underwent a longer curing period than the test shaft. Finally, because the test shaft was loaded incrementally and the creep specimens were loaded instantaneously, the test shaft should creep less.

Although there were discrepancies in the curing and loading procedure of the test shaft and creep specimens, it was felt that the data obtained from the creep studies would be valuable in the estimation of trends of creep strain for the test shaft. These discrepancies did, however, pose one problem; the value of the modulus of elasticity obtained from conventional concrete tests ($5.6 \times 10^6$ psi) was larger than that estimated by the instantaneous loading of the creep specimens. It was felt that for the analyses the output from the creep specimens for the instantaneous loadings should be made to fit the modulus of elasticity

projected by the laboratory testing. The multiplication factor which converts circuit strain to concrete strain was adjusted to bring the results from the creep specimens into agreement. A discussion of some of the findings of past researchers concerning the multiplication factor is given later and shows that such factors can show considerable variation from one test to the next. Therefore, it is believed that the method used in this study was reasonable.

The creep specimens were initially loaded on July 17, 1973. The output from the gages was monitored hourly for the first three days and then daily for about a week. At present the creep specimens are monitored twice monthly. Concrete strain versus time is shown plotted in Appendix C for each of the four creep specimens. It can be seen that the rate of creep is high at the initial time of loading and then decreases with time. This phenomenon has been reported by many authors who have dealt with creep. Troxell et. al. (1958) found that 18 to 38 per cent of the total creep deformation after 20 years of loading was accumulated in the first two weeks, 40 to 70 per cent was accumulated in the first three months, and 64 to 84 per cent within the first year.

In Fig. 5.4 the representation of the decrease in the modulus of elasticity versus time is shown. This plot was constructed from the data from the creep specimens. It can be seen that a perfectly straight line through the data points cannot be constructed; however, the lines which are shown are thought to be of sufficient accuracy. For the instantaneous loading of the creep specimens, the data suggest a large reduction of the modulus of elasticity during the initial month. If the

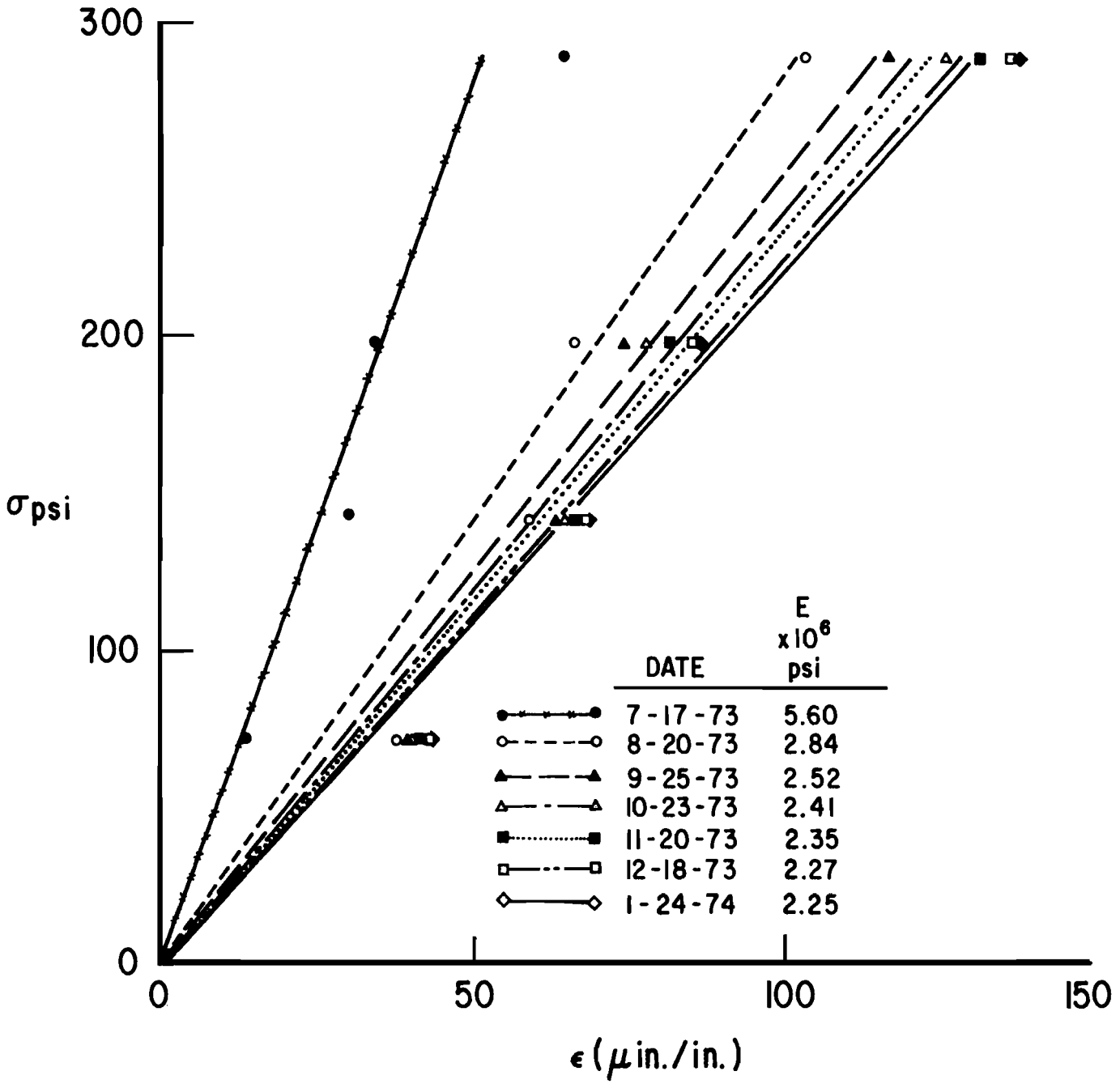


Fig. 5.4 Modulus of Elasticity as Determined by Creep Specimens

maximum stress levels attained in the creep specimens were reached after incrementally applied stresses, as is the case for the concrete in the drilled shaft, it seems reasonable that the creep rates would not be as rapid. Depending upon the magnitude of the increments, and upon the speed of load application, the value of the modulus of elasticity will decrease from the initial value along different paths. The path traced by the modulus of elasticity versus time for an instantaneous loading is shown in Fig. 5.5. This instantaneous relationship was constructed from Fig. 5.4. Also shown in that figure are various other paths which could occur for variations of the loading procedure. Curve "a" represents a loading phase similar to an instantaneous load. Curve "b" represents a three-increment loading phase, with the final increment bringing the value of stress to approximately that of the instantaneous load. Curve "c" represents a very slowly applied load that requires a long time to achieve ultimate load. The instantaneous curve tends to be asymptotic to some value of modulus of elasticity. This value corresponds to the point of ultimate creep. It can be seen that that value for this concrete is about $2.0 \times 10^6$ psi.

In reducing the data obtained from the test shaft, values for the modulus of elasticity can only be approximated. It is evident, due to the loading scheme in the field, that the relationship between the modulus of elasticity and time lies somewhere between the value for instantaneous loading and the value unaffected by creep ($5.6 \times 10^6$ psi). By studying the loading scheme in the field, it was possible to approximate the actual paths which the concrete in the test shaft took. Due to the inability to duplicate in the laboratory the precise conditions of

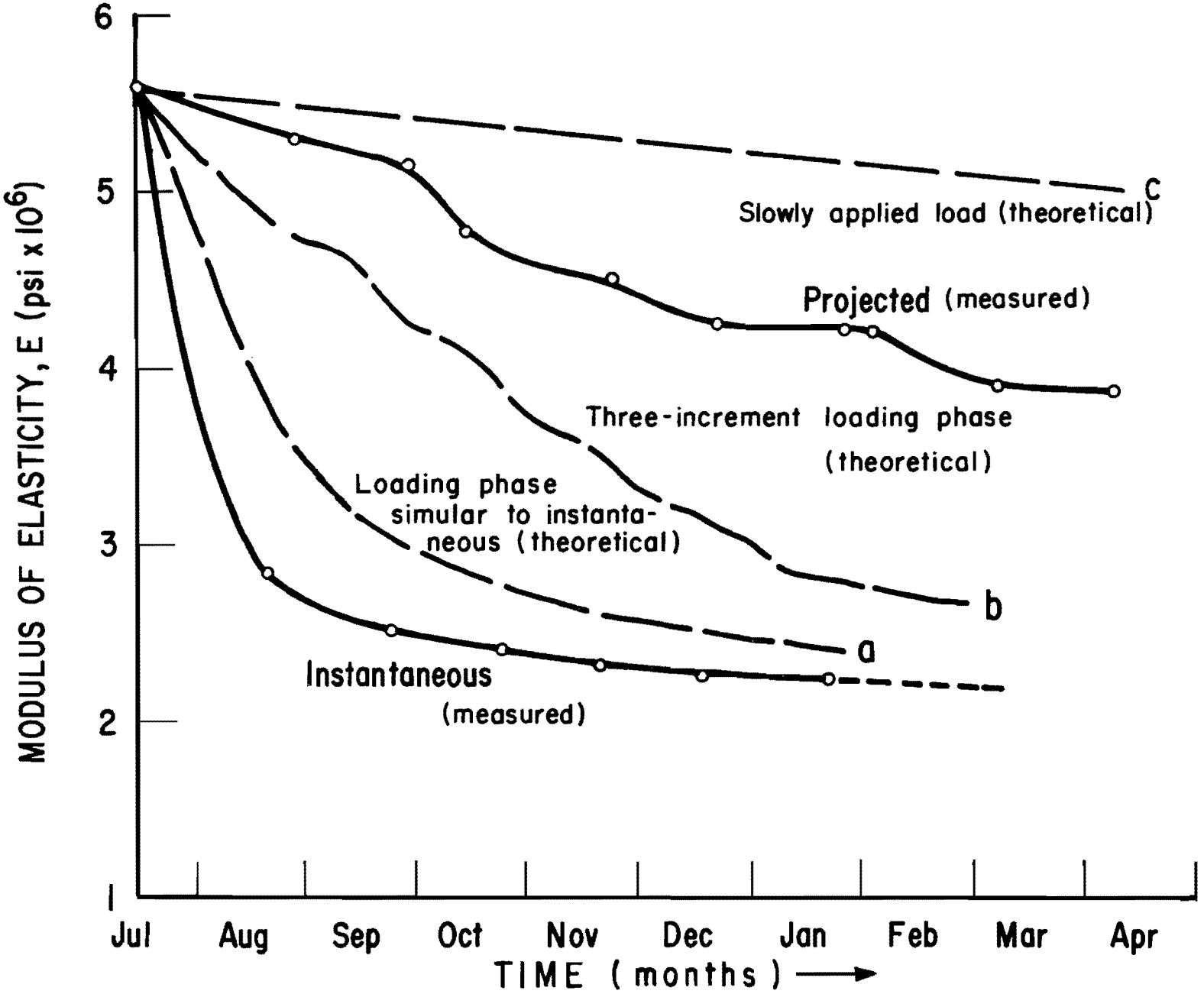


Fig. 5.5 Modulus of Elasticity Vs. Time

curing and loading of the field concrete, the creep specimens overestimate the amount of creep in the field by a substantial amount. Therefore, representative values for creep were selected which would in turn enable the load data to approximate the estimated load induced by the structure. Table 5.1 shows values of the modulus used. The values are plotted in Fig. 5.5 relative to the instantaneous modulus.

Table 5.1

Modulus of Elasticity Vs. Time

| Date | Modulus (Psi) |
|---|---|
| 3-15 - 1973 | $5.6 \times 10^6$ (Instantaneous modulus) |
| 4-28 | 5.29 |
| 5-29 | 5.17 |
| 5-30 | 5.17 |
| 6-13 | 4.76 |
| 7-26 | 4.48 |
| 8-22 | 4.24 |
| 9-25, 26 | 4.24 |
| 10-03 | 4.24 |
| 11-07 | 3.86 |
| 12-11 | 3.86 |
| 2-07 - 1974 | 3.42 |

# CHAPTER VI

# ANALYSIS OF LOAD DATA

## Mustran Cell Performance

As in any research project, the credibility of the results depends on the accuracy with which certain phenomena are measured. For this project, the bulk of the measurements was made by the Mustran cell, with some contribution coming from the vibrating wire gages. Therefore, the accuracy of the results is highly dependent on the reliability of the Mustran cell. As mentioned in an earlier section, the Mustran cell can be adversely affected by many hazards of its hostile environment. To insure that any faulty gages can be identified, readings of the Mustran cells were taken periodically from the time of the concrete placement through the loading sequence.

The readings recorded on January 26, 1973, were selected as the "base line" readings because they were the last set of readings taken before any significant load was applied. In other words, these readings are assumed to be for a "no-load" condition. The accumulation of gage output relative to the base line readings in units of strain, is shown plotted against time in Appendix D. By studying these plots, it is possible to recognize gages which were possibly malfunctioning. Gages showing erratic jumps and jagged traces have questionable integrity. Gages showing excessively high output compared to gages in nearby levels are also suspect of being faulty. The tendency should be for all the gages

to show a general increase in output with time, due to the increased load and creep. Also, the gages in the upper levels should show a steeper slope than the gages in lower levels, and there should be a smooth transition of slopes from steep to gentle as the gage depth increases. Gages not keeping with these general tendencies were considered carefully in the analysis.

Another valuable set of plots in the identification of faulty gages is shown in Appendix E. These plots show the variation of gage output over a 40-hour period. Readings were taken at various intervals, and the gage readings were plotted relative to the first readings. It can be seen that the maximum deviation is about 20 microunits of circuit strain. This deviation can be caused by gage drift, temperature variations, and systematic error. In terms of concrete strain, 20 mircounits of circuit strain would be about four microinches of concrete strain or about 3000 pounds of load. This seems to be an acceptable error. All of the gages except gage F-1 show approximately the same behavior. Gage F-1 plotted irregularly, well above and below the axis is shown in Appendix E.

In general, most of the Mustran cells have performed quite well. There do exist some discrepancies, however. The top level of gages seems to give an extremely high value of output compared to the second and third levels. This would suggest a very large load transfer from the first level (at three feet) to the second level (at five feet). This suggested load transfer would be about 0.4 tons per square foot (tsf) for a load of around 100 tons. By consulting with load transfer figures supplied by Touma and Reese, this much load transfer seems exceptionally

high. Not only that, the second and third levels indicate a smaller load in the shaft than do the next three lower levels. Therefore, the top level of gages would appear to overestimate the load while the next two levels underestimate it. When gages present such anomalies, the reason for their erratic behavior is left to speculation. There are many factors that could be involved, such as damage to the gages, improper embedment of the gages, tendencies for the concrete to be less dense near the top, misorientation of gages, and the improper selection of base line values.

In order to develop load-distribution curves for the top of the shaft, the output from the lower cells in the shaft was used to reconstruct that portion of the load-distribution curves through the faulty gages. This method, along with consulting the low-load behavior of the Touma G-1 shaft, and a graphical average of the three questionable gages yielded a reasonable solution to the problem.

Another minor problem was the tendency for some gages to indicate tensile load, a phenomenon which was felt to be impossible for this shaft. After much consideration, it was felt that this discrepancy was caused by the imperfect sensitivity of the gage itself, by errors in the calibration of the reading instrument before readings were taken, and by errors in reading. Instead of eliminating such gages immediately, they were considered carefully and some of them seemed to function satisfactorily later and were used in the final analysis.

## Reduction of Data

Before the output from the Mustran cells could be interpreted, the selection of the modulus of elasticity to be used for each load and date had to be made. A discussion of that process is contained in the preceding chapter. Under the assumption that the modulus of elasticity has been adequately estimated, the multiplication factor relating concrete strain to circuit strain must be considered. This factor is a complex function of the concrete properties, the fabrication of the Mustran cell, and the bonding of the concrete. The multiplication factor is difficult to predict due to the many variables involved. O'Neill and Reese (1970) suggested a value of 7.3, while analytical analysis suggested 7.6. Tests run by Barker and Reese (1970) showed the factor to be 5.5. Back calculation based on data from the six test shafts studied by Touma yielded multiplication factors that varied from 8.2 to 10.9. Although Touma's Mustran cells were of a slightly different design than the ones employed in the long-term test, the variation of this factor suggests an inability to predict it accurately.

The first sets of data from the long-term test shaft instrumentation were reduced using a multiplication factor of 7.3. To check the value of 7.3, readings were taken in the field immediately after the bent cap had been placed. Calculations of the volume of concrete at that time estimated a load of about 75,000 pounds, while the factor of 7.3 yielded a calculated load of 65,000 pounds. In order to get the calculated load and the estimated load to converge, a factor of 5.6 was required. It was felt that because there were so many indeterminate factors contributing

to the multiplication factor, a change from 7.3 to 5.6 was totally justified. So, in the reduction of test shaft data, the circuit output was divided by 5.6 to convert to concrete strain.

For the creep specimens, however, a factor was chosen that would yield a value of the instantaneous modulus of elasticity for those specimens of $5.6 \times 10^6$ psi. This factor turned out to be about 8.1. This factor is considerably higher than the 5.6 used for field calculations. It is believed that the discrepancy between laboratory and field values of the instantaneous moduli of elasticity reflects experimental error in the loading system used for the laboratory creep studies rather than errors in the Mustran system. Because the creep specimens have been relegated only to predicting "trends" of creep performance, this large deviation in multiplication factors is acceptable.

After the modulus of elasticity and multiplication factor were established, conversion from strain output to load was completed. Computation of load was accomplished by use of a digital computer. Conversion factors were computed for each date of loading by making use of the appropriate value of the modulus of elasticity. The conversion factors were expressed as pounds of load in the shaft per division of gage output. The change in the conversion factor as a function of time is shown plotted in Fig. 6.1. It is seen that the factor decreases with time as a result of the increase in strain output with time because of creep.

To facilitate the plotting of load-distribution curves and the calculation of load transfer, the program DARES was employed. DARES (Barker and Reese, 1970) is a program primarily used for the reduction of

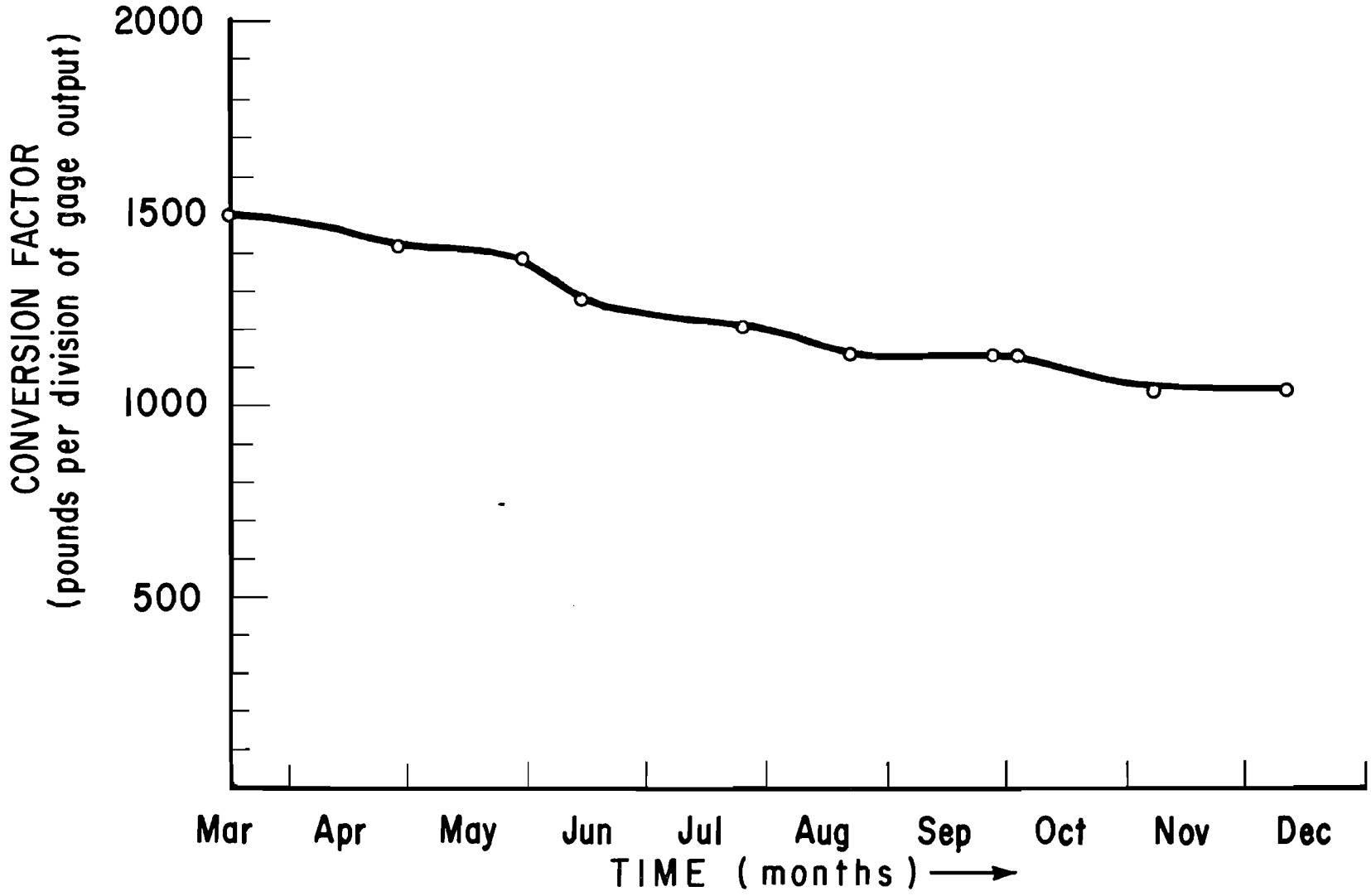


Fig. 6.1 Conversion Factor Vs. Time

data from short-term load tests. Use of the program requires a calibration level of gages and known values of applied loads. Because the sustained load test yields neither of these values, modifications were made to facilitate the use of the program. The conversion factors already discussed proved valuable here. Data for a level of gages at ground elevation was simply back calculated to fit the projected curve for the top three levels of gages. Results from this method proved to be satisfactory. Due to the scatter of data points, a second-order curve, rather than a higher order, was needed to fit the data satisfactorily without showing excessive reverse curvature.

Values of load were also calculated using the output from the vibrating wire gages. The same values for the moduli of elasticity and for the cross-sectional area were employed as in the Mustran cell data reduction. Some malfunction of the vibrating wire gages was also noted in that the top levels gave excessively high load values, similar to the Mustran cells. Both gages at the bottom level also proved inoperable. Good correlation between the Mustran cells and vibrating wire gages existed at the other two levels.

## Results of Analysis of Load Data

Figure 6.2 shows the plots of load versus depth as obtained by program DARES. Individual plots are shown for each value of load in Appendix F. In Appendix F, data points shown by crosses are those of the Mustran cells, while the circles represent the output from the vibrating wire gages. The data for each date were run independently of each other to facilitate the alteration of the modulus of elasticity.

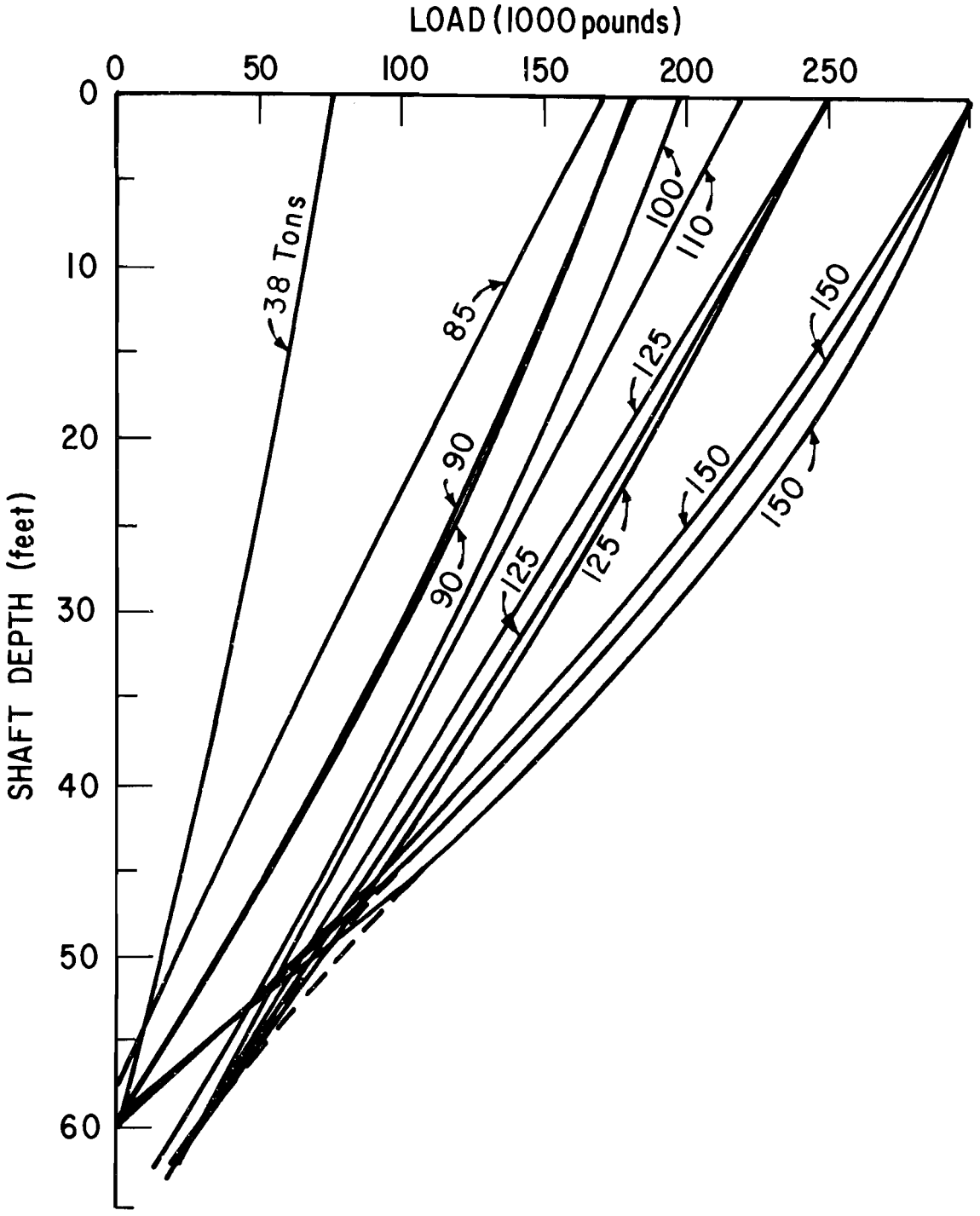


Fig. 6.2 Load Distribution Curves for Various Loads

Figure 6.3 shows plots of load transfer versus depth. These plots were constructed from values computed by program DARES. These plots are straight lines because they are the first derivative of the load-distribution curves, which were selected to be second-order curves. The curves in Figs. 6.2 and 6.3 will be discussed in the next chapter.

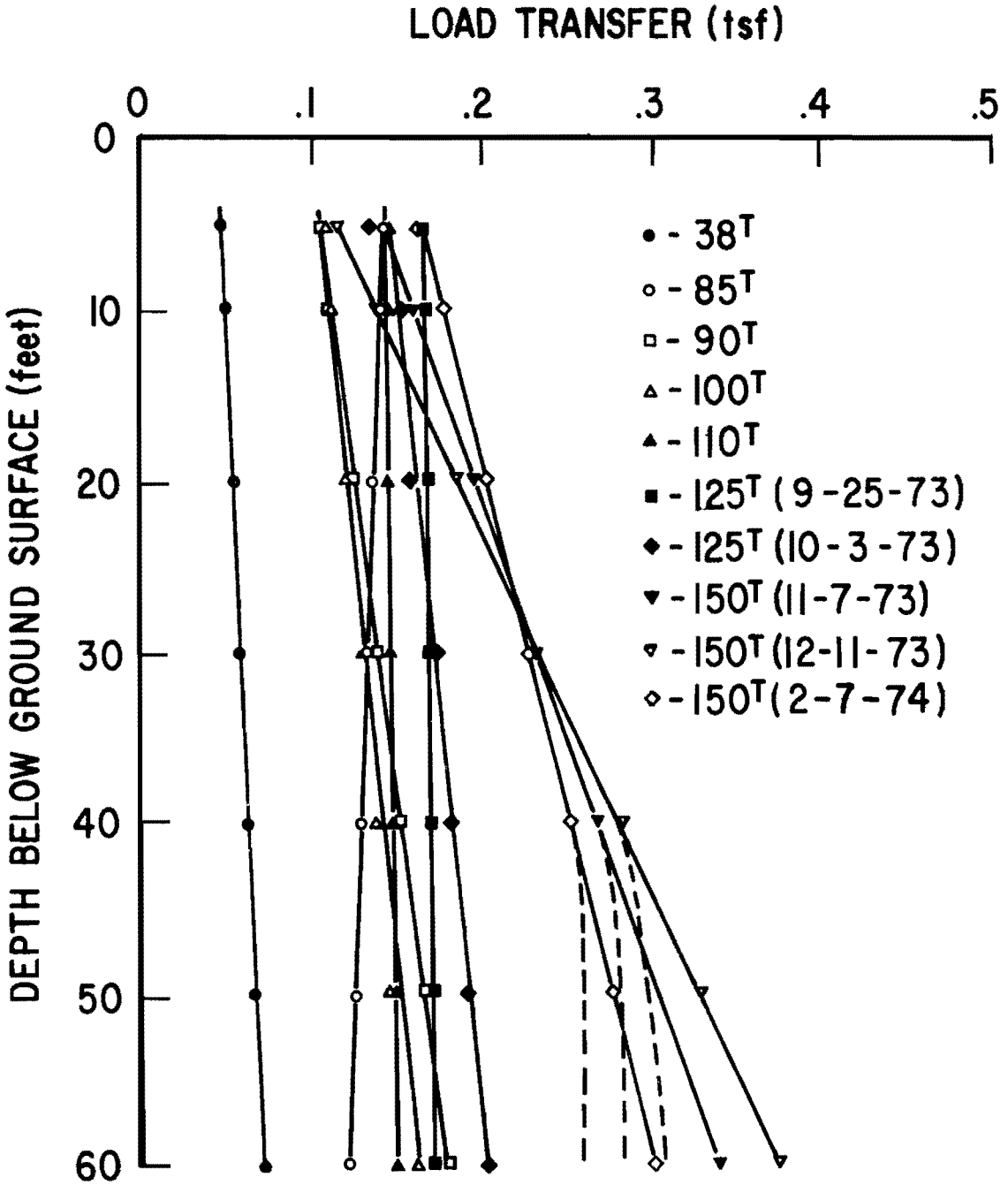


Fig. 6.3 Load Transfer Curves for Various Loads

# CHAPTER VII

# INTERPRETATION OF RESULTS

## Validity

In the analysis of experimental data the magnitude of experimental error must be considered. Much of the data that were taken in the course of this research project are known to possess such errors; furthermore, there were additional difficulties because the design of the experiment, consistent with practical considerations, did not allow all important parameters to be measured with high precision. Therefore, some simplifying assumptions were required before the analyses undertaken in this report could be completed. The primary factors which influence the results of the analysis are the selection of the various moduli of elasticity, and the selection of the strain gage multiplication factors.

One method which was used to check the accuracy of the analysis, in the absence of any externally measured load, was to estimate the weight of concrete above the drilled shaft. The total dead load as estimated by the Texas Highway Department is 414,000 pounds. However, the calculated load from the strain gage output was only 300,000 pounds as of the 7th of February, 1974. This date essentially corresponds to the completion of the structure. The method of analysis, therefore, underestimates the load projected by the Texas Highway Department by about 25%. The relationship between calculated load and time is shown in Fig. 7.1; also, in that figure is shown the estimated Texas Highway Department dead load.

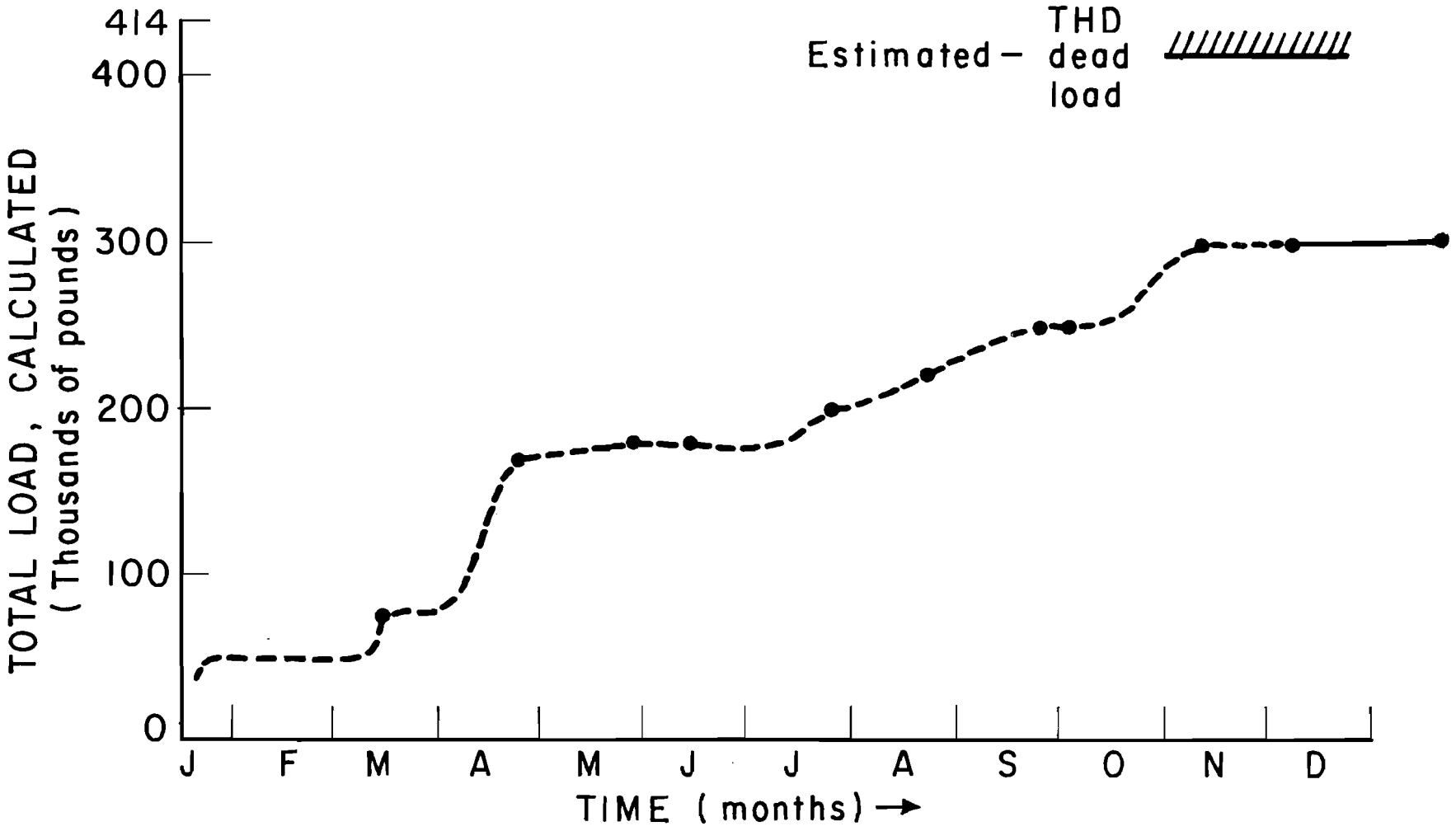


Fig. 7.1 Calculated Load Vs. Time

The significance of the lack of agreement between estimated and calculated loads is questionable. Many things could cause the estimated load of 414,000 pounds to be in error. Alteration of either, or both, of the multiplication factor and the modulus of elasticity could make the calculated value agree with that estimated. While there is no guarantee that the analysis is totally correct, results are presented of the same order of magnitude as engineering estimates and, as will be shown in the following sections, conclusions can be reached about the sustained-load behavior of drilled shafts.

## Implications

A consideration of the relationship between the actual load and the computed capacity is of interest before discussing the implications of the research results. Values of side resistance in the portion of the shaft in clay can be computed using the method proposed by O'Neill and Reese (1970) and the capacity of the tip and the side resistance of the portion of the shaft in sand can be computed using criteria proposed by Touma and Reese (1972). Both of these methods are justifiably conservative and this fact must be kept in mind. For the clay, the capacity of the shaft in side resistance can be expressed as

$$Q_{ss} = \alpha_{avg} \cdot s \cdot A_s \quad \ldots\ldots\ldots\ldots \quad (7.1)$$

where

$\alpha_{avg}$ = reduction factor

s = average shear strength of clay

$A_s$ = peripheral area of the shaft.

For the sustained load test, the length of penetration of the shaft into clay is about 32 feet, while the circumference is 10.99 feet. The average shear strength for that portion of the shaft, as described by Touma, is 0.9 tsf, and the recommended value of $\alpha_{avg}$ is 0.5. From Eq. 7.1, neglecting the top 5 feet as was recommended, the total capacity of the portion of the shaft in clay is 135 tons.

For the sand,

$$Q_{ss} = \alpha\ C \cdot \int_0^H p'\ \tan\ \phi'\ dh \quad . \quad . \quad . \quad . \quad . \quad . \quad . \quad . \quad (7.2)$$

where

$\alpha$ = reduction factor

C = circumference of shaft

p' = effective overburden pressure

$\phi'$ = effective friction angle of sand

H = depth of embedment.

The penetration of the shaft into sand is from a depth of 32 feet to a depth of 62 feet. In calculating the capacity of the sand, the average value for p' tan $\phi'$, as obtained from Touma and Reese (1972), is about

1.7 tsf. Following Touma's recommendations, the average value of $\alpha$ is suggested to be between 0.5 and 0.6. For these caluclations, a conservative value of 0.5 was used. Using the above data, Eq. 7.2 yields a capacity of side resistance in sand of 260 tons. Following Touma's recommendations, the allowable failure stress of the tip of the shaft, assuming a tolerable settlement of one inch, is 12 tsf. For the base area of 9.62 square feet, the capacity of the tip of the shaft is 115 tons. The addition of three components of capacity suggests that the total capacity for the drilled shaft is about 510 tons, or 1020 kips.

The calculations of load based on strain gage output suggest a load of less than one-third of that capacity. It is evident that the actual load of the test shaft is substantially lower than its ultimate capacity. The fact that the load in the shaft is so small will result in small stresses in the concrete, and, therefore, small strains. Small strains result in low strain gage output, and, therefore, difficulties in measuring. Low shaft load will also result in the shear stress in the soil being quite low compared to the shear strength of the soil. This point will be discussed in a later section.

## Settlement Results

Although the installation of the settlement-measuring apparatus was delayed, due to the construction procedures used in completing the test shaft, the system seems to be functioning satisfactorily. The initial set of readings was taken in December, 1973, almost a full year after the installation of the test shaft. This delay in acquisition of

data is not believed to be detrimental to the long-term results of the settlement system, because the bulk of the expected settlement will occur as a function of time due to either load shedding or consolidation. The readings taken two months after the installation of the settlement equipment revealed a settlement of 0.002 feet for the two interior shafts, and 0.001 feet for the two exterior shafts in the test bent. The accuracy of the system is believed to be about 0.005 feet; therefore, these readings correspond to essentially zero settlement during the time period involved. These data do not imply the absence of settlement altogether. Certainly, some settlement occurred during the period before the installation of the settlement measuring devices. The magnitude of this settlement is uncertain, but it is believed that any additional settlement related to time phenomena will be accurately measured.

## Load Distribution Curves

The load distribution curves which were plotted with the aid of the program DARES are shown in Fig. 6.2; each curve is shown individually in Appendix F. Inspection of these curves reveals several apparent findings. It can be seen that the values for load in the shaft show an increase with time until the 7th of November, 1973; thereafter the load remains constant. The increase in load can be accounted for by the actual addition of load to the structure due to construction progress. The construction was essentially completed by the 7th of November, 1973.

For the first several sets of load distribution curves, an almost linear decrease of load versus depth can be noted. This particular

shape of the load distribution curves is probably related to the second-order curve fitting that was employed, but it should be noted that Touma and Reese (1972) reported very similar results for low values of applied load for test shaft G-1.

For all the load distribution curves, the load at the tip of the shaft is exceptionally small. By the 13th of June, 1973, the tip load was still equal to zero. For all the other sets of readings, the tip load is approximately 10 to 15 tons. It should be noted that the tip loads for the last three sets of load distribution curves had to be extrapolated due to erroneous data. These maximum tip loads of only 15 tons suggest an interesting point. Based upon the relationships suggested by Touma and Reese (1972) for tip pressure versus relative settlement for drilled shafts in sand, a load of 15 tons would result in a settlement of only about 0.08 inches. This very small settlement has been partially substantiated by the data produced by the settlement-measuring device, even though the device was not installed at the beginning of the test.

As of the last set of readings, taken on February 7, 1974, there is no evidence of any load shedding taking place. The tip load has been shown to remain quite low throughout the term studied in this report. Had there been load shedding, the tip load would have increased.

There is some question as to how long a period of time is required for a substantial amount of load shedding to occur. Because the load shedding effect is related to creep, and because the effect of creep is most seriously felt soon after the loading sequence is initiated, if load shedding were to occur, some signs of it should have appeared. As

time passes, the creep-prone viscous contact points of the soil will transfer their stress to the frictional contact points which are not prone to large creep deformation. Therefore, if any load shedding were to occur as a result of creep, it seems likely that such an occurrence would be felt soon after the load was applied.

The apparent absence of creep is probably due primarily to the low magnitude of load relative to the capacity of the shaft. Such small service loads result in relatively small stress levels in the soil adjacent to the shaft. The small stress levels have an obvious effect, when viewed in light of the two components of strength. With relatively small stress levels, it is probable that the bulk of the stress will be carried by the frictional component of strength. Because the frictional capacity is probably larger than the actual stress in the soil, the cohesive, or viscous component of strength will transfer its stress to the frictional component before much creep has occurred. This will result in very little perceptible creep, and therefore, little load shedding. This action has been substantiated by the behavior of the shaft as observed to date. While little load shedding is anticipated in the future, based upon the small settlement and small tip loads, the monitoring of field instrumentation should be continued to verify or refute this conjecture.

## Load Transfer Curves

From the load transfer curves shown in Fig. 6.3, it can be seen that the values for load transfer fall mainly between 0.1 and 0.2 tsf. These values tend to increase for the loads of 150 tons. Because the

three loadings of 150 tons all yielded approximately the same load transfer curves, it appears, once again, that load shedding is not present. The values of load transfer will be discussed with relationship to the $\alpha$ factor in the following section.

Unit Load Transfer Values

The unit load transfer values ($s_z$) relate the transferred shear stress to the shear strength of a soil at a given load. The unit load transfer value can be calculated for any load. For the ultimate load, the unit load transfer value becomes equal to the $\alpha$ factor described by Touma and Reese (1972). If $s_z$ is 1.0, the soil is carrying a stress which is equal to its shear strength. The unit load transfer values shown in Table 7.1 were calculated by dividing the load transfer at any depth by the shear strength of the soil at that depth. The shear strength used in these calculations was that projected by Touma and, therefore, is subject to the time phenomena described in previous chapters. The values in Table 7.1 are plotted in Fig. 7.2. These values, for any depth, increase with time because of the accumulation of load.

The values of $s_z$ show a general decrease with depth for any particular load. Similar behavior has been reported for all the short-term load tests carried out by The University of Texas. The decrease in the unit load transfer values with depth is caused partially because the shear strength tends to increase with depth at a faster rate than the load transfer. For the load of 150 tons, however, the values of $s_z$ do not decrease as rapidly as for the 125 ton loading in the upper portion of the shaft.

Table 7.1

Unit Load Transfer Values ($s_z$) for Various Depths and Various Loads

| LOAD | $38^T$ | $85^T$ | $90^T$ | $90^T$ | $100^T$ | $110^T$ | $125^T$ | $125^T$ | $125^T$ | $150^T$ | $150^T$ | $150^T$ |
|---|---|---|---|---|---|---|---|---|---|---|---|---|
| DATE | (3-15) 1973 | (4-28) | (5-29) | (6-13) | (7-26) | (8-22) | (9-25) | (9-26) | (10-3) | (11-7) | (12-11) | (2-7) 1974 |
| 10' | .07 | .20 | .16 | .16 | .16 | .21 | .24 | .22 | .21 | .22 | .20 | .25 |
| 20' | .05 | .14 | .12 | .13 | .12 | .15 | .17 | .16 | .16 | .20 | .19 | .20 |
| 30' | .05 | .11 | .11 | .11 | .10 | .12 | .14 | .13 | .14 | .18 | .19 | .18 |
| 40' | .04 | .09 | .11 | .11 | .10 | .10 | .12 | .13 | .13 | .19 | .20 | .18 |
| 50' | .04 | .07 | .10 | .10 | .09 | .09 | .10 | .11 | .11 | .15* | .15* | .15* |
| 60' | .03 | .06 | .09 | .09 | .08 | .07 | .09 | .09 | .10 | .10* | .10* | .10* |

* Extrapolated values

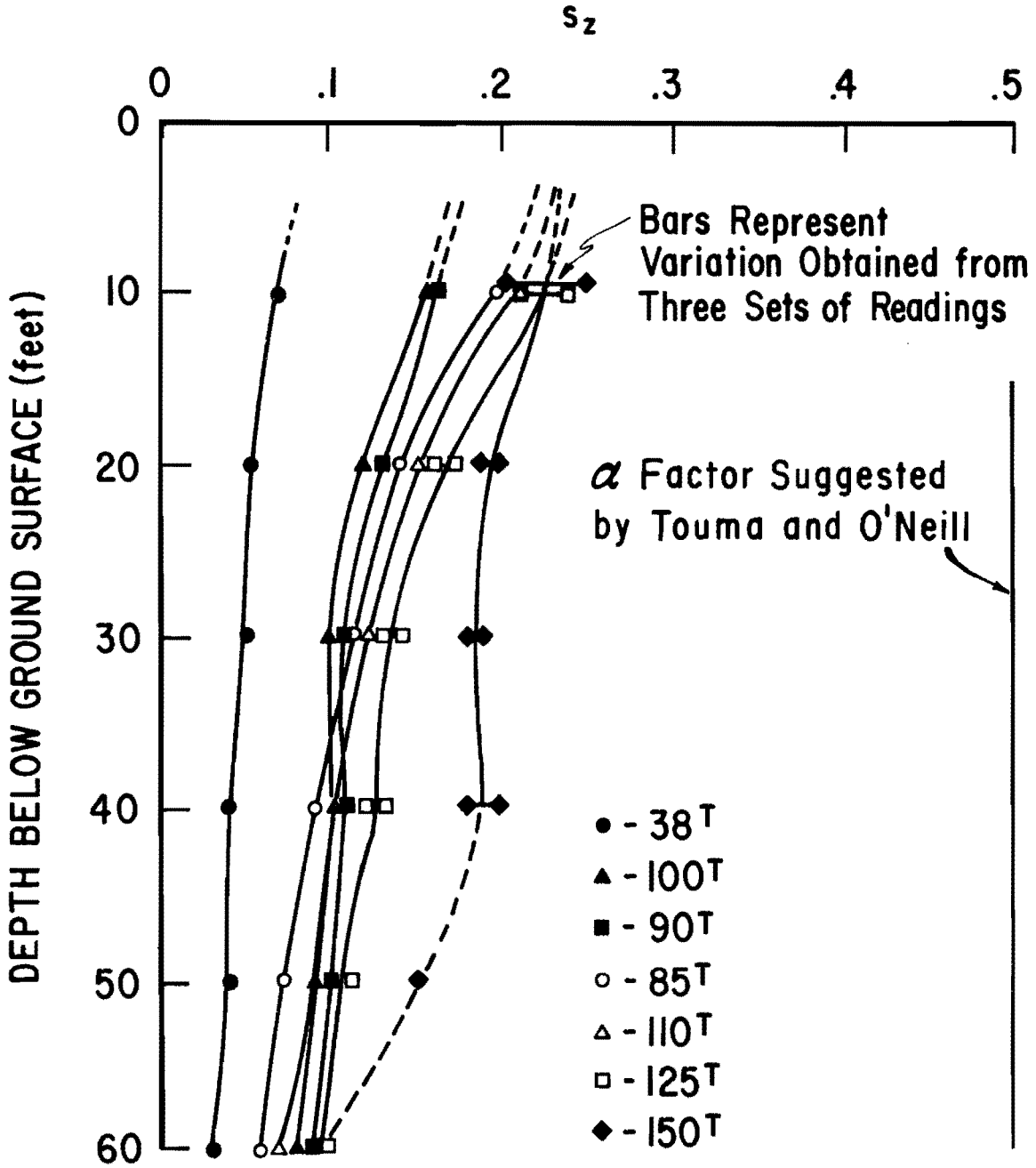


Fig. 7.2 Variation of $s_z$ Factors with Depth for Various Loads

The values do decrease rapidly in the last 20 feet of the shaft. This is depicted in Fig. 7.2.

The change in the behavior of the values of $s_z$ from the 125-ton loading suggests that the soil in the middle portion of the shaft was "stressed up" as a result of the additional 25 tons of load, and not that load shedding was occurring. Had load shedding occurred, the plots of $s_z$ for the three 150-ton loadings would be widely variable. Conversely, the plots for $s_z$ fall very closely together for the three dates of the 150-ton loading. Therefore, it looks as if little load shedding has occurred.

## Concluding Remarks

With regard to the previous discussions presented in this chapter, it appears that little load shedding has occurred in the sustained-load shaft described. This conclusion is based upon the exceptionally small tip loads and the almost imperceptible settlement. Tip loads and settlement can be affected by load shedding and are two prime considerations in the design of a drilled shaft. Because this long-term shaft appears to show no ill effects due to load shedding, and because the $s_z$ values are considerably lower than the $\alpha$ factors suggested by Touma and O'Neill, it can be reasoned that for these soil conditions and for this particular drilled shaft, the design procedure based upon short-term load tests is totally acceptable. Caution should be used, however, when other soil conditions are encountered.

The soil conditions at this site consist of sand overlain by an over-consolidated clay. The action of this shaft in this soil cannot necessarily be extrapolated to a similar shaft in either an under-consolidated clay or an expansive clay. In an under-consolidated clay a drilled shaft may be exposed to negative skin friction. Negative skin friction will result in a phenomenon known as downdrag. Essentially what happens is that the soil adjacent to the shaft settles and exerts a downward force on the shaft. Instead of offering resistance to load, the soil is actually inducing an additional load into the shaft. This condition has serious implications in design.

Another soil in which designs should be made with caution is expansive clay. Expansive clay undergoes large volume changes as the moisture content changes. When exposed to abundant supplies of water, these soils can greatly increase their volume; when completely desiccated, they shrink excessively. When the soil expands it can exert great tensile forces on the shaft, and these tensile forces can have detrimental effects on unreinforced sections of a drilled shaft. When the clay shrinks, as a result of desiccation, the soil may crack and separate from the drilled shaft in the upper portions of the soil-pier interface, resulting in a reduction of the load-carrying ability of the shaft.

Although the long-term test results show no serious defects in the design criteria for the soil conditions tested, care must be taken in the application of the results of this report to other soil conditions.

# CHAPTER VIII

# CONCLUSIONS AND RECOMMENDATIONS

Research of drilled shafts has been carried out by The University of Texas for almost a decade. During that time span significant advances have been made in the understanding of the behavior of drilled shafts in a variety of soil conditions. It is hoped that the results contained in this report will provide a useful complement to the existing knowledge.

Because the actual structure and its loading were incorporated into a full-scale project, information pertaining to the behavior of shafts in actual field conditions has been acquired. This information will be valuable in evaluating present design methods.

## Conclusions

### General Behavior of Shafts

From the literature reviewed in the writing of this report, it became evident that the behavior of a drilled shaft under long-term loading is a complex matter. The slow loading rates and the time-related phenomena of creep and consolidation contribute to the change in shear strength of a soil after a period of sustained loading.

Research has shown that, in the course of loading, a soil can experience excessive creep deformations. These creep deformations can

lead to a phenomenon known as load shedding. Load shedding is the transfer of load to lower regions of the shaft. This condition can result in high tip loads and excessive settlements. It can be concluded from the literature studies that creep and load shedding are realities and can constitute problems under some conditions of loading and soil characteristics.

## Instrumentation

Although some of the data acquisition was complicated by time and by environmental conditions, most of the instrumentation employed in this test project behaved satisfactorily. However, it was concluded that the vibrating wire gage employed in this study does not possess sufficient reliability, sensitivity, or repeatability for the purposes of the experiment.

The Mustran cell did perform satisfactorily. The Mustran cells were simple to read and produced reasonable data; also, the cells appeared to remain stable over an extended period of time.

The settlement-measuring equipment, although simple, provided valuable and accurate data concerning the settlement of the test shaft and the neighboring shafts. By taking settlement data at regular dates, it was concluded that any significant movements of the shaft can be monitored. The accuracy of the system is sufficient for measurement of such movements.

## Houston Long-Term Test Shaft

Although the possibility of load shedding exists for drilled shafts under sustained load, no evidence of load shedding was present for the long-term test shaft. The magnitude of tip load remained very low for the duration of testing, and little settlement was noted. It was concluded that load shedding was substantially absent at this site for the period of the test.

It is believed that the absence of load shedding can be attributed to the relatively low stress levels of the soil. The low stress levels of the soil can be graphically substantiated by the small $\alpha$ factors. If the stress levels were increased, the possibility of load shedding would also be increased. The test, therefore, reveals that the design methods used are satisfactory.

## Recommendations

While it has been discussed that the possibility of load shedding for this shaft seems remote, it is recommended that the monitoring of the instrumentation at the test site be continued. Because the instrumentation has already been installed, the expense of acquiring additional data is relatively small.

Due to the obstacles which a service structure presents to the acquisition of data, it is believed that any future attempt to install a long-term test in a public structure should not be considered. The absence of load calibration and the indefinite magnitude of the applied load present difficulties that are too severe.

The possibility of future long-term load tests, however, should be carefully considered. There is still much knowledge to be gained from additional long-term testing if a controlled testing environment could be attained. A well-organized, long-term load test which was designed solely for research should be successful.

Such a test could consist of a single drilled shaft subjected to a constant load. The diameter of the test shaft should be selected so that stress levels in the soil can be made to approach the failure stress, if desired. A site should be selected with soil of such a character that meaningful laboratory creep studies could be performed. By varying the stress level in such tests a better understanding can be attained as to how the stress level is related to the rate of creep and, therefore, to load shedding in the shaft.

While the test outlined above would be valuable with respect to the problem of load shedding, the problems posed by under-consolidated clays and expansive clays must also be considered. Independent research studies will be required on these topics.

# APPENDIX A

# RESULTS OF SOIL INVESTIGATION PROGRAM

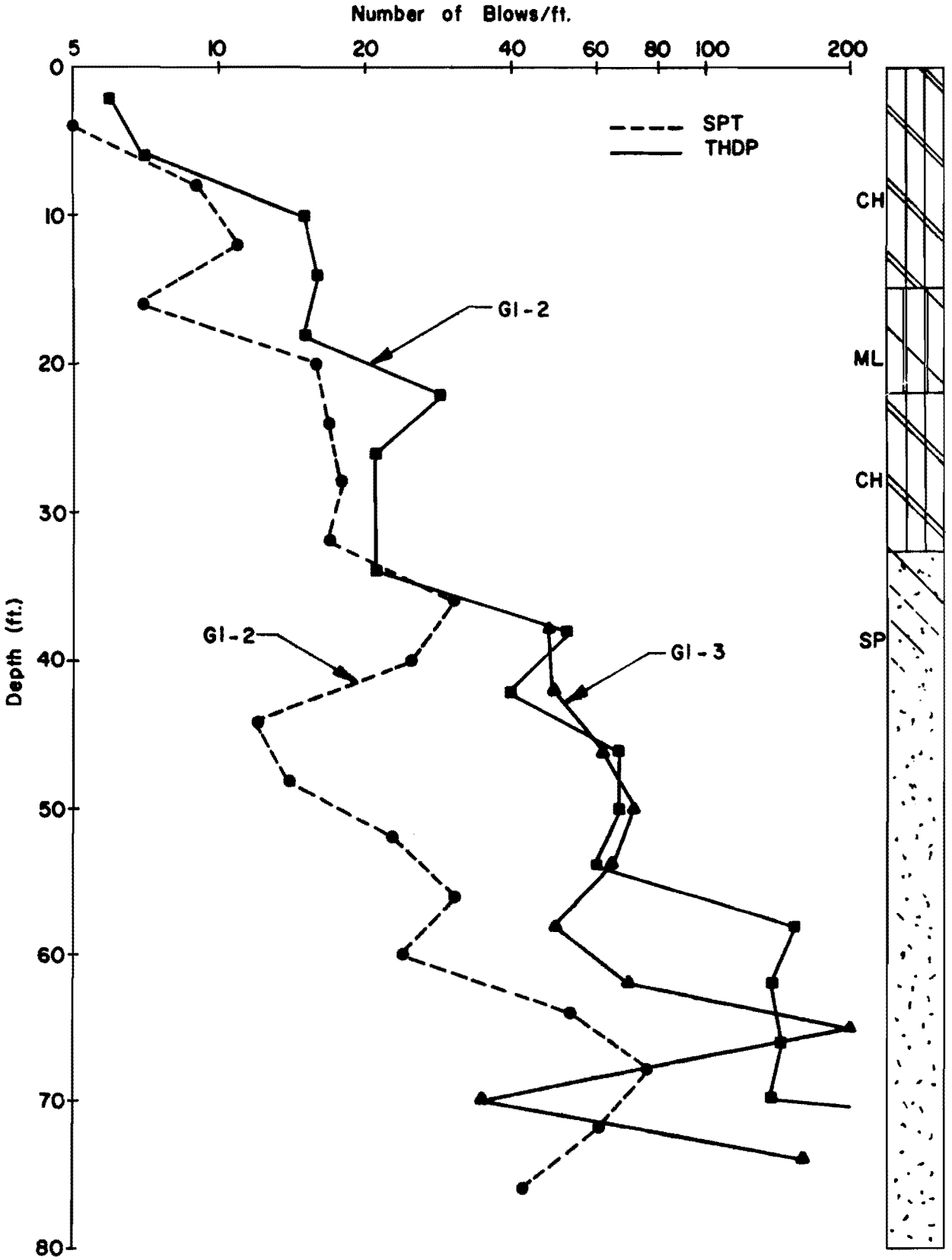


Fig. A1 Dynamic Penetration Tests - G1 Site (after Touma and Reese, 1972)

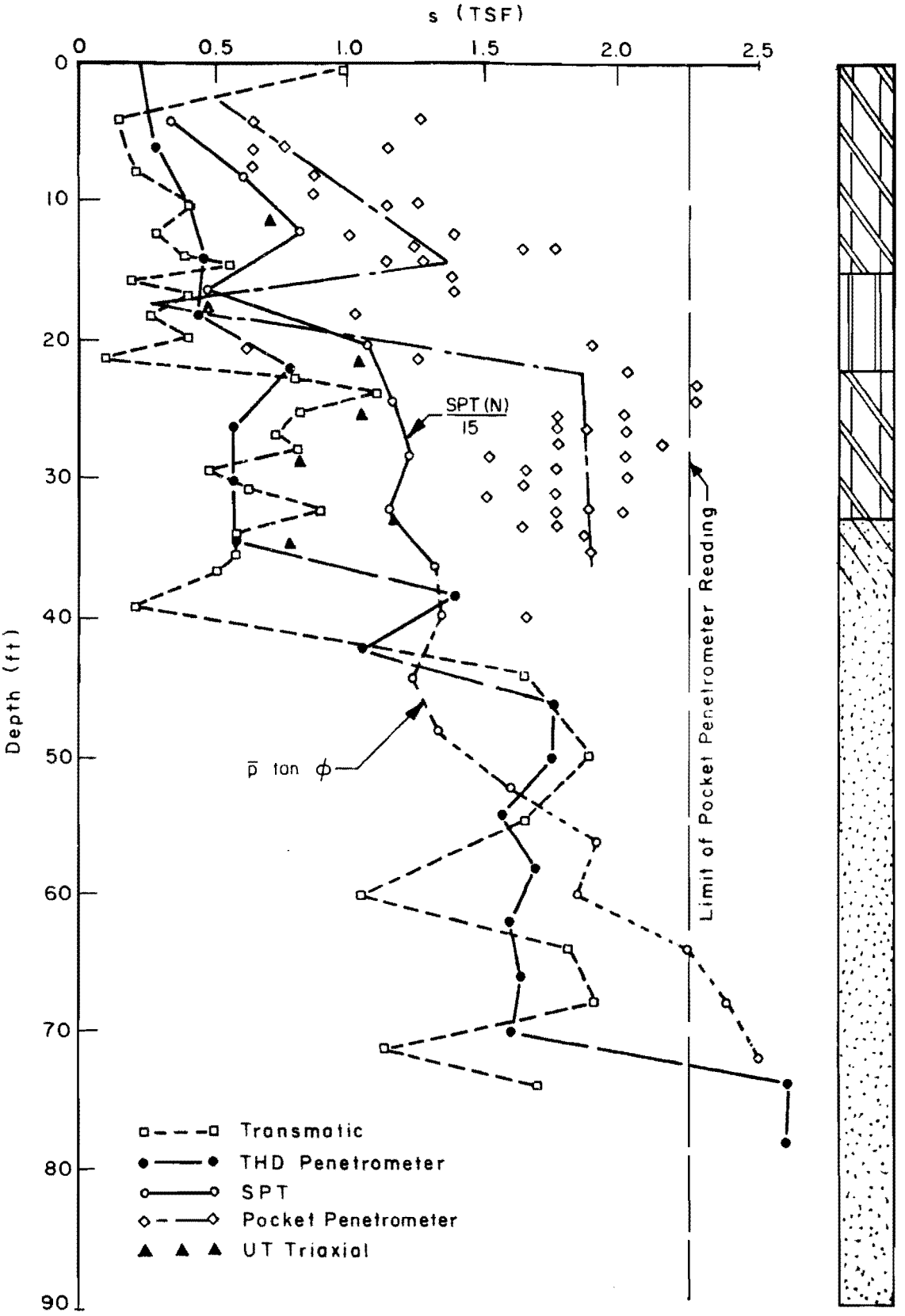


Fig. A2 Shear Strength Profile - G1 Site (after Touma and Reese, 1972)

# APPENDIX B

## CALIBRATION CURVES FOR FOUR SETS OF CREEP LOADING SPRINGS

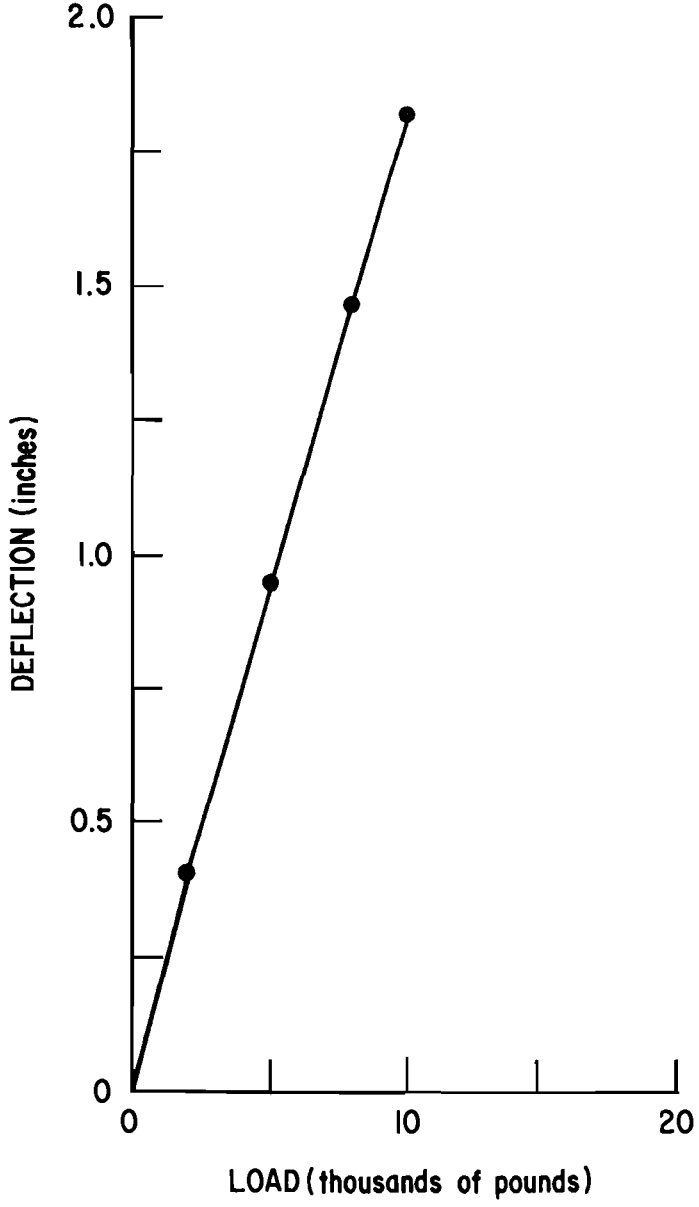


Fig. B1 Calibration Curve for Spring Set No. 1

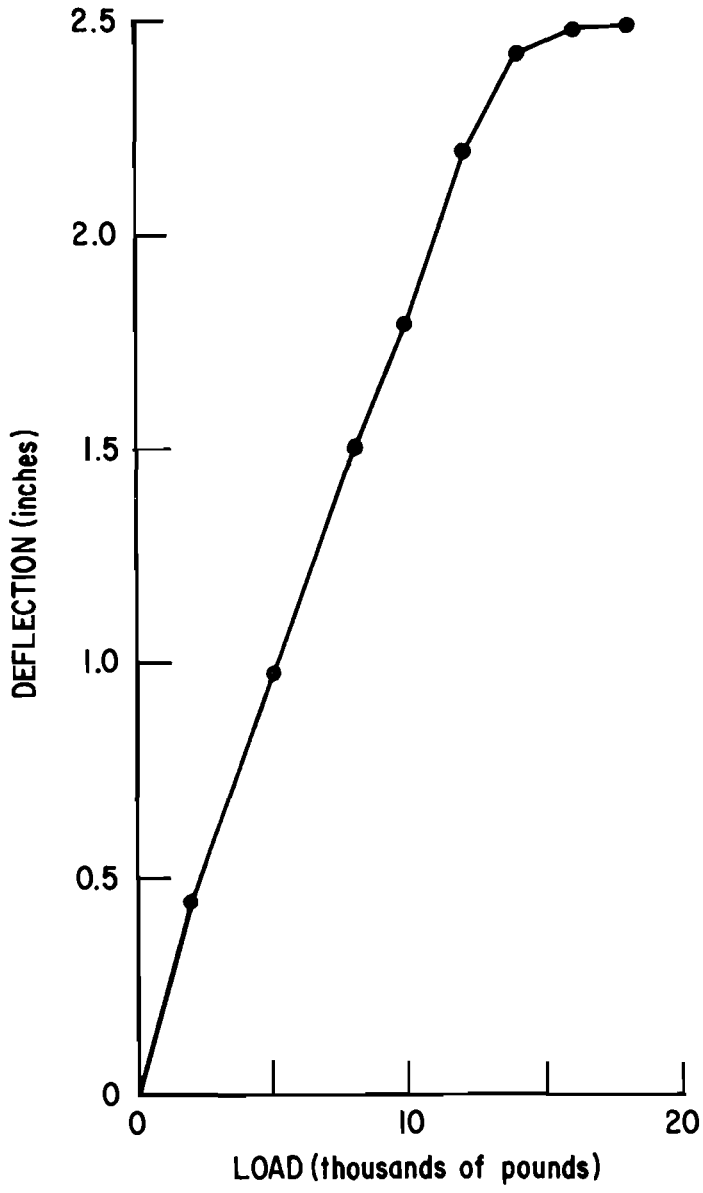


Fig. B2 Calibration Curve for Spring Set No. 2

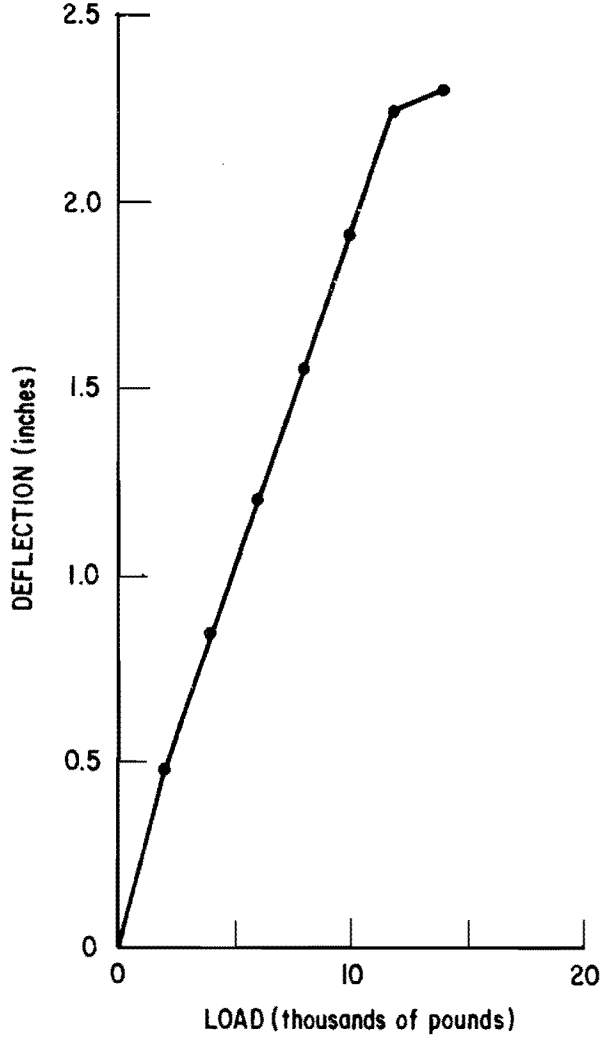


Fig. B3 Calibration Curve for Spring Set No. 3

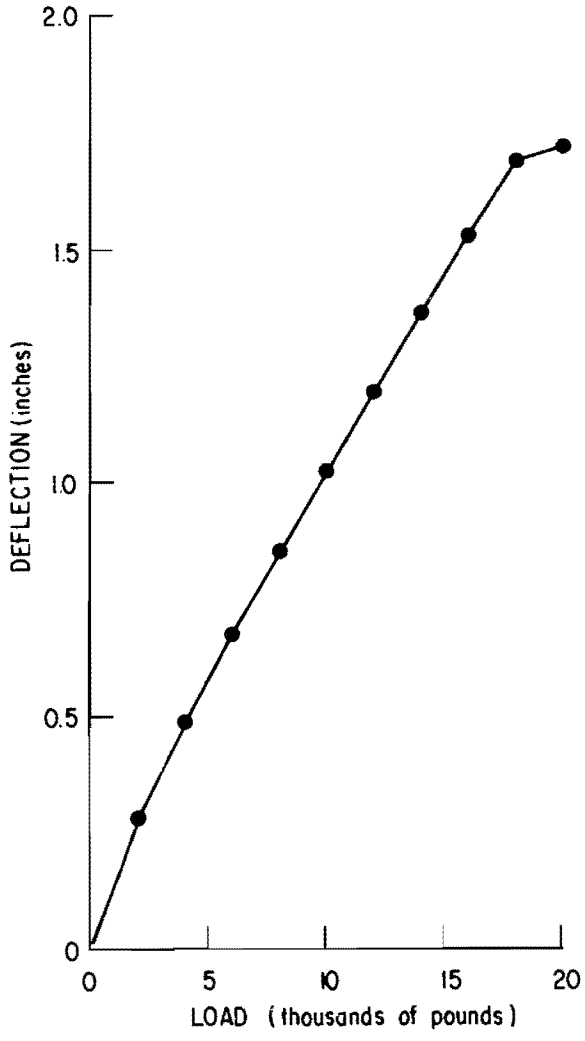


Fig. B4 Calibration Curve for Spring Set No. 4

# APPENDIX C

## CONCRETE STRAIN VS. TIME FOR FOUR CREEP SPECIMENS

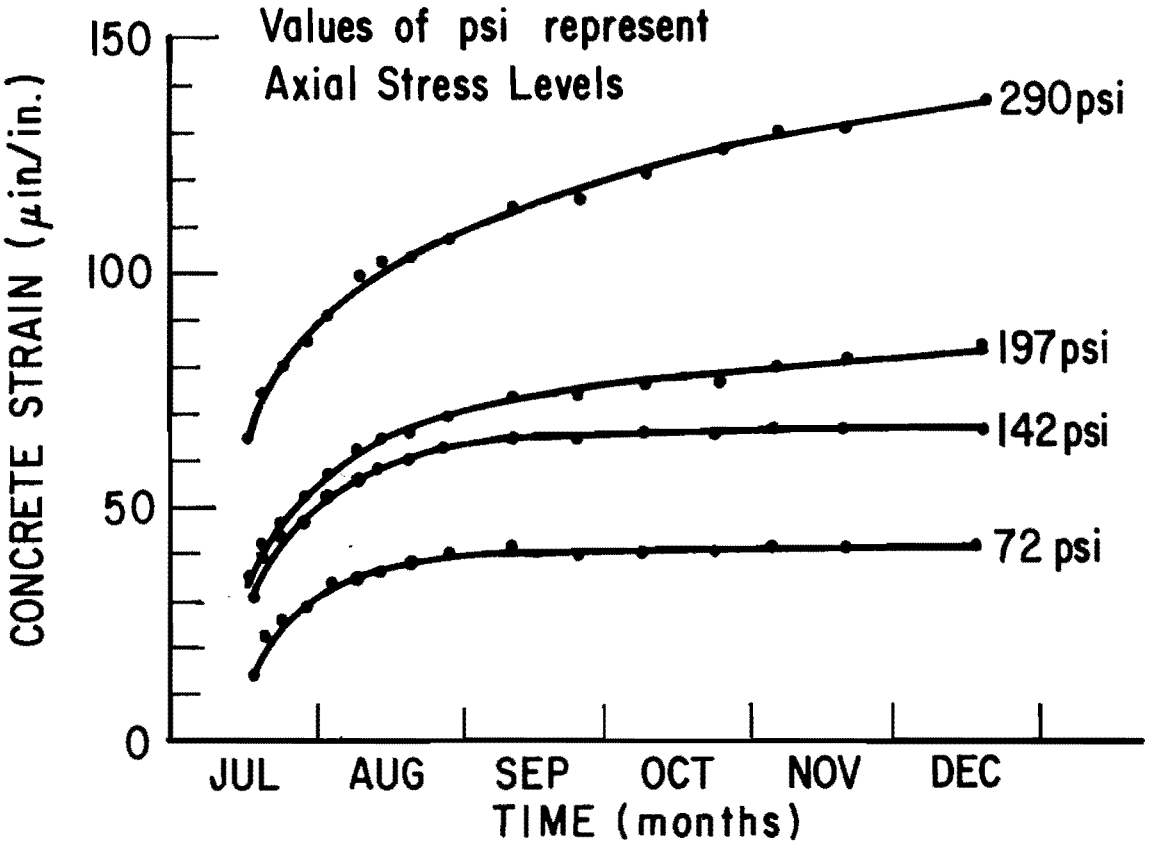


Fig. C1 Concrete Strain Vs. Time for Four Creep Specimens

# APPENDIX D

## VARIATION OF CONCRETE STRAIN VS. TIME FOR MUSTRAN CELLS

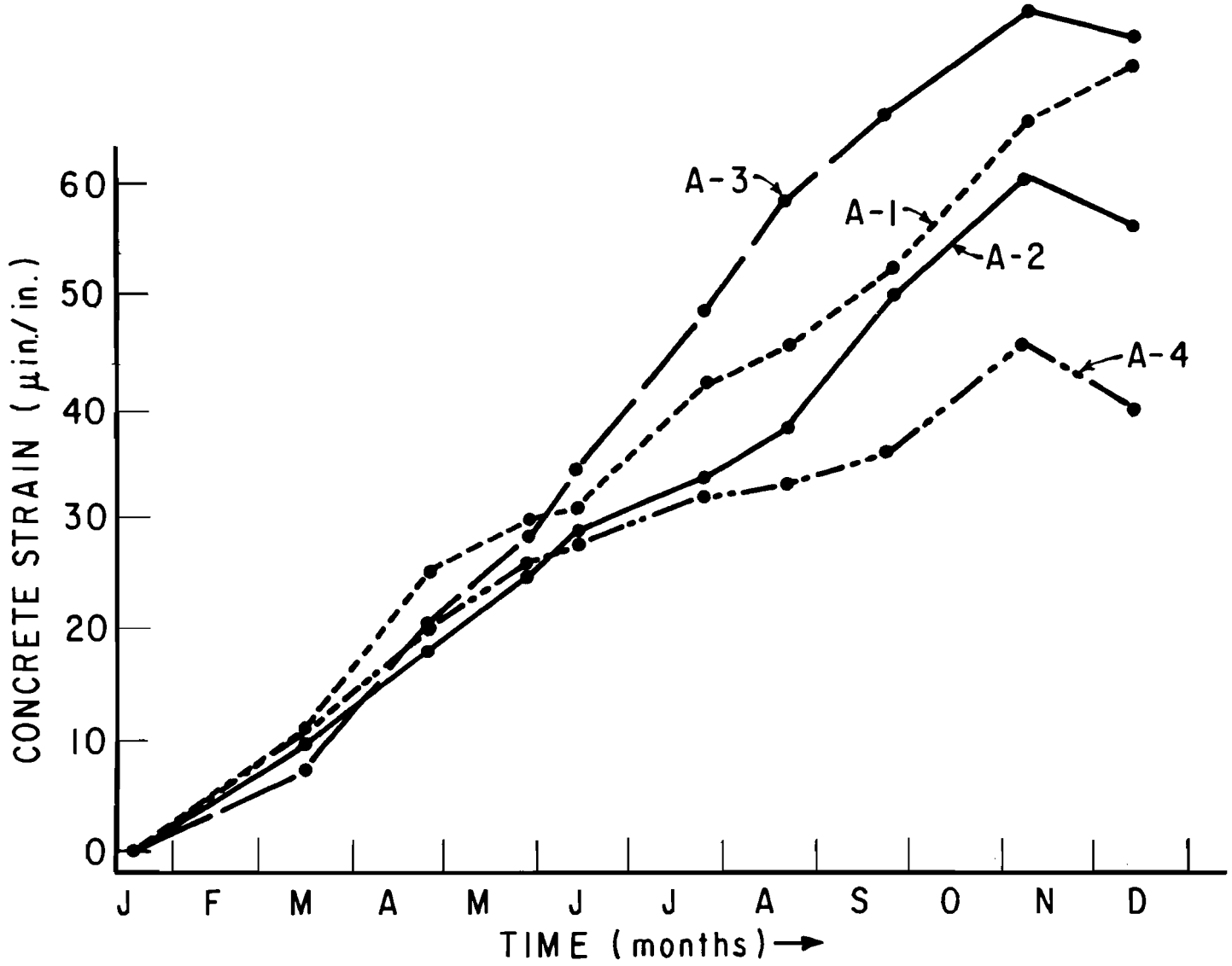


Fig. D1 Concrete Strain Vs. Time for Gages at Level A (3')

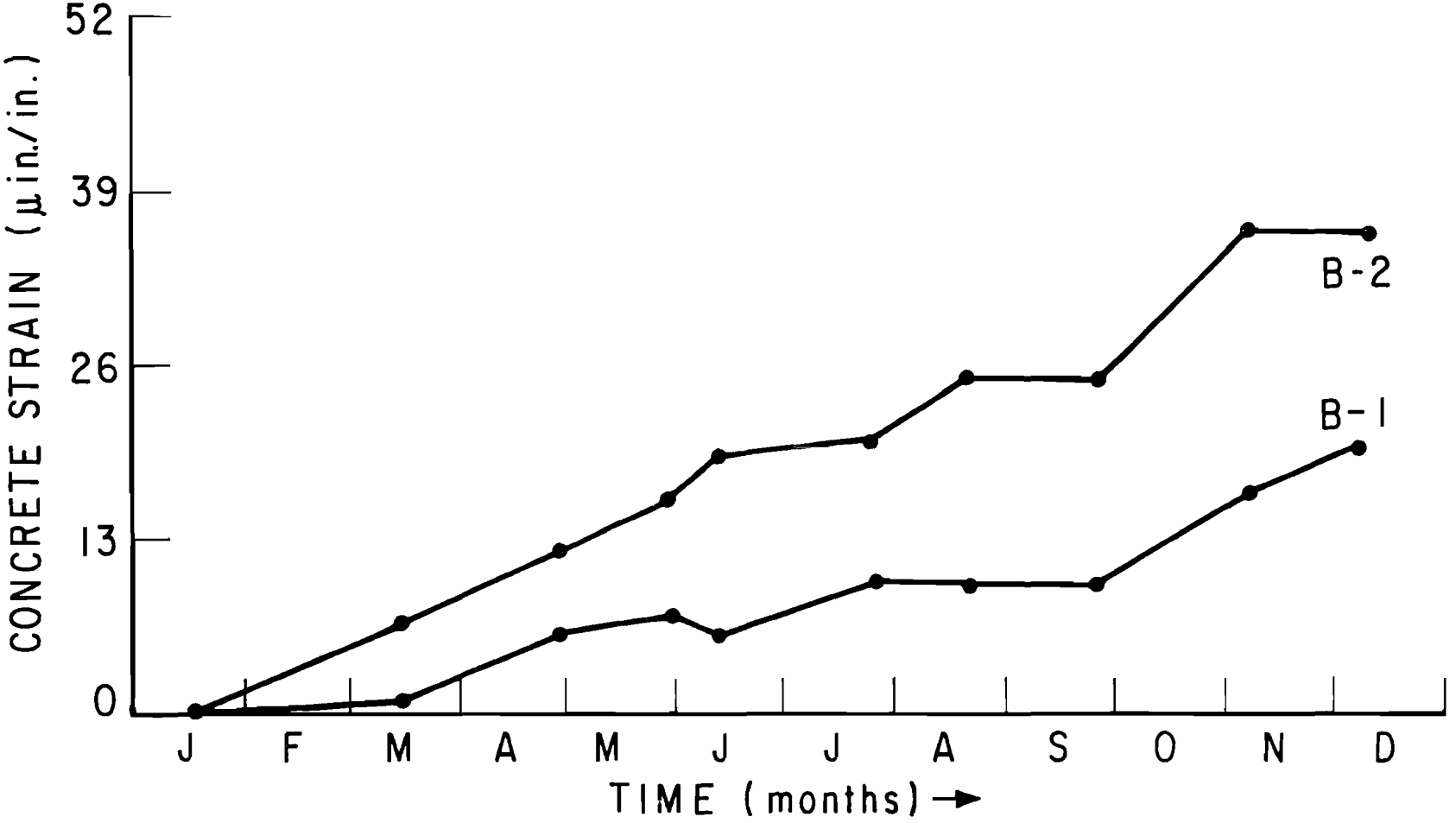


Fig. D2 Concrete Strain Vs. Time for Gages at Level B (5')

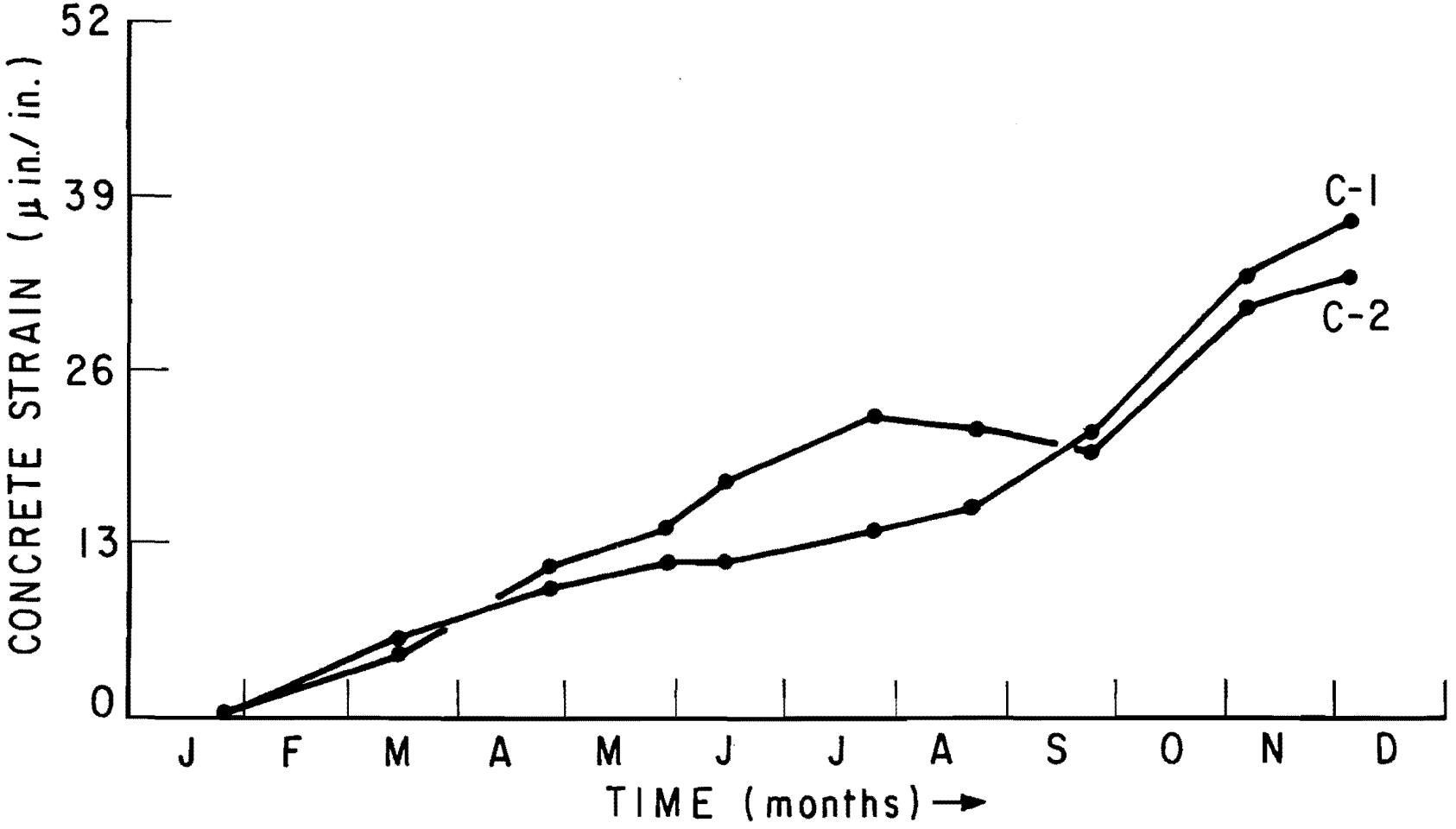


Fig. D3 Concrete Strain Vs. Time for Gages at Level C (11')

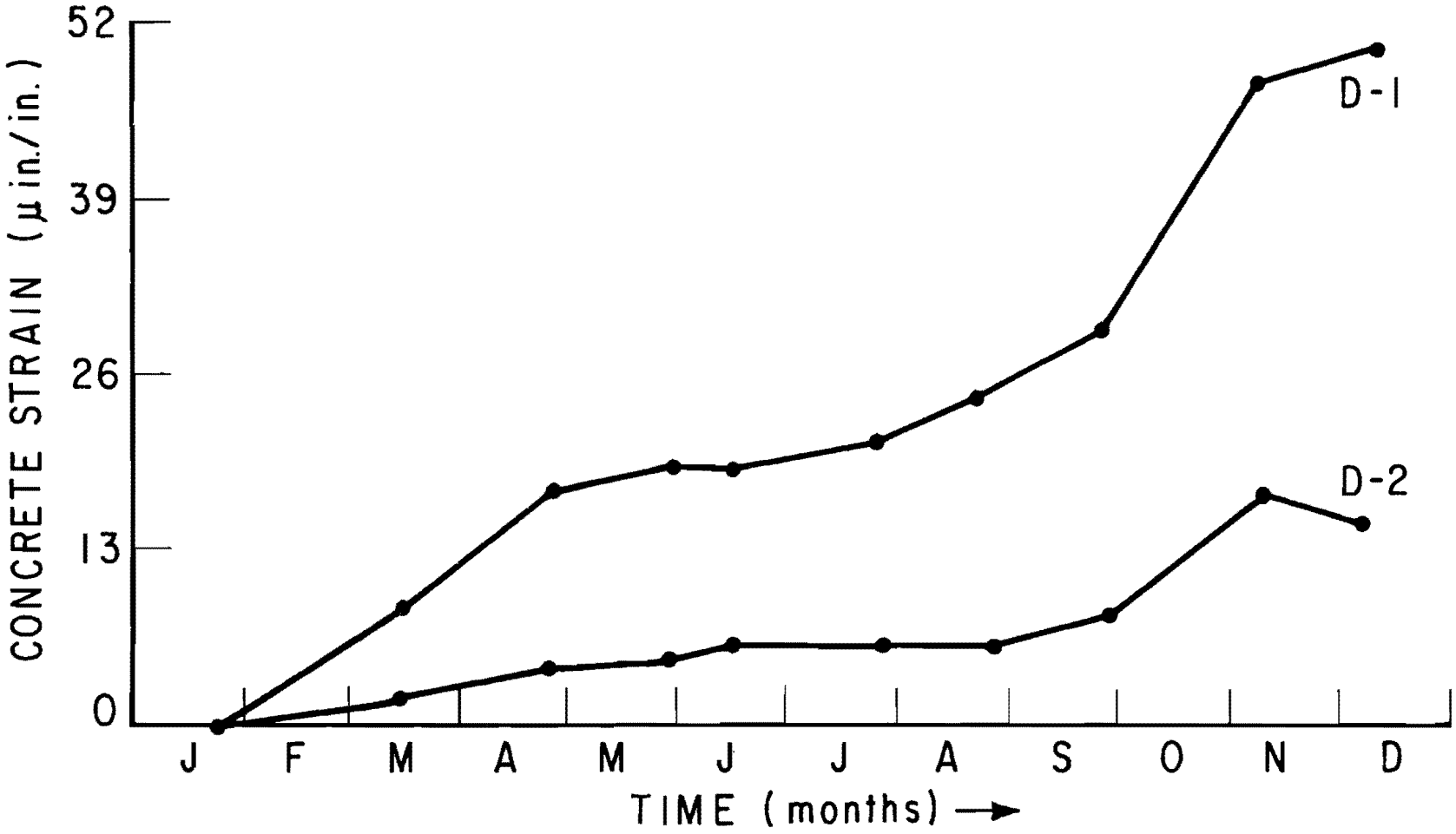


Fig. D4 Concrete Strain Vs. Time for Gages at Level D (17')

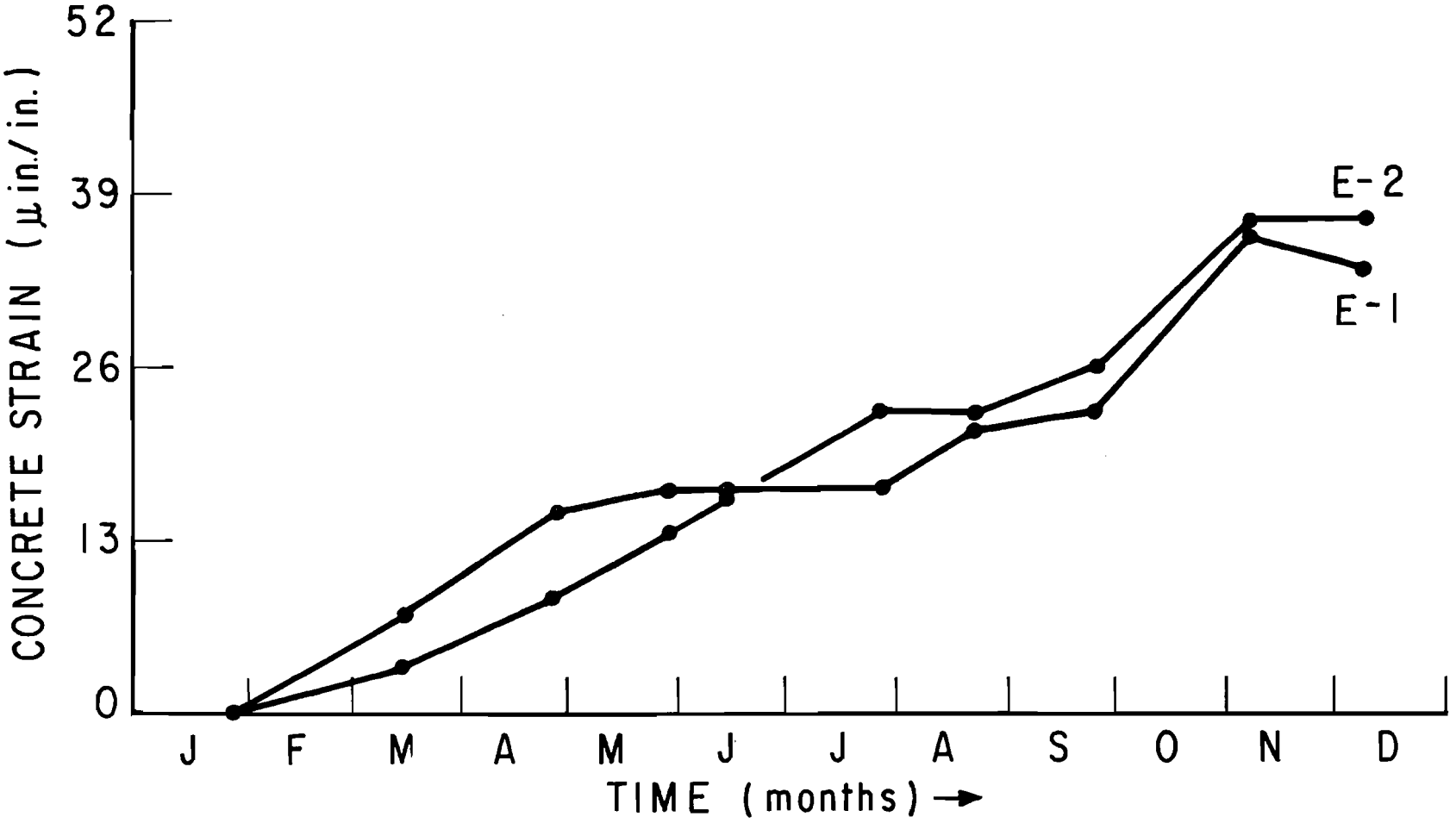


Fig. D5 Concrete Strain Vs. Time for Gages at Level E (23')

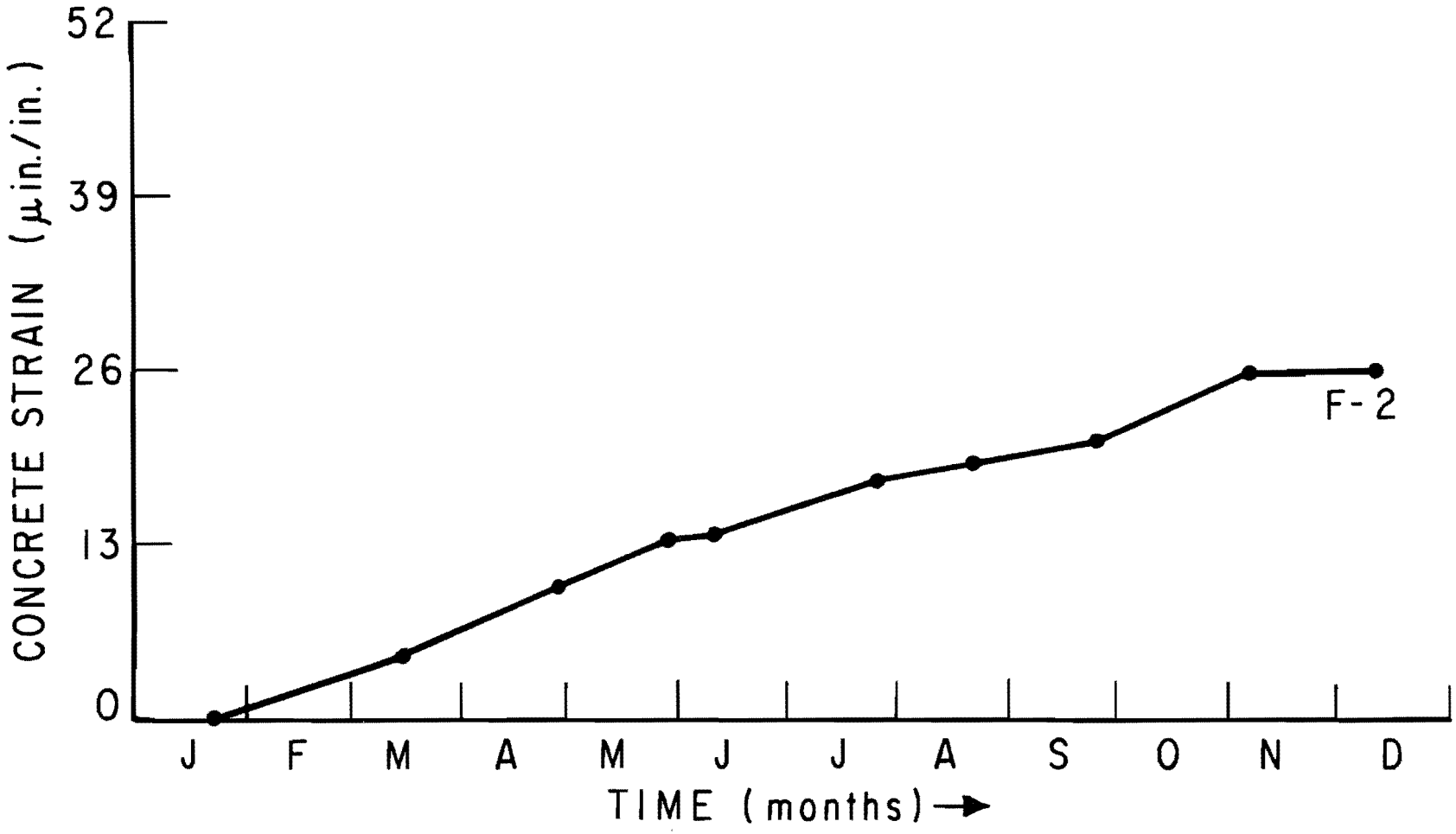


Fig. D6 Concrete Strain Vs. Time for Gages at Level F (29')

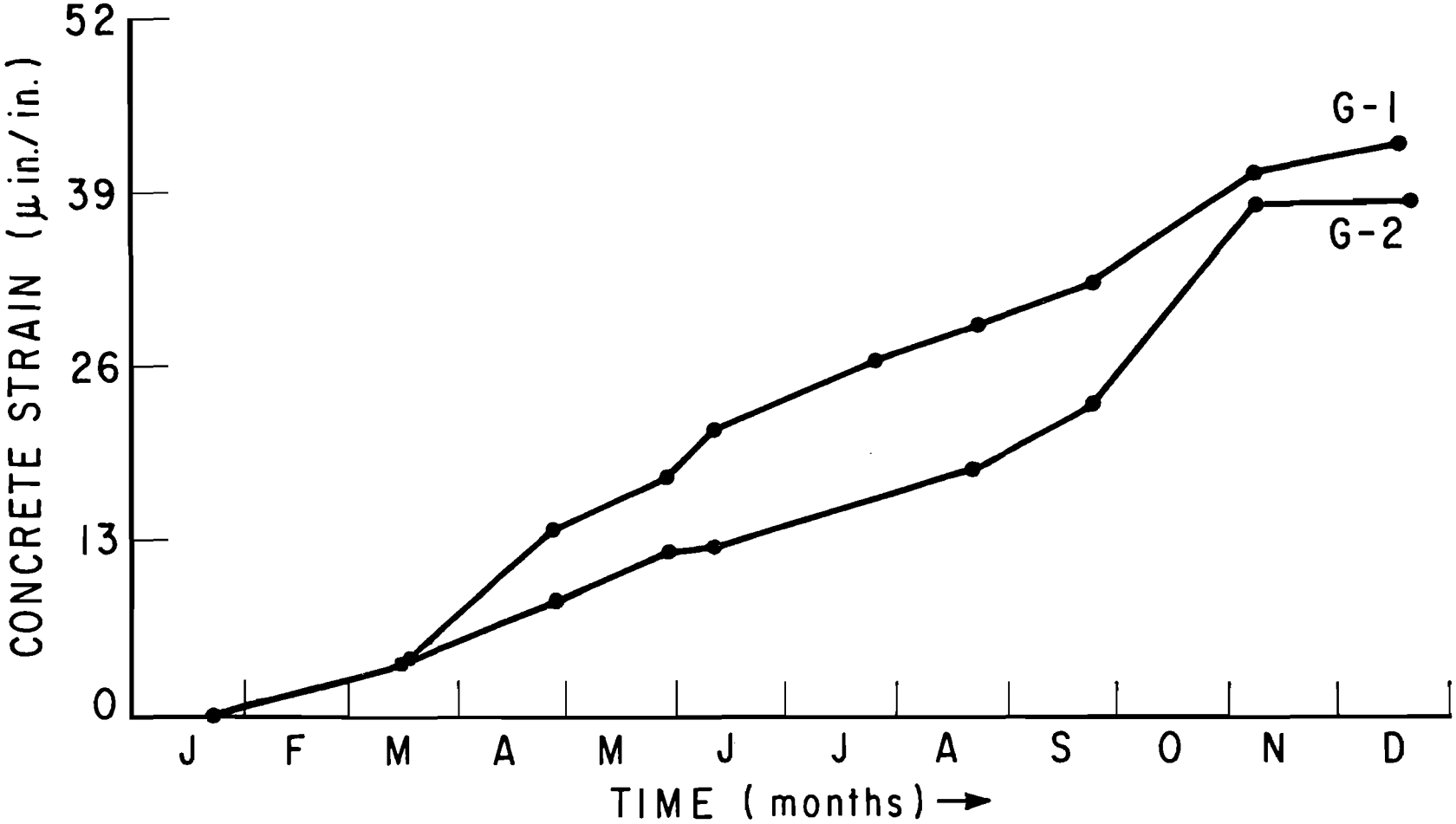


Fig. D7 Concrete Strain Vs. Time for Gage at Level G (32')

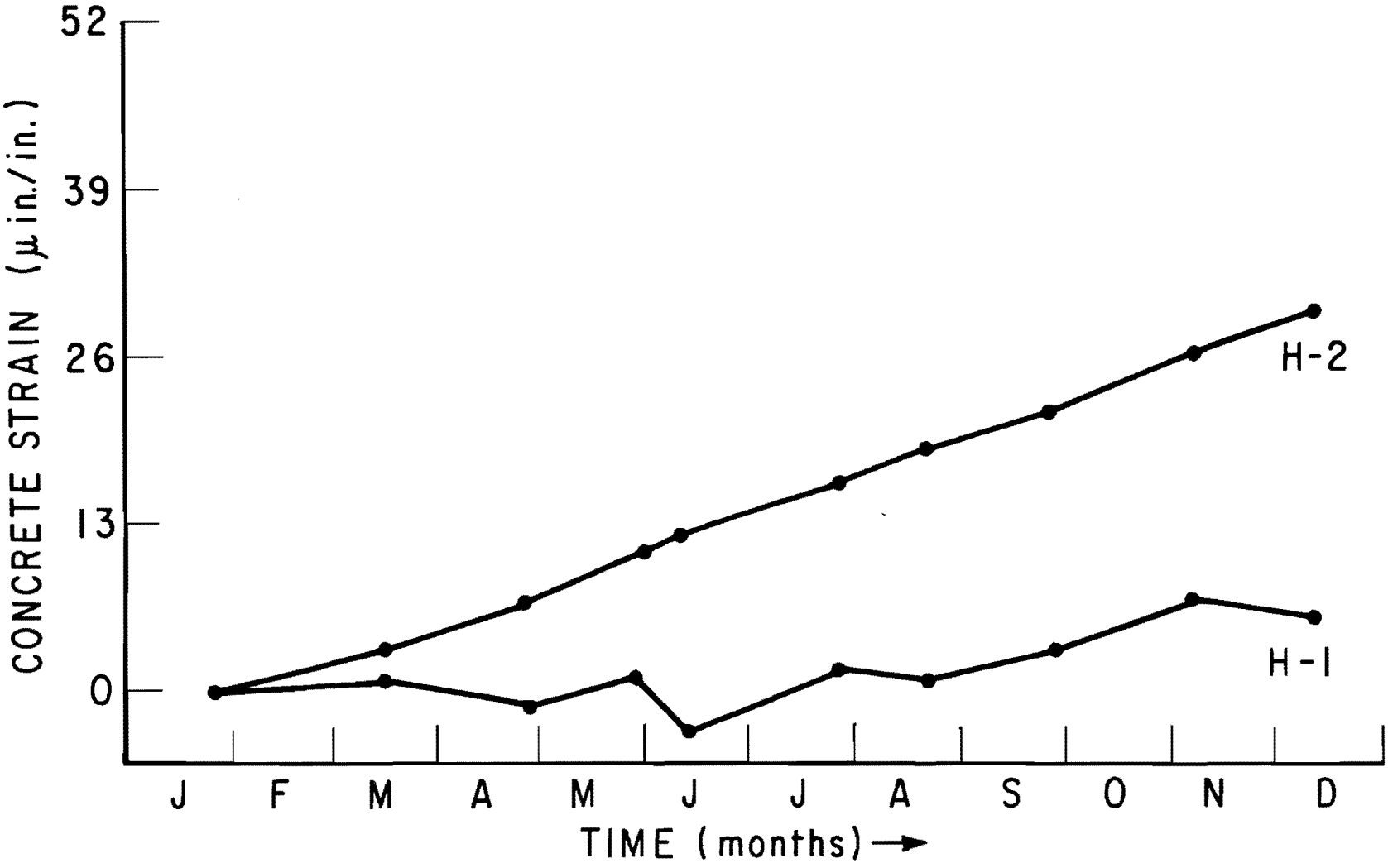


Fig. D8 Concrete Strain Vs. Time for Gages at Level H (41')

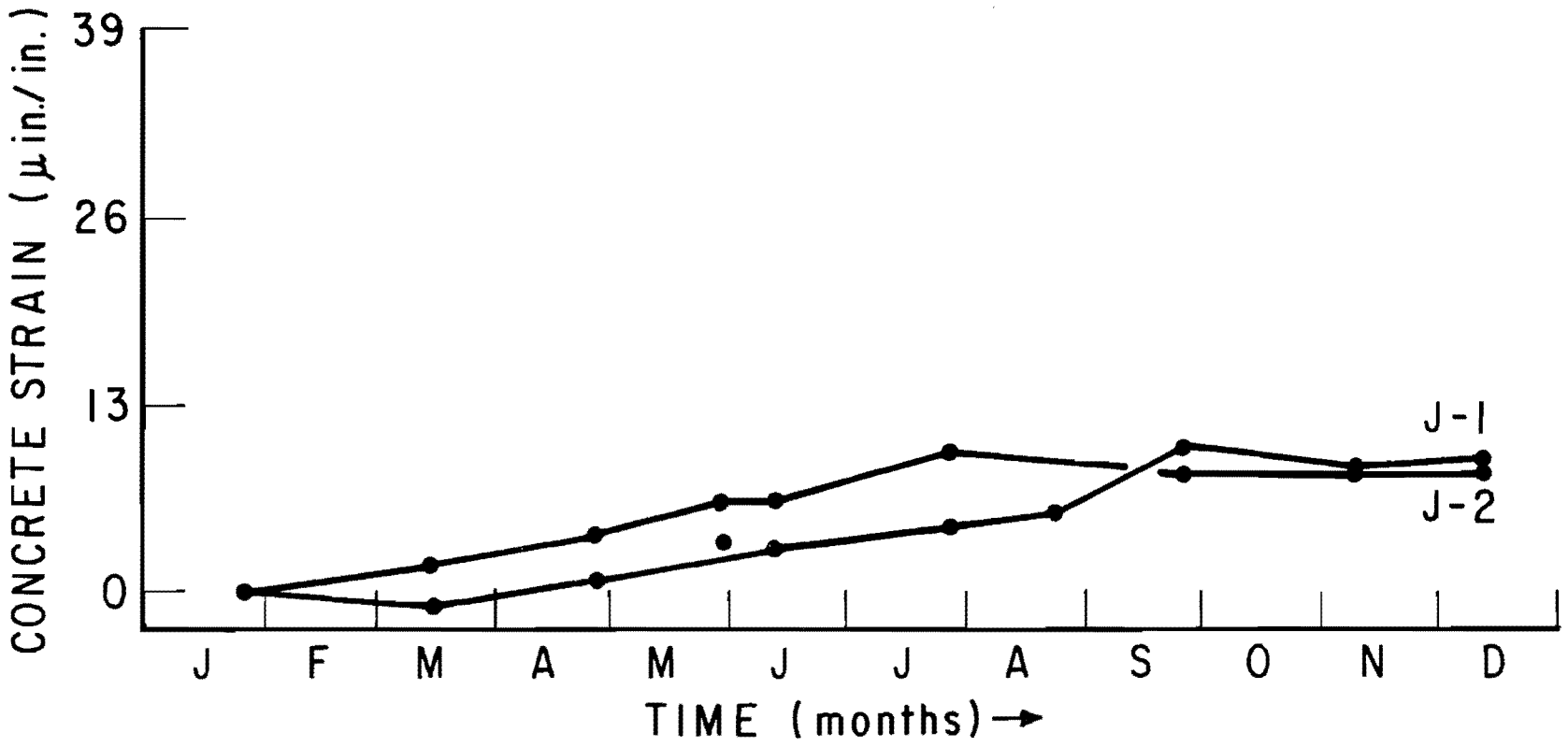


Fig. D9 Concrete Strain Vs. Time for Gages at Level J (47')

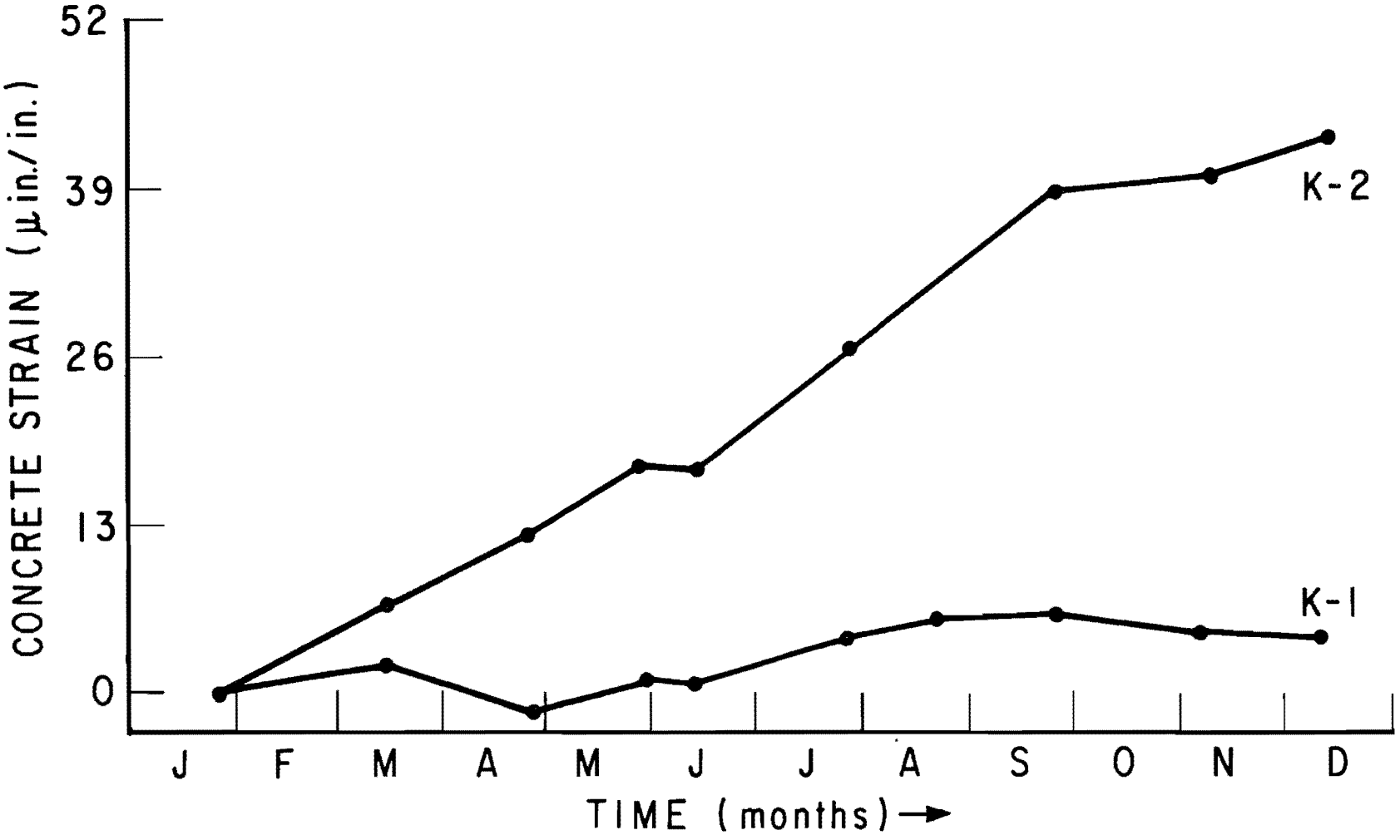


Fig. D10 Concrete Strain Vs. Time for Gages at Level K (53')

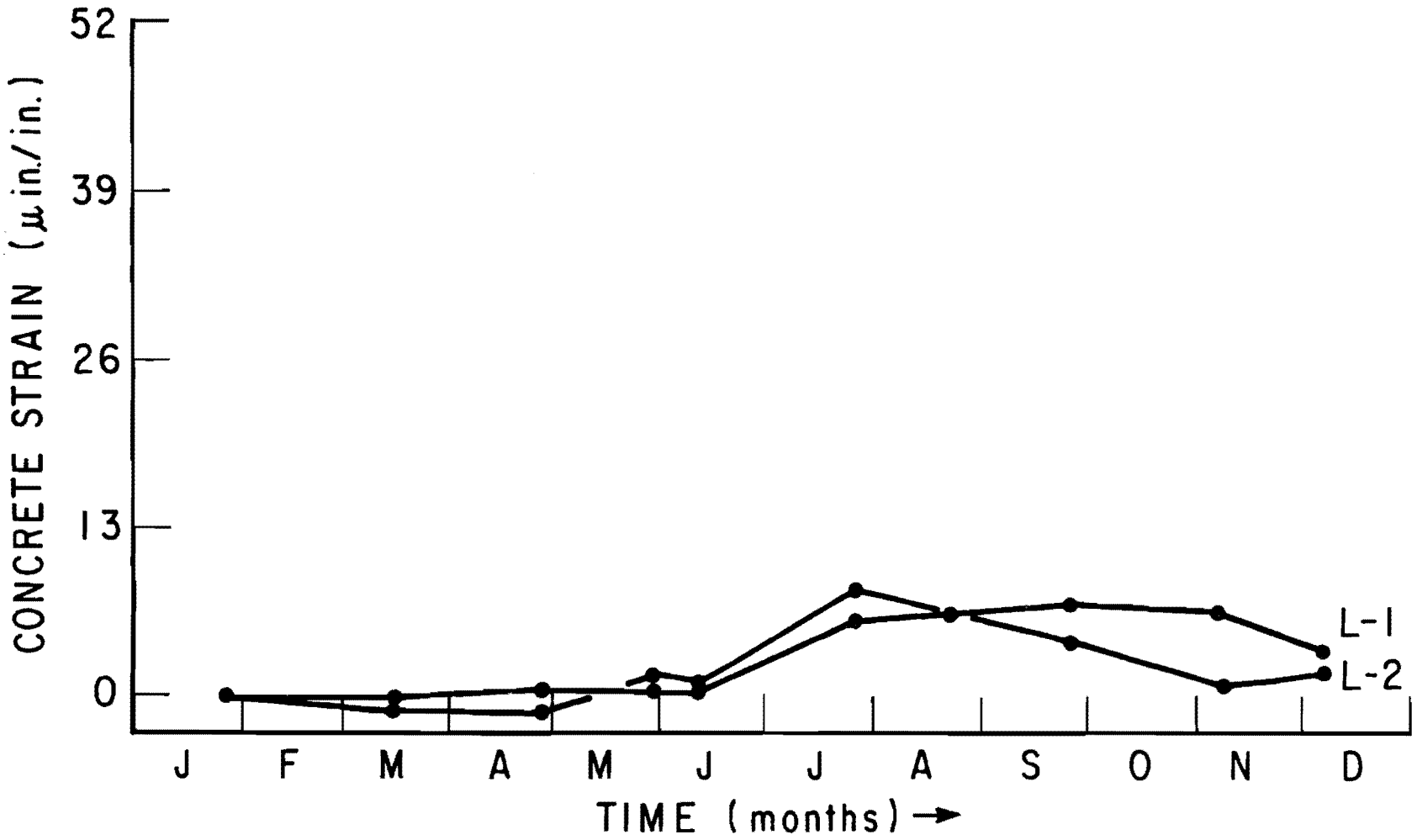


Fig. D11 Concrete Strain Vs. Time for Gages at Level L (57')

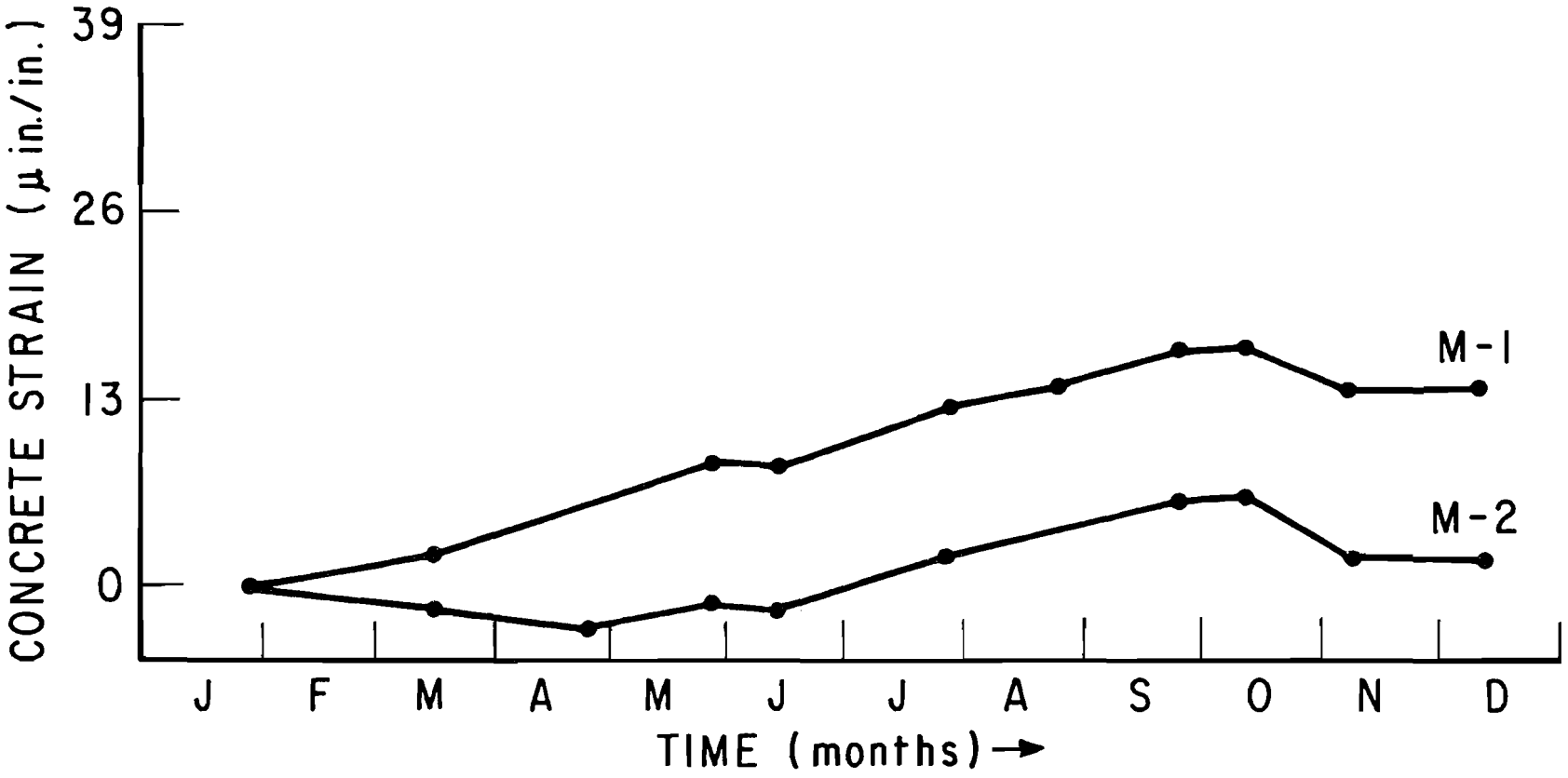


Fig. D12 Concrete Strain Vs. Time for Gages at Level M (61')

# APPENDIX E

## CIRCUIT STRAIN VARIATIONS OVER A 40 HOUR PERIOD FOR MUSTRAN CELLS

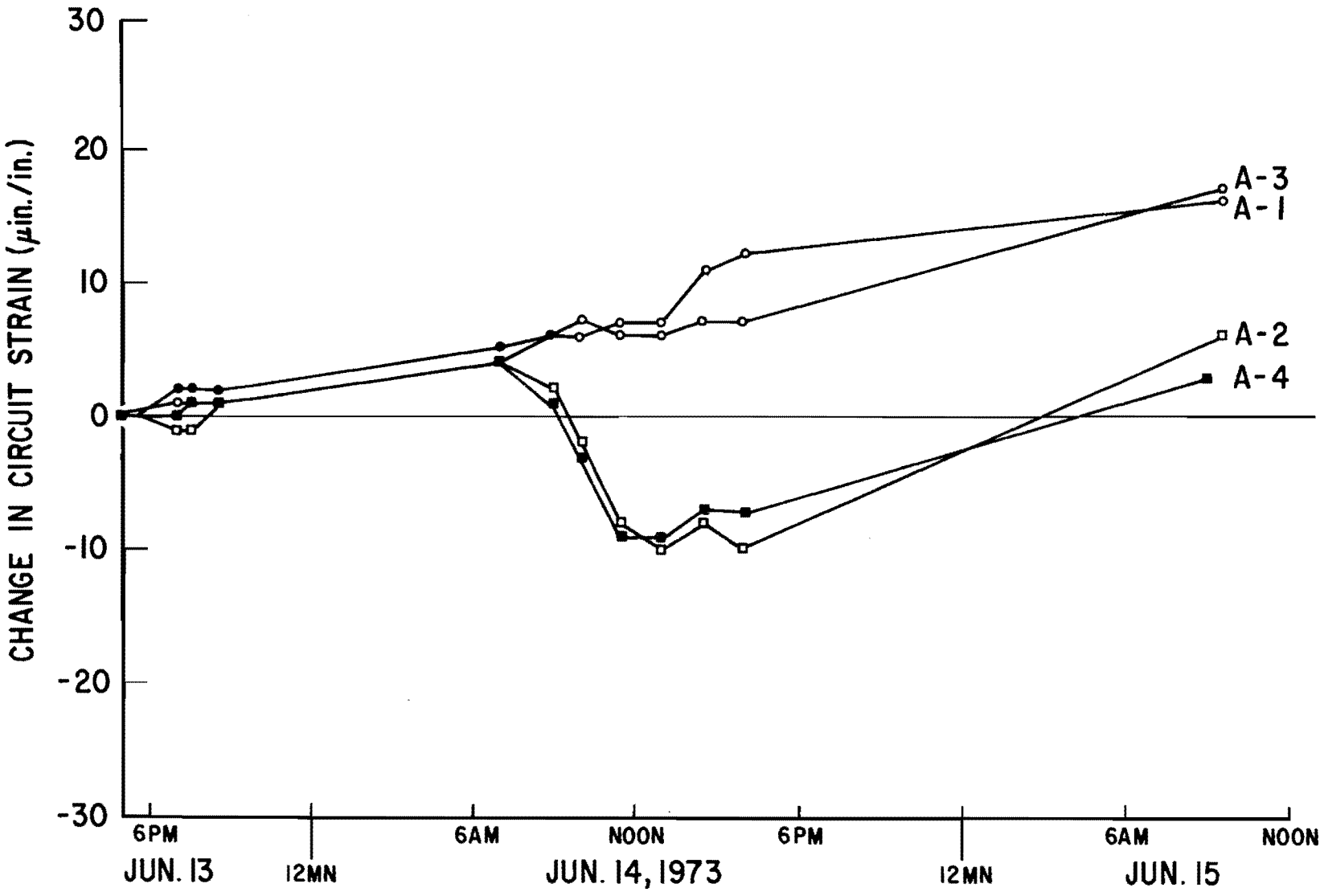


Fig. E1 Variation of Circuit Strain for Gages at Level A (3') Over a 40 Hour Period

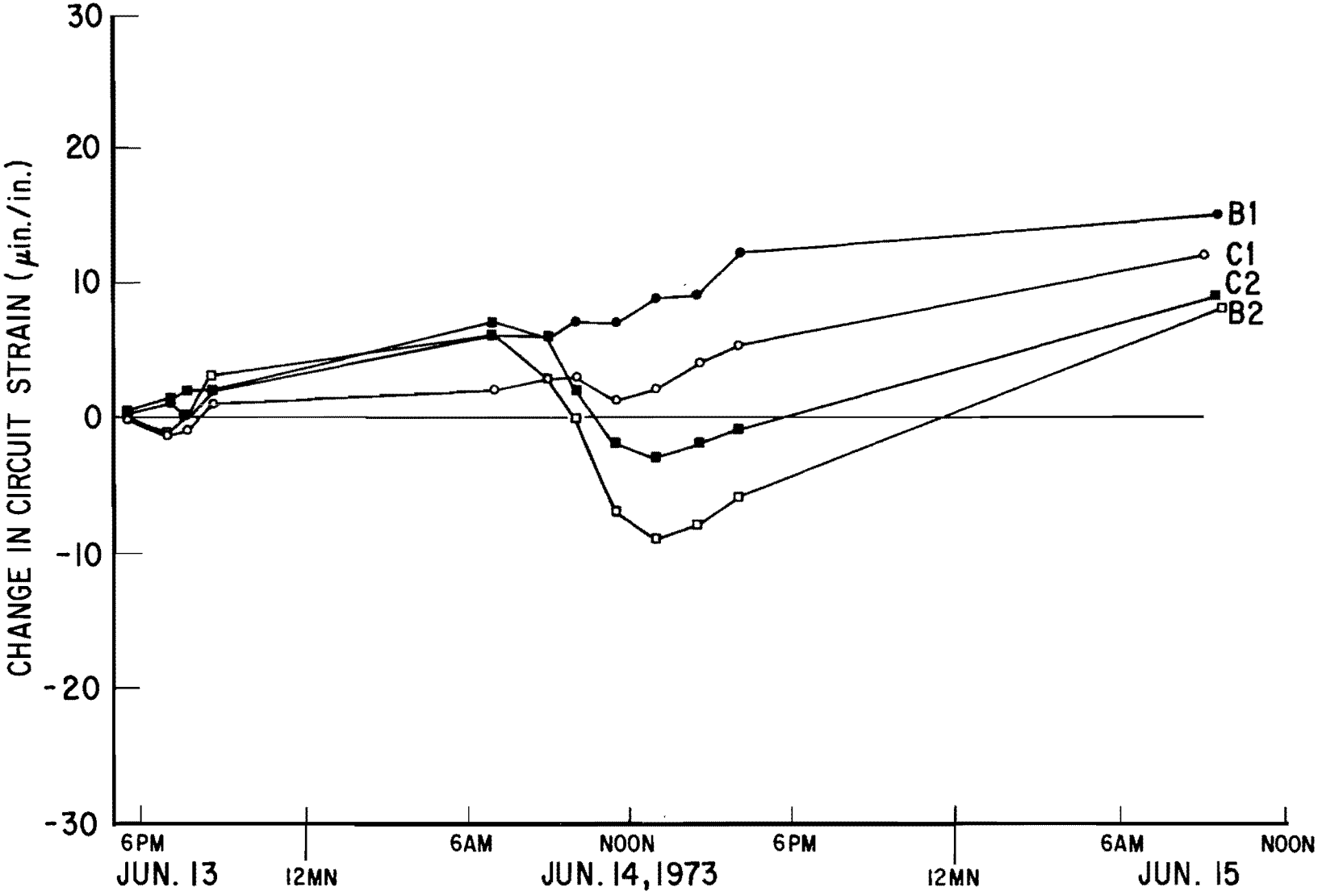


Fig. E2 Variation of Circuit Strain for Gages at Levels B (5') and C (11') Over a 40 Hour Period

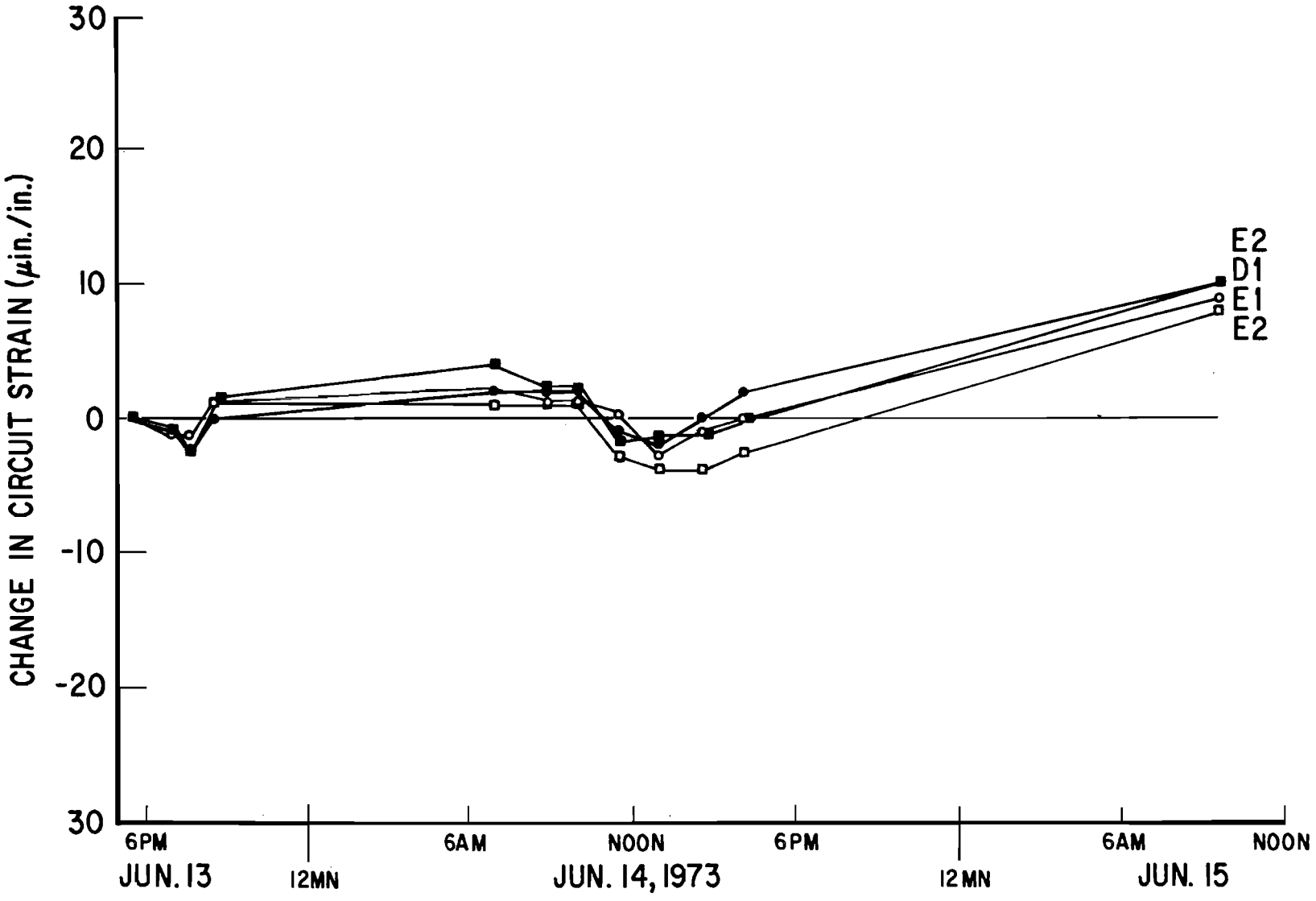


Fig. E3 Variation of Circuit Strain for Gages at Levels D (17') and E (23') Over a 40 Hour Period

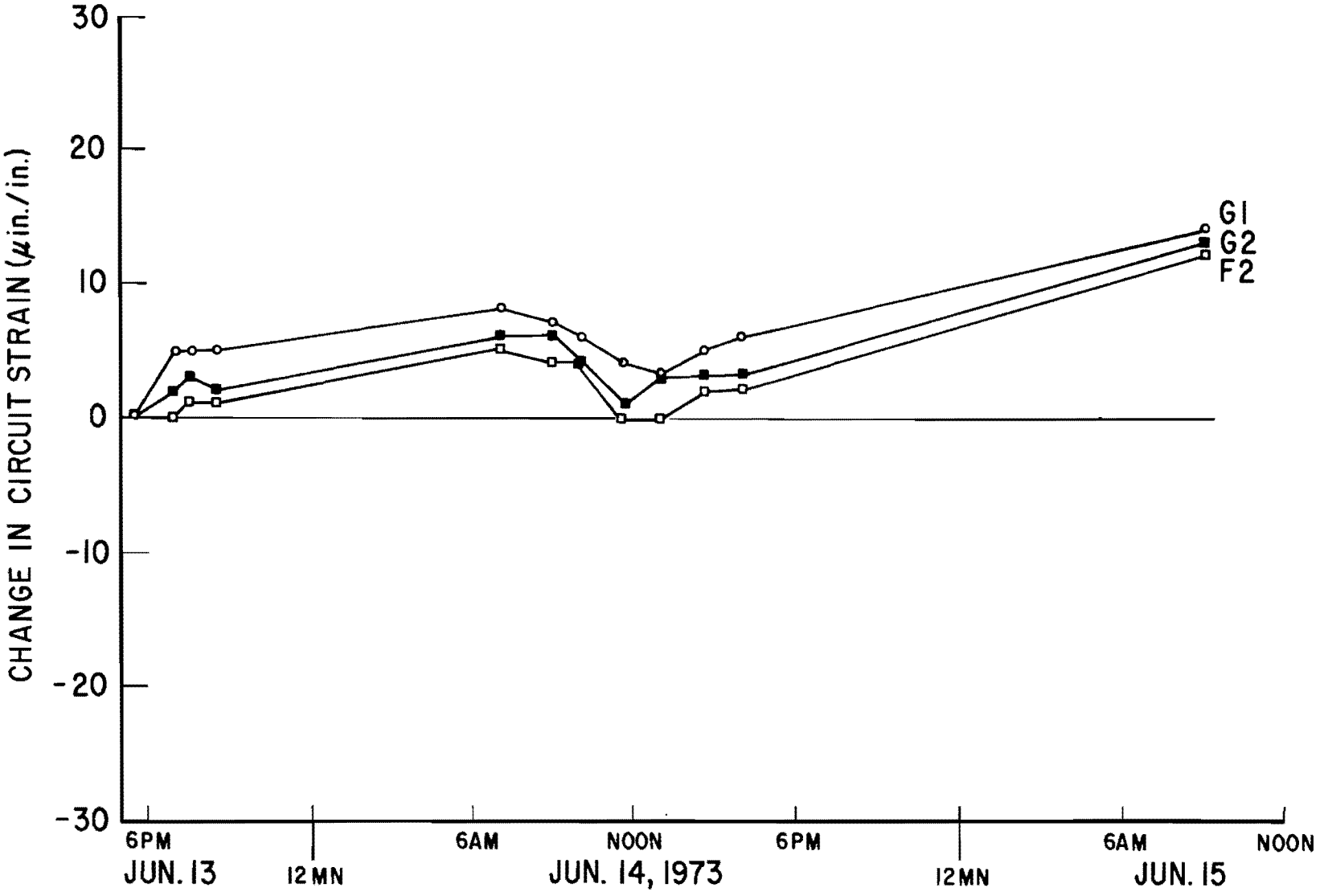


Fig. E4 Variation of Circuit Strain for Gages at Levels F (29') and G (32') Over a 40 Hour Period

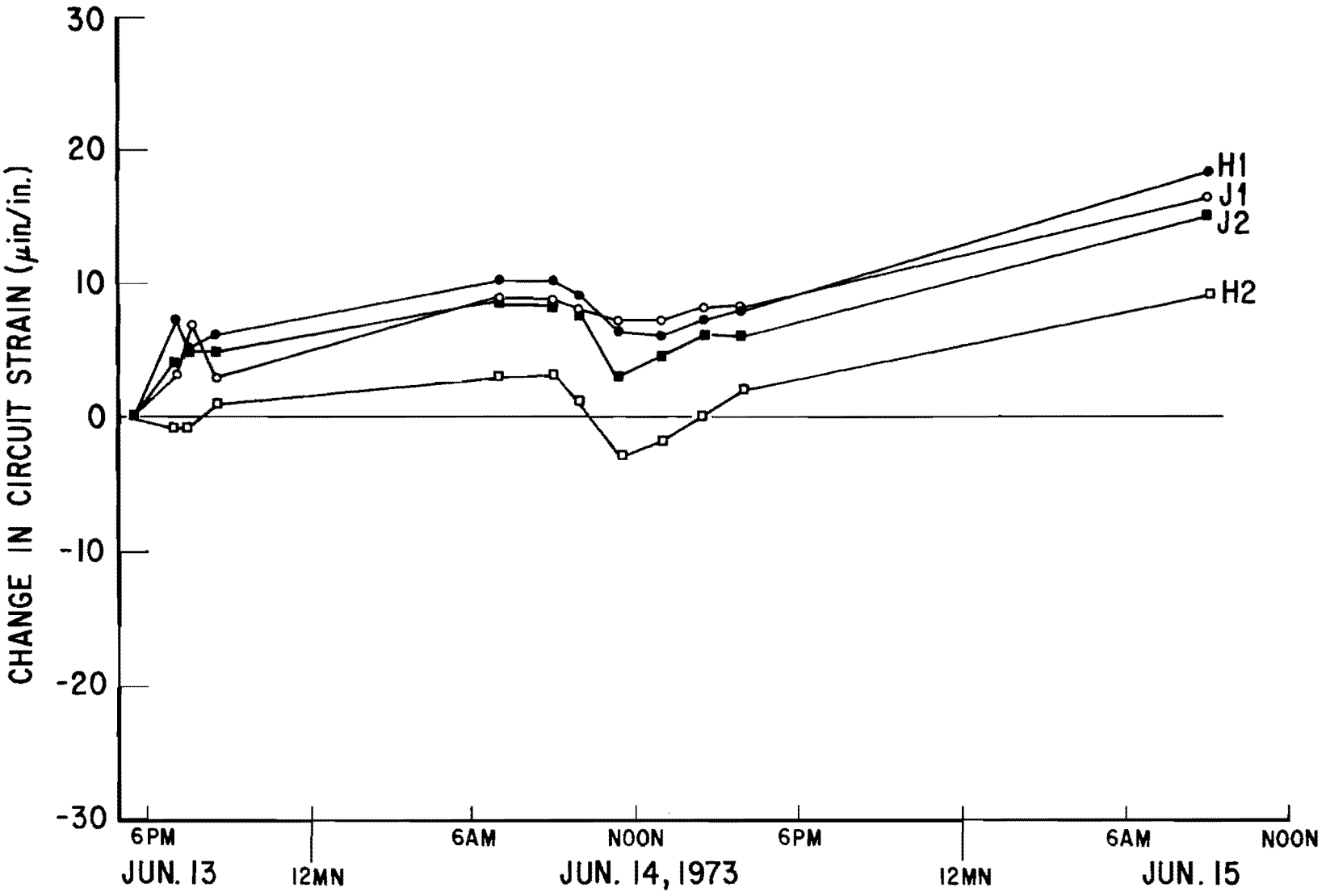


Fig. E5 Variation of Circuit Strain for Gages at Levels H (41') and J (47') Over a 40 Hour Period

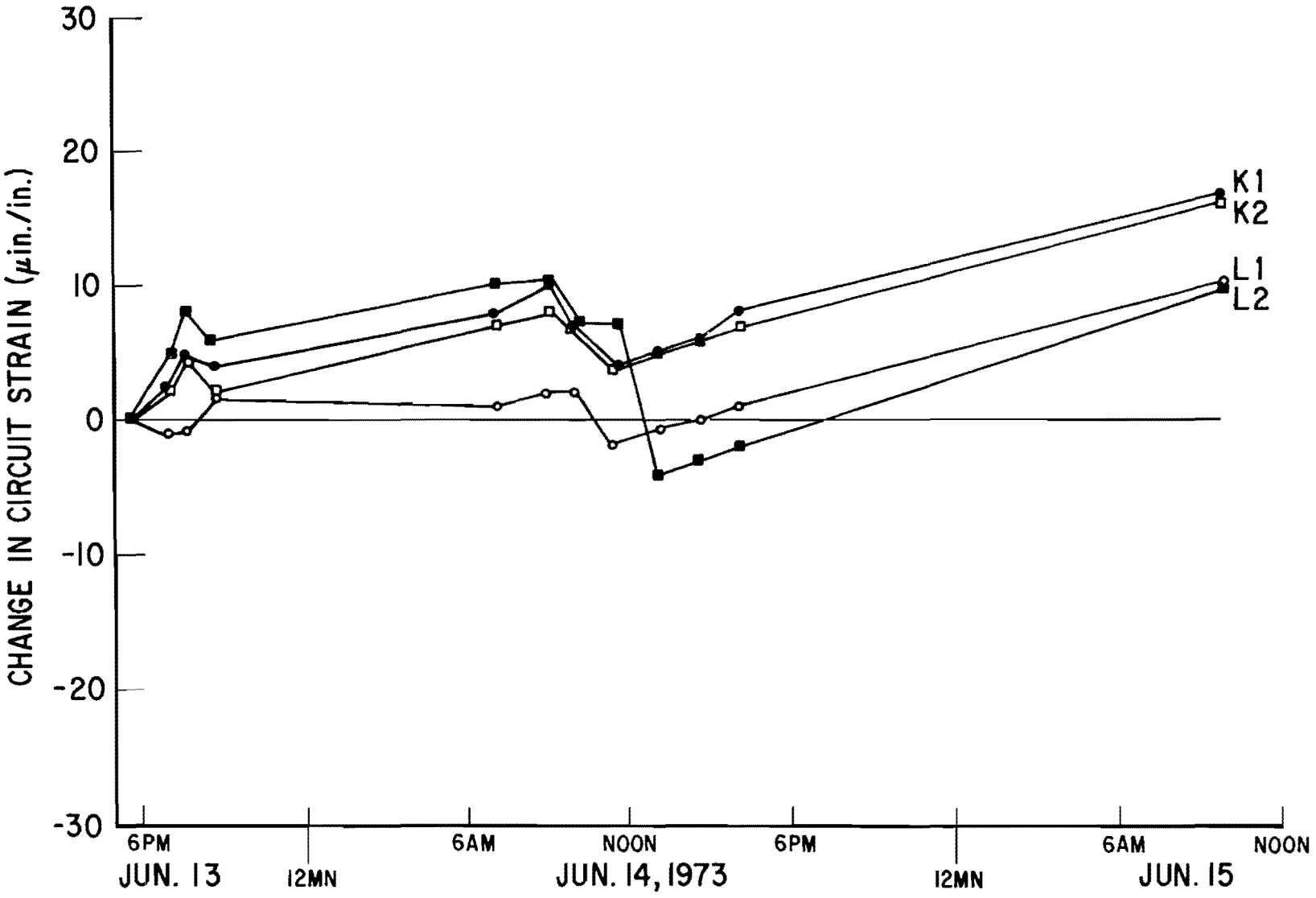


Fig. E6 Variation of Circuit Strain for Gages at Levels K (53') and L (57') Over a 40 Hour Period

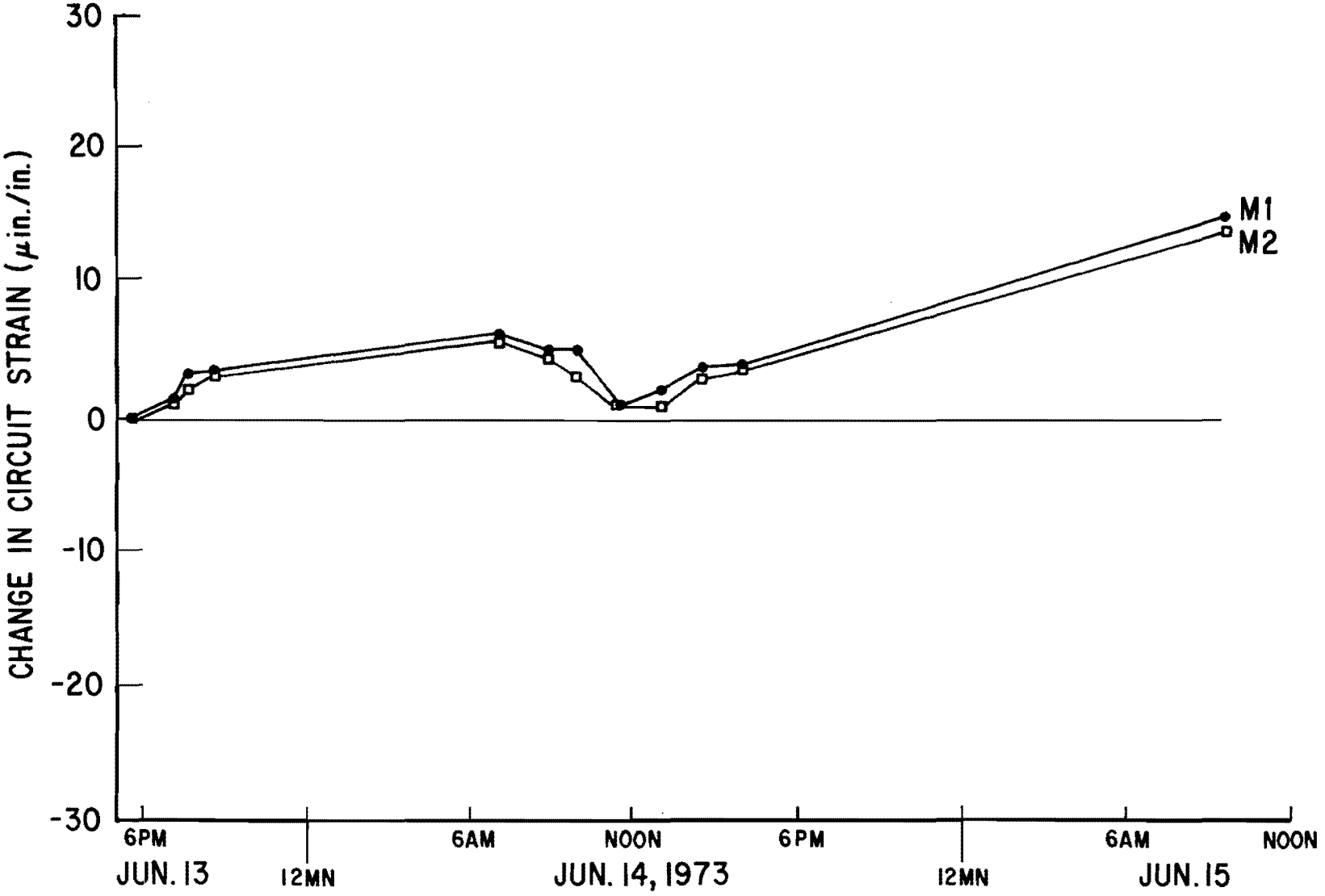


Fig. E7 Variation of Circuit Strain of Gages at Level M (61') Over a 40 Hour Period

# APPENDIX F

# LOAD DISTRIBUTION CURVES

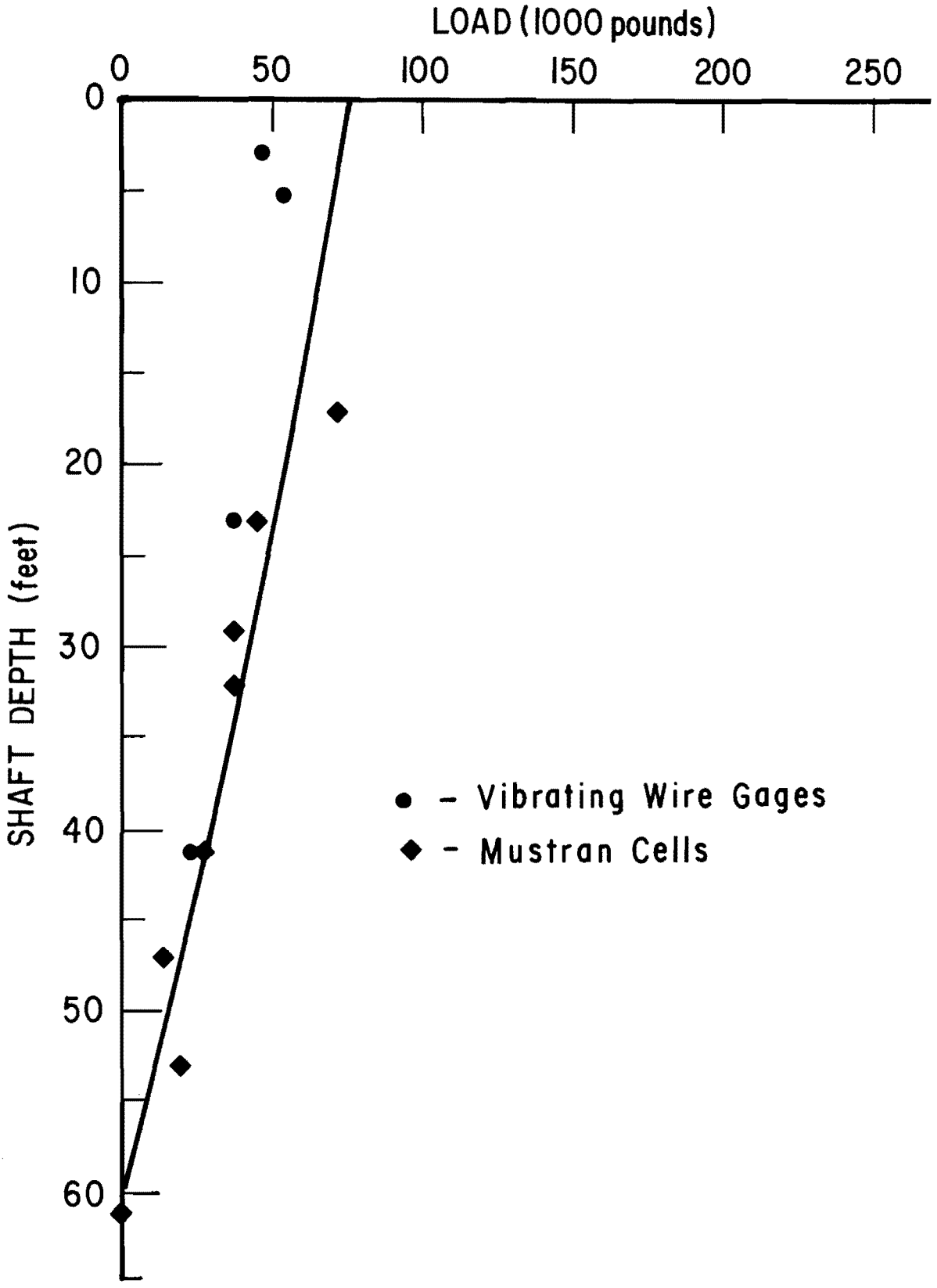


Fig. F1 Load Distribution Curve for March 15, 1973 (Load = 38 tons)

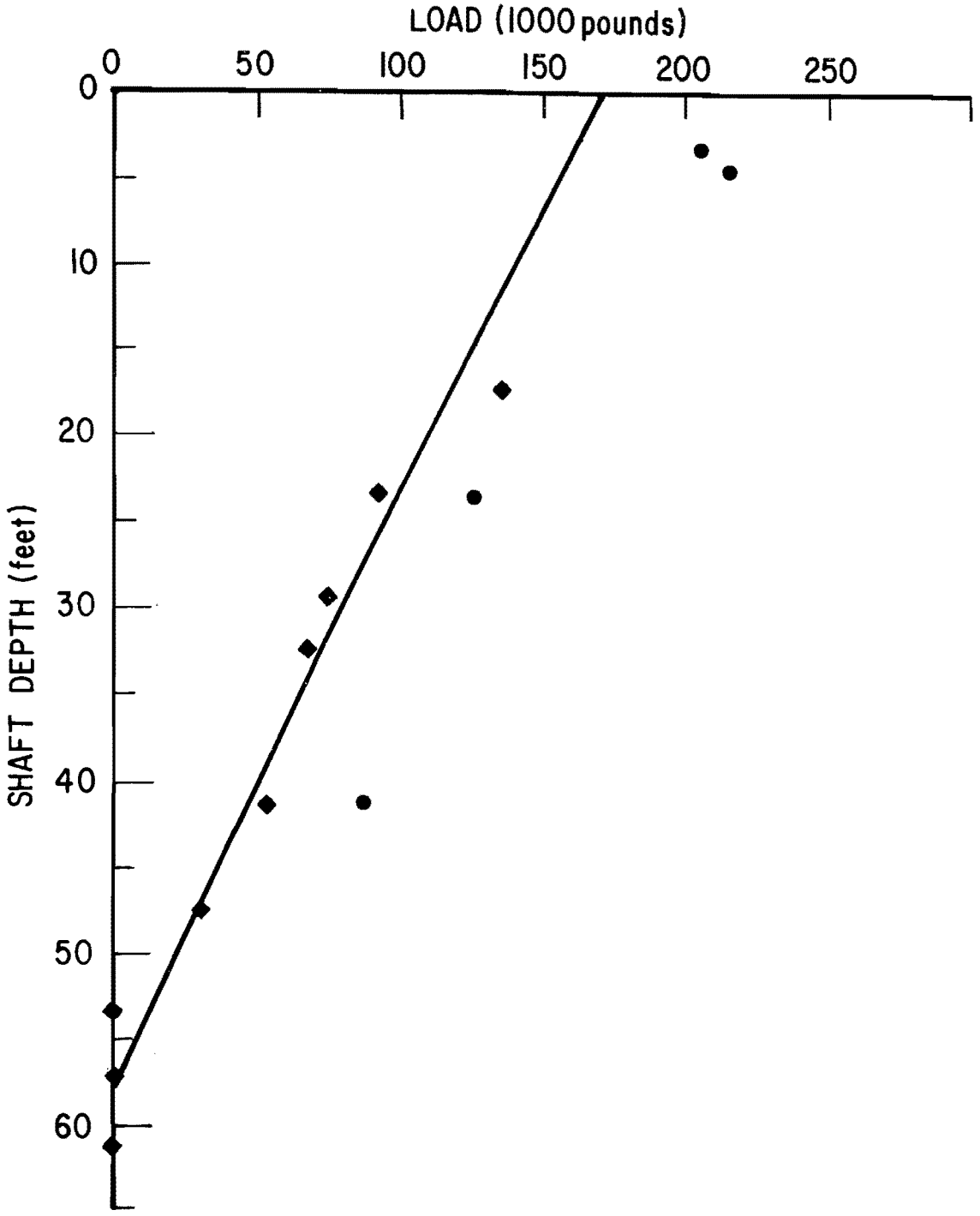


Fig. F2

Load Distribution Curve for April 28, 1973 (Load = 85 tons)

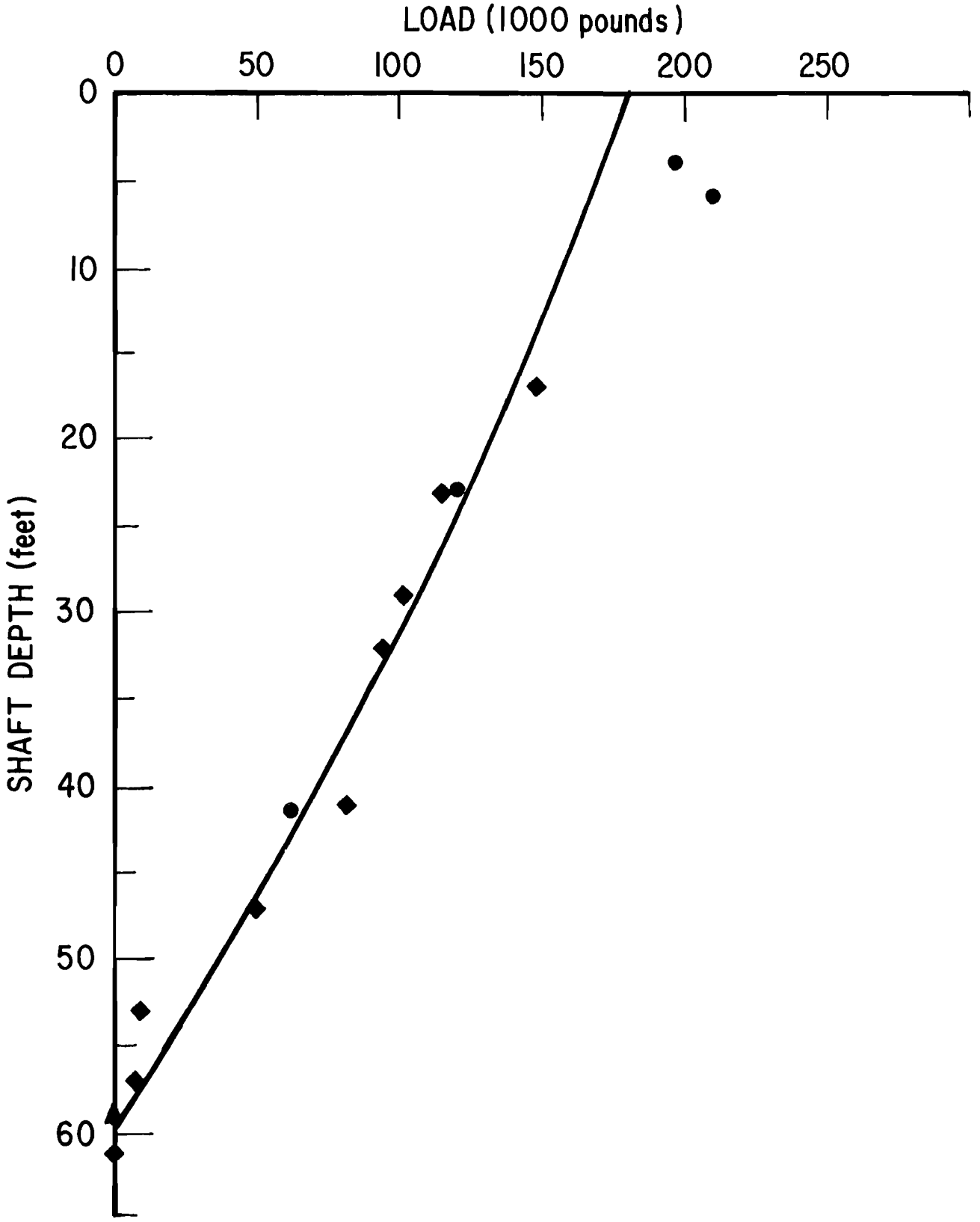


Fig. F3

Load Distribution Curve for May 29, 1973 (Load = 85 tons)

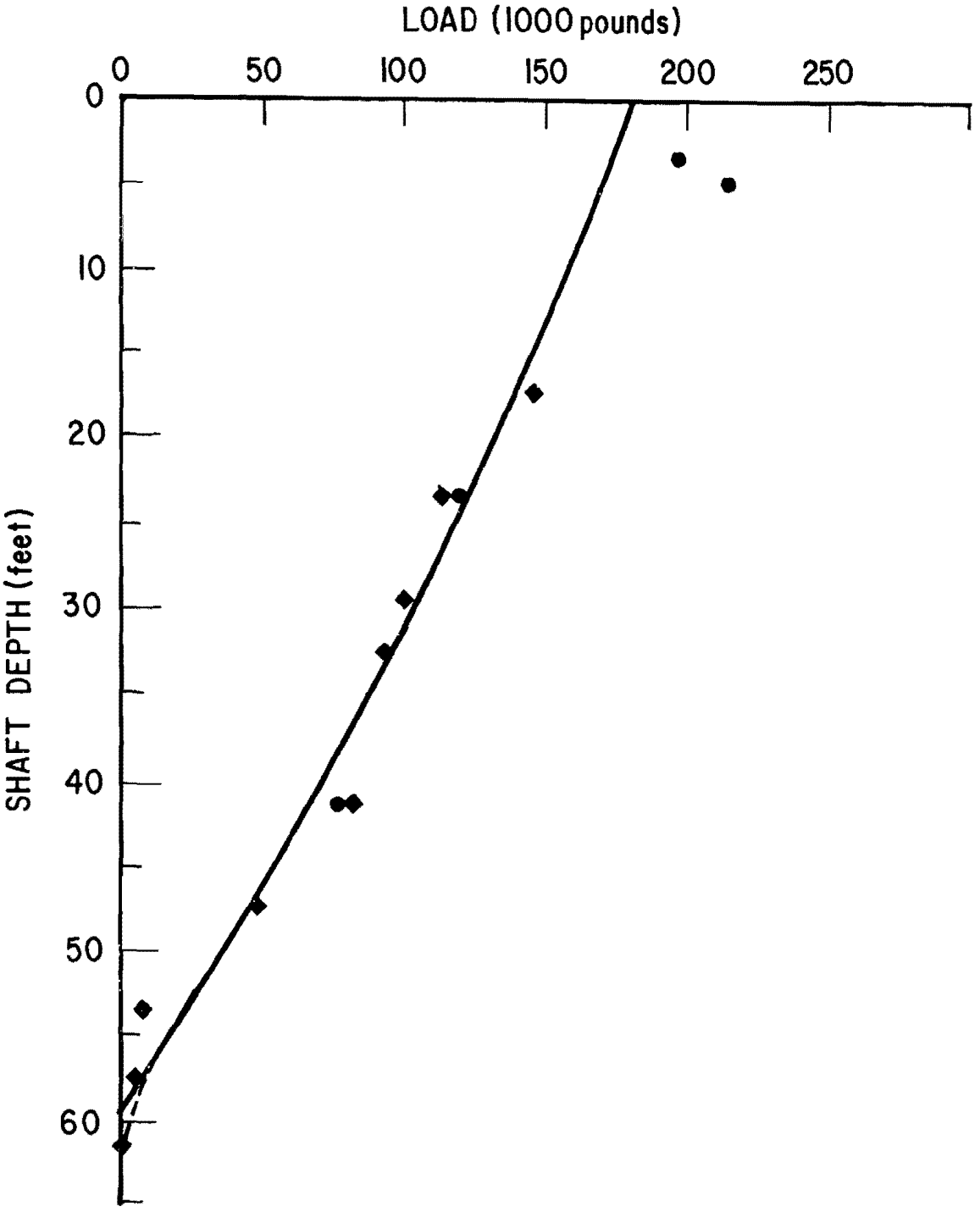


Fig. F4

Load Distribution Curve for May 30, 1973 (Load = 85 tons)

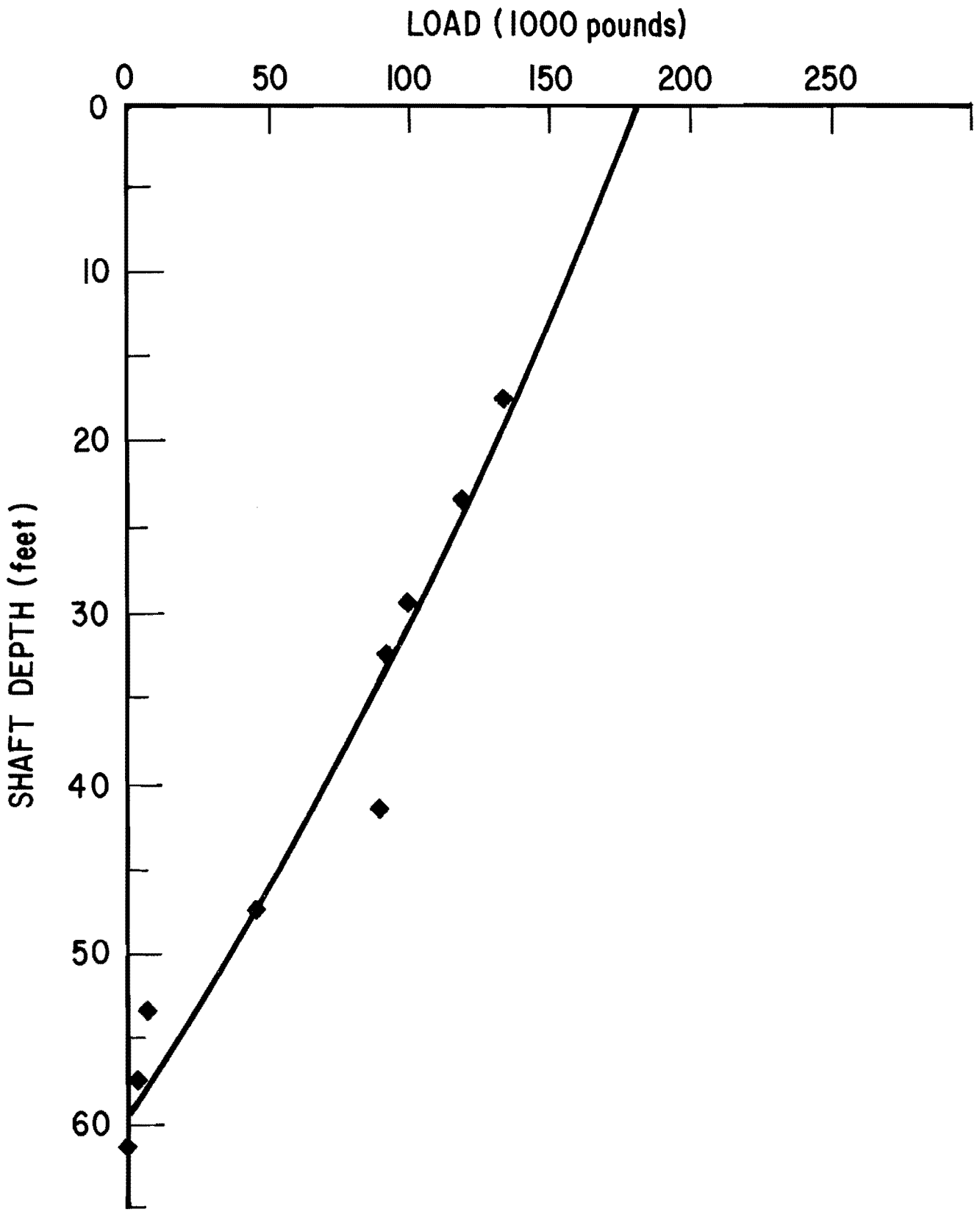


Fig. F5

Load Distribution Curve for June 13, 1973 (Load = 85 tons)

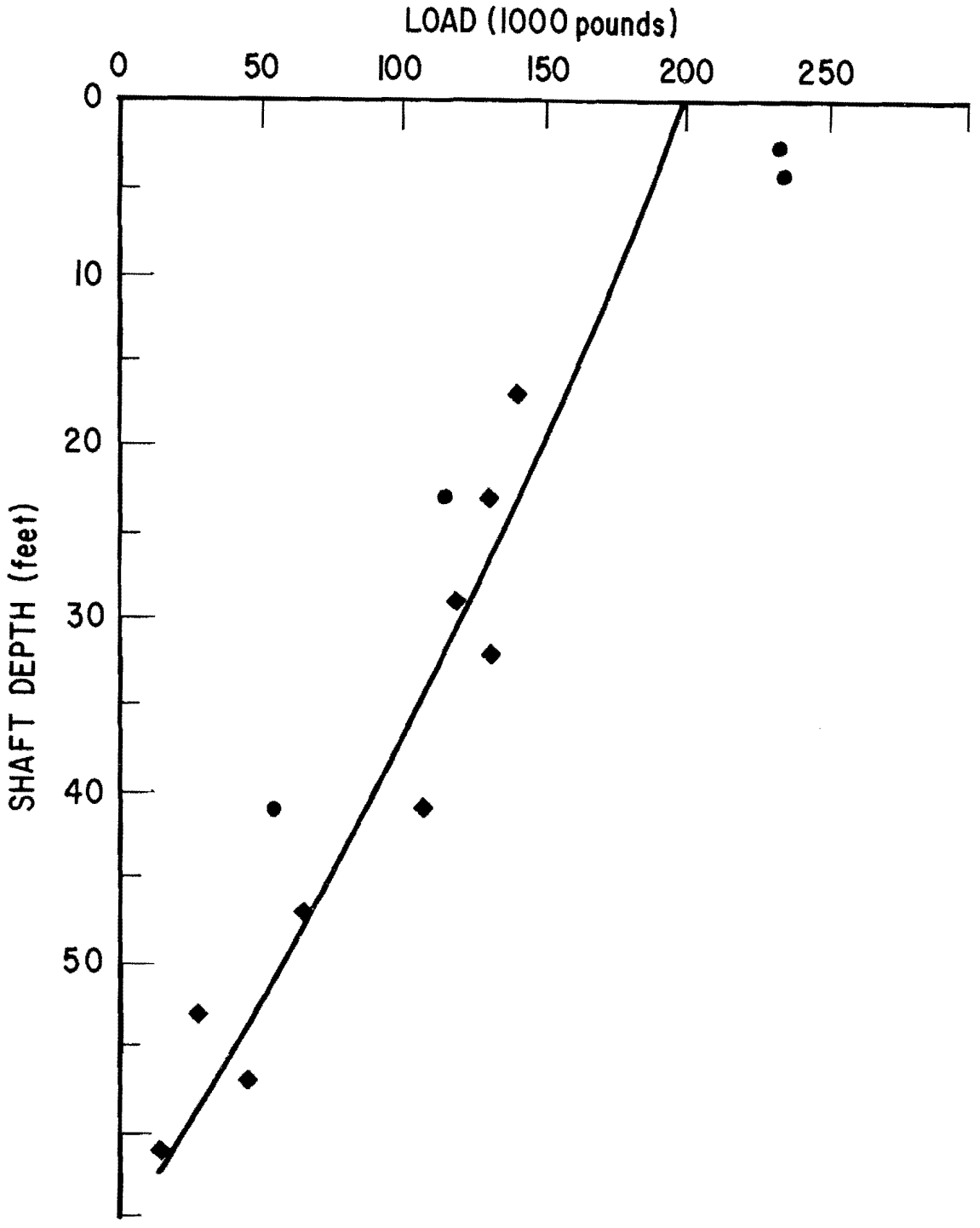


Fig. F6

Load Distribution Curve for July 26, 1973 (Load = 100 tons)

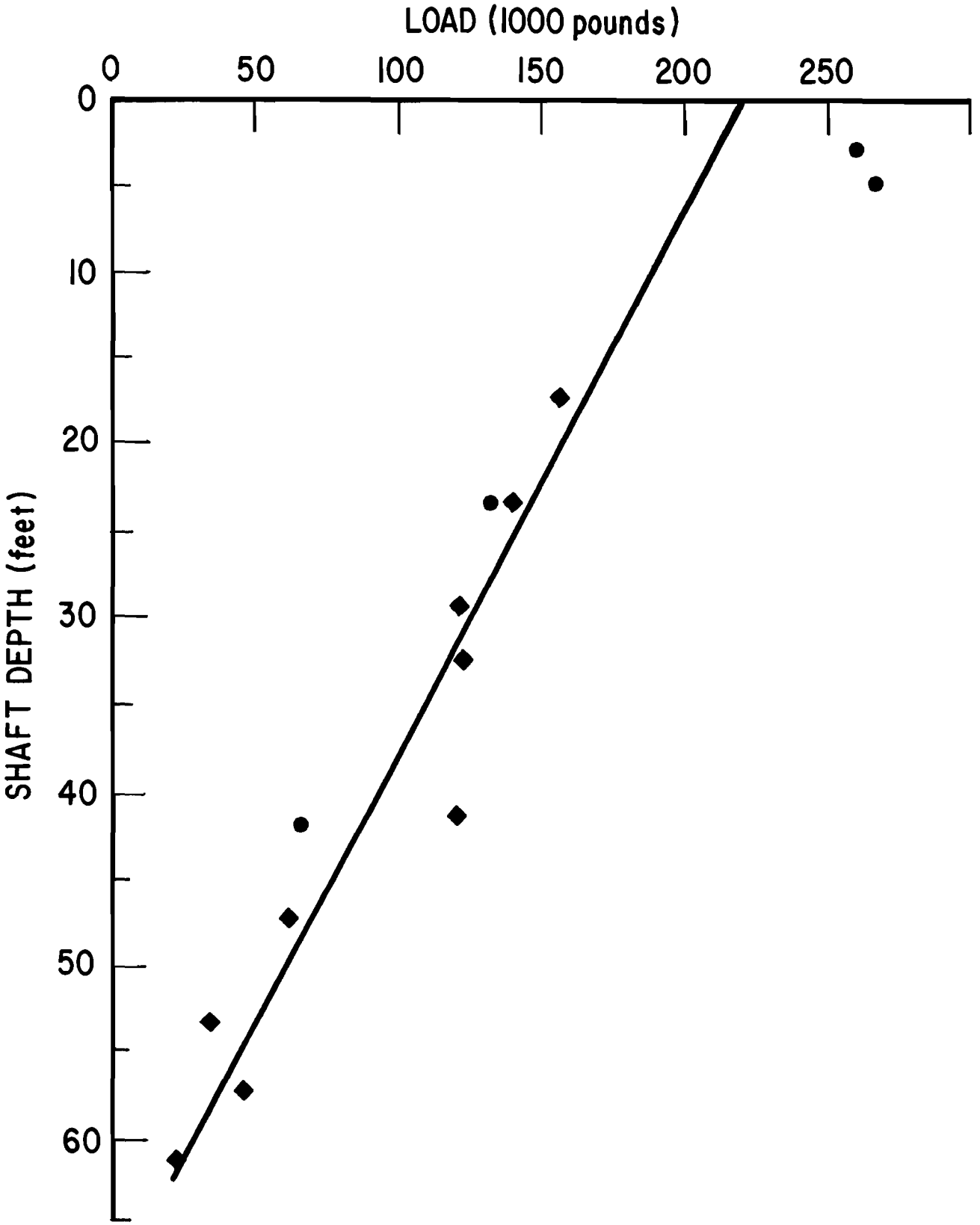


Fig. F7

Load Distribution Curve for August 22, 1973 (Load = 110 tons)

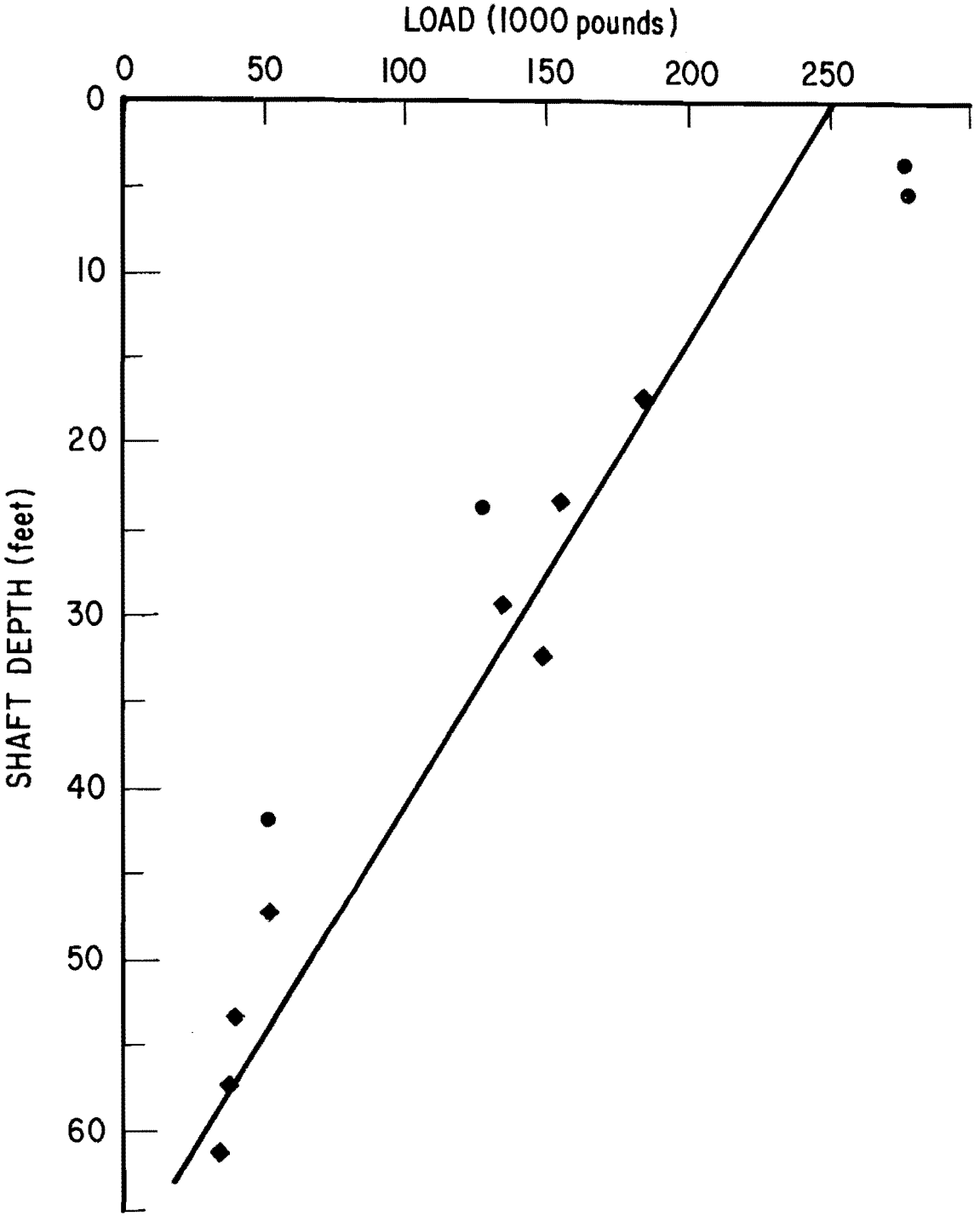


Fig. F8

Load Distribution Curve for September 25, 1973 (Load = 125 tons)

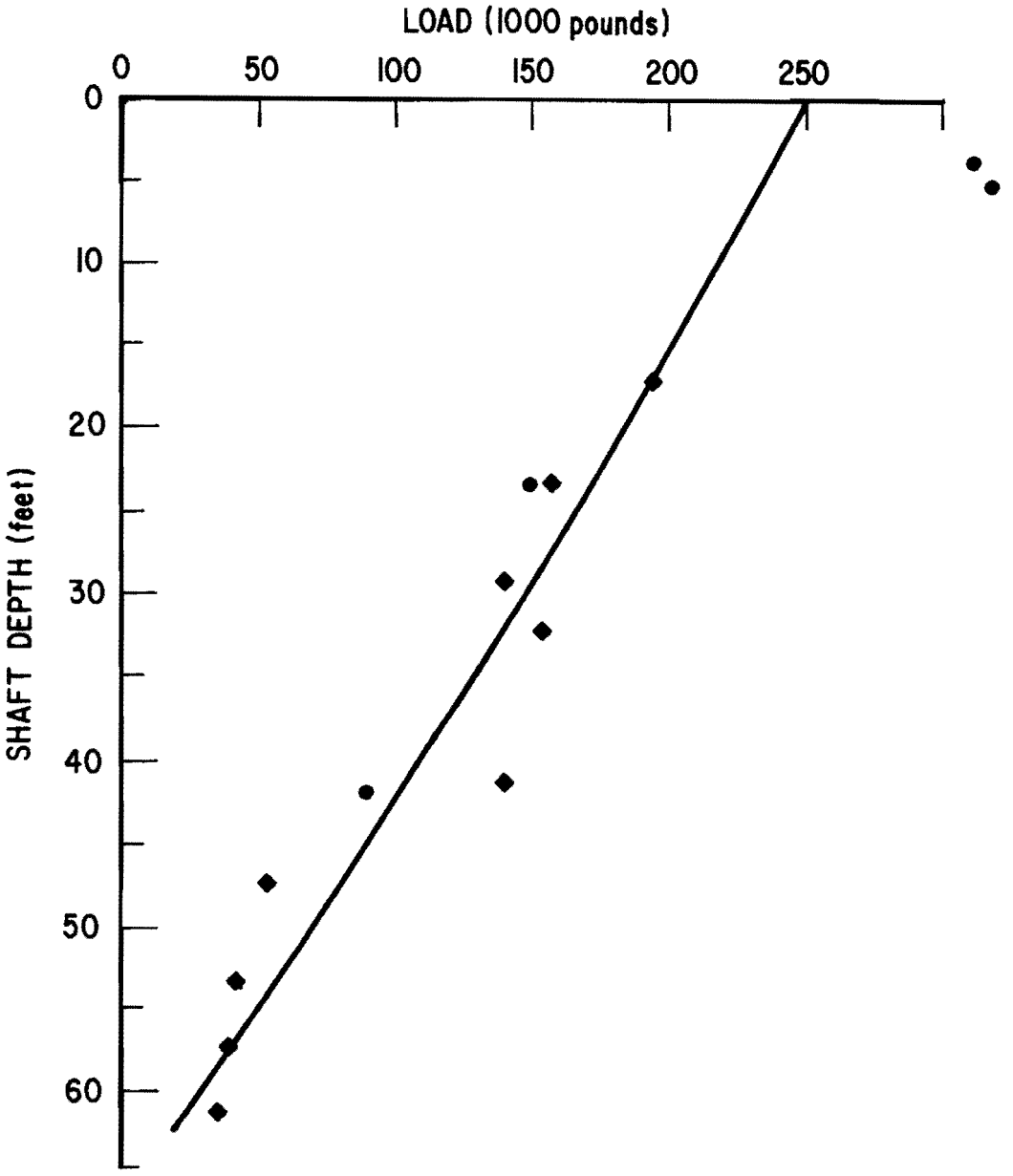


Fig. F9

Load Distribution Curve for September 29, 1973 (Load = 125 tons)

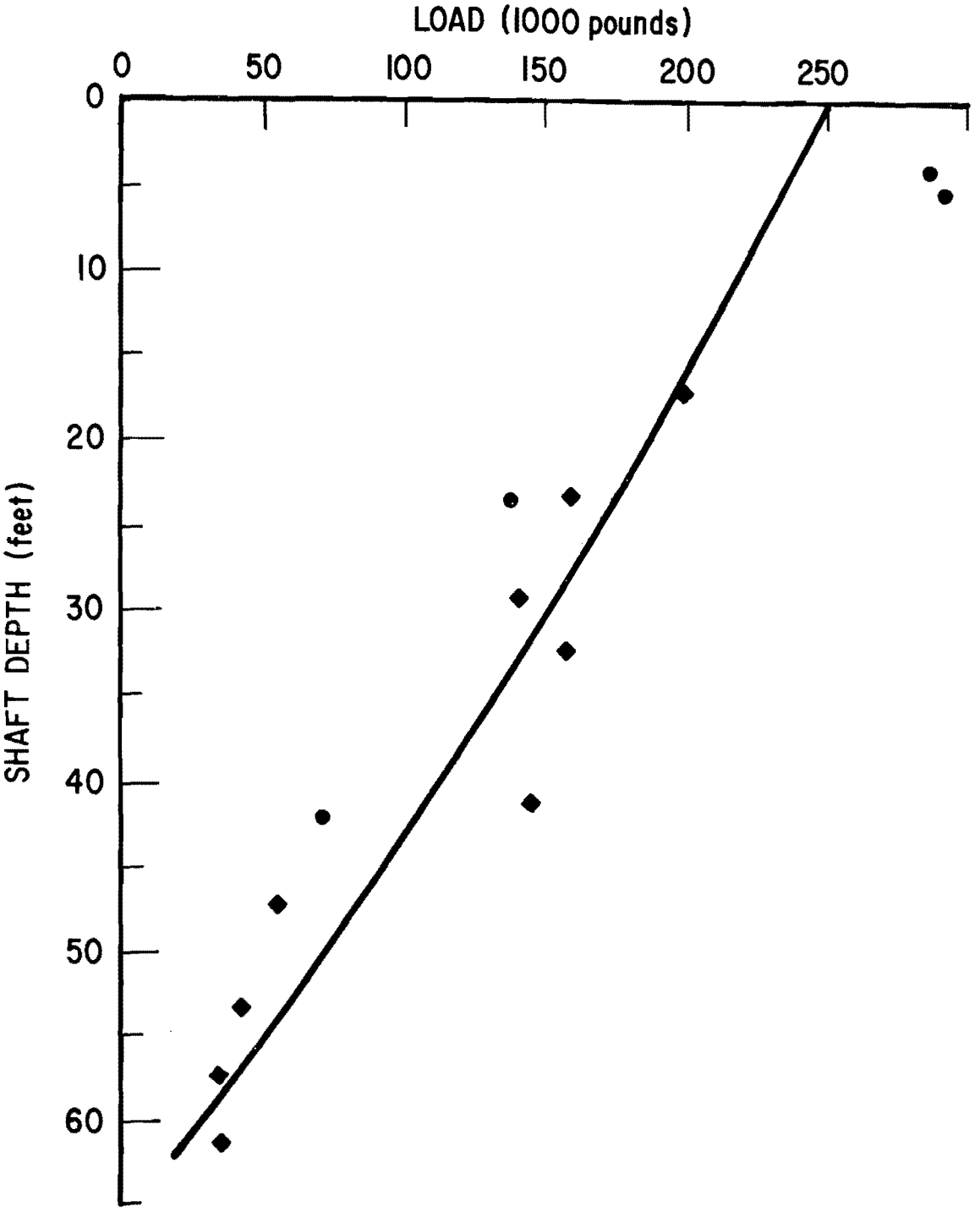


Fig. F10

Load Distribution Curve for October 3, 1973 (Load = 125 tons)

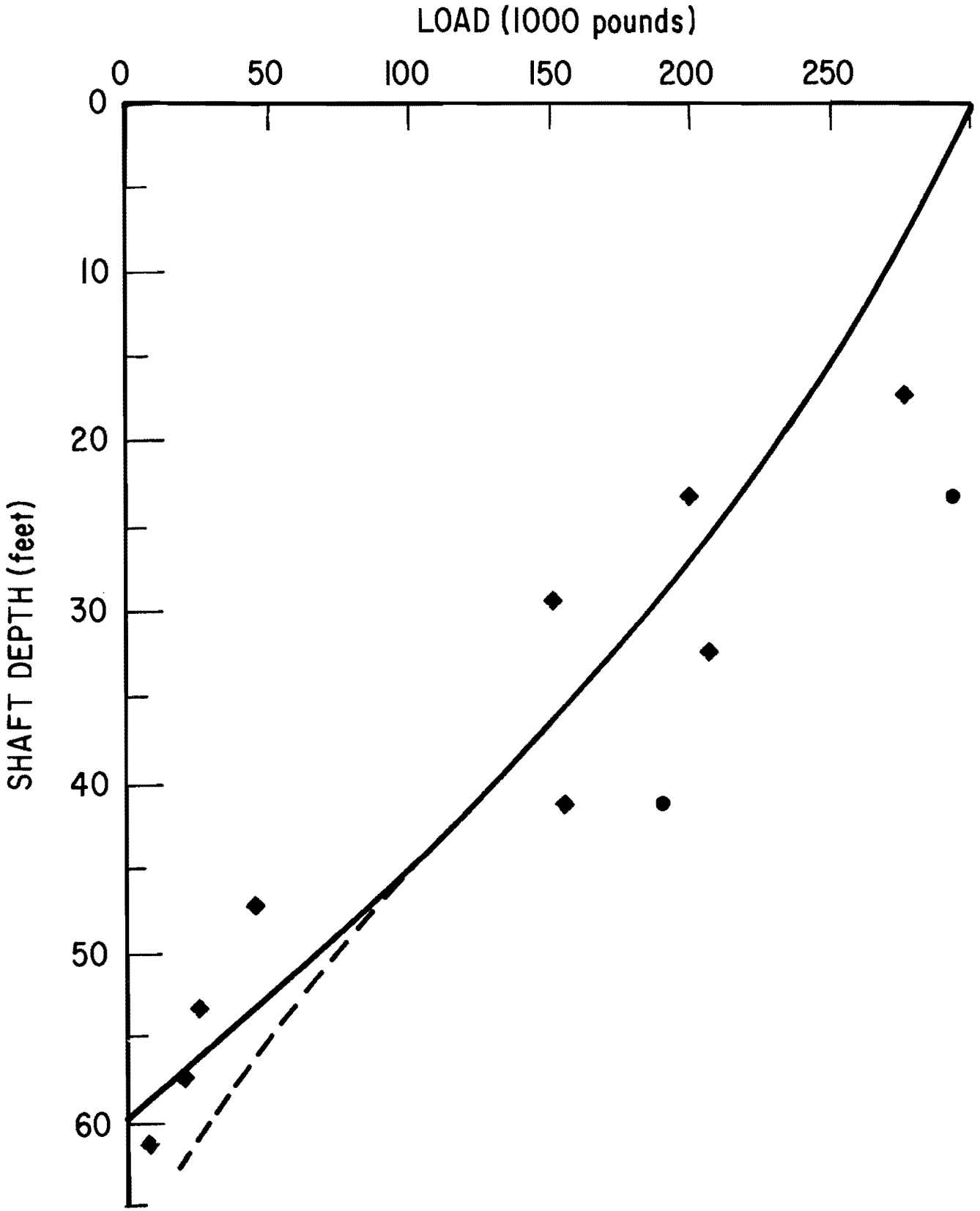


Fig. F11

Load Distribution Curve for November 7, 1973 (Load = 150 tons)

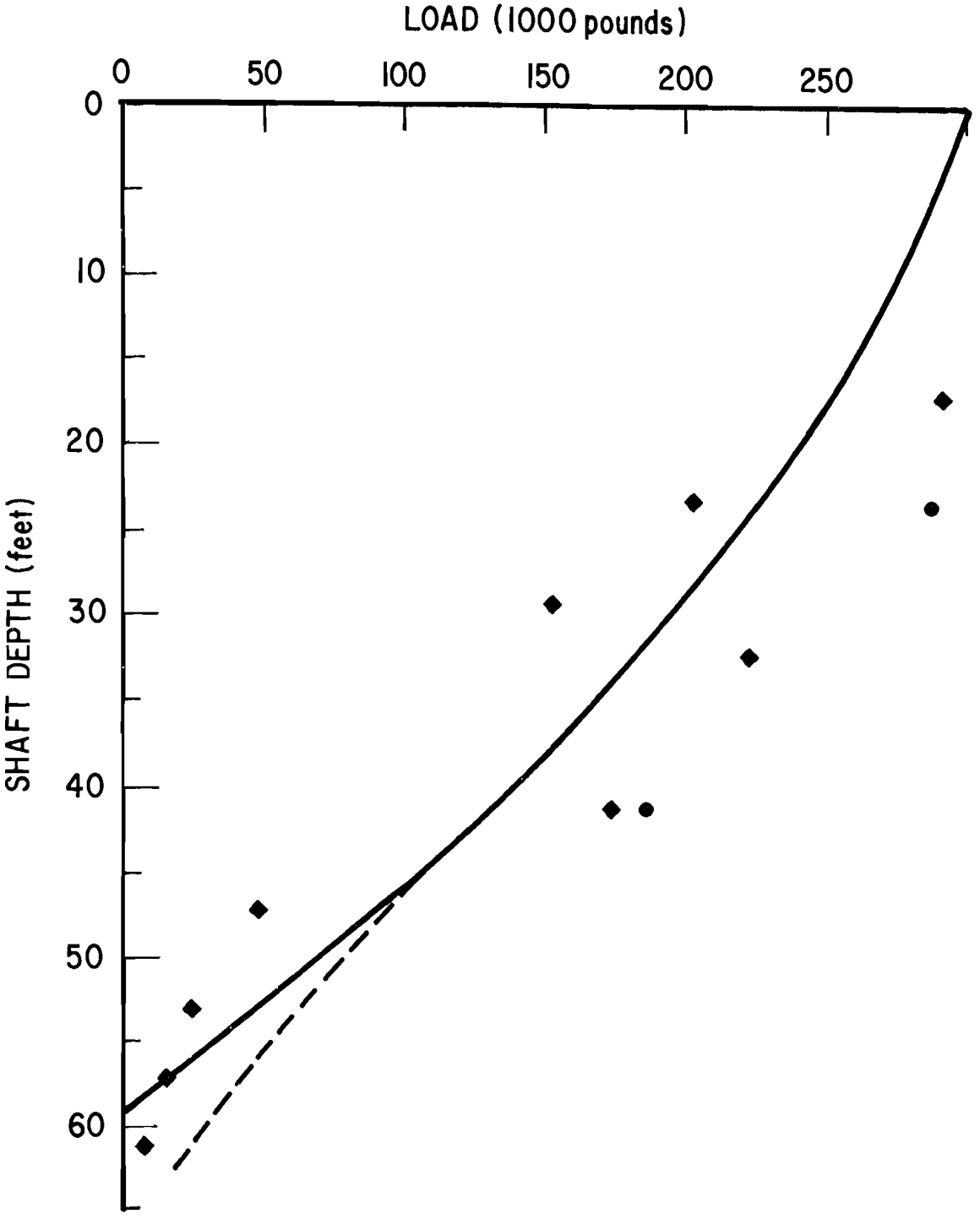


Fig. F12

Load Distribution Curve for December 11, 1973 (Load = 150 tons)

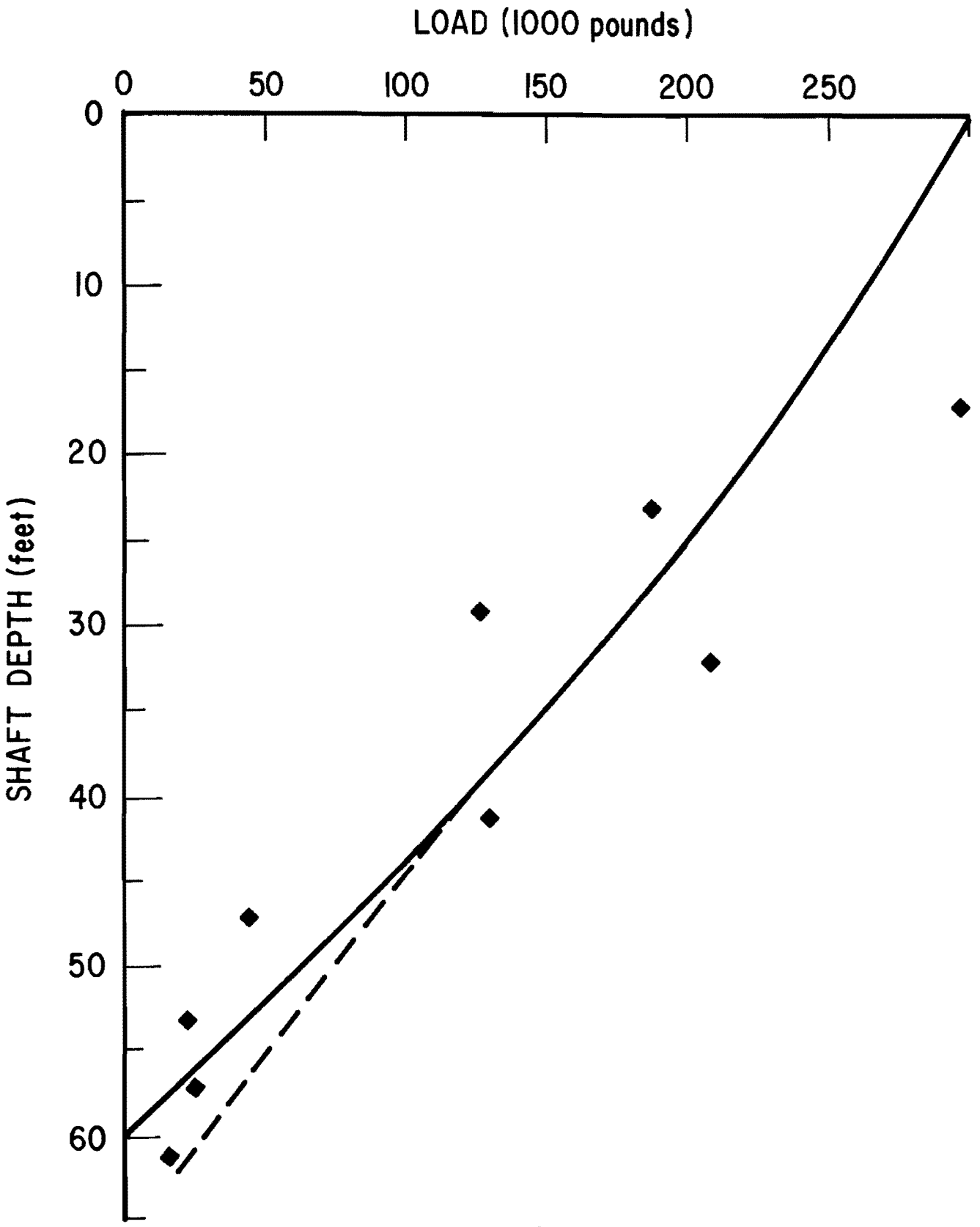


Fig. F13

Load Distribution Curve for February 7, 1974 (Load = 150 tons)

# REFERENCES


Barker, W. R. and L. C. Reese (1969), Instrumentation for Measurement of Axial Load in Drilled Shafts, Research Report 89-6, Center for Highway Research, University of Texas, Austin, November, 1969.

Barker, W. R. and L. C. Reese (1970), Load-Carrying Characteristics for Drilled Shafts Constructed with the Aid of Drilling Fluids, Research Report 89-9, Center for Highway Research, University of Texas, Austin, August, 1970.

Berre, T. and L. Bjerrum (1973), "Shear Strength of Normally Consolidated Clays," Proceedings of the Eighth International Conference on Soil Mechanics and Foundation Engineering, Session 4, Moscow, 1973.

Bishop, A. W. and H. T. Lovenbury (1969), "Creep Characteristics of Two Undisturbed Clays," Proceedings of the Seventh International Conference on Soil Mechanics and Foundation Engineering, Vol. 1, pp. 29-37, Mexico City, 1969.

Bjerrum, L. (1973), "Problems of Soil Mechanics and Construction on Soft Clays and Structurally Unstable Soils," Proceedings of the Eighth International Conference on Soil Mechanics and Foundation Engineering, Session 4, Moscow, 1973.

Casagrande, S. and S. D. Wilson (1951), "Effect of Rate of Loading on the Strength of Clays and Shales at Constant Water Content," Geotechnique, Vol. 2, No. 3, pp. 251-263, 1951.

Chuang, J. W., T. W. Kennedy, and E. S. Perry (1970), An Approach to Estimating Long-Term Multiaxial Creep Behavior from Short-Term Uniaxial Creep Results, Research Report 2864-3, Department of Civil Engineering, University of Texas, Austin, June, 1970.

Eide, O., J. N. Hutchinson, and A. Landva (1961), "Short and Long-Term Test Loading of a Friction Pile in Clay," Proceedings of the Fifth International Conference on Soil Mechanics and Foundation Engineering, Vol. 2, pp. 45-53, Paris, 1961.

Eide, O., G. Aas, and T. Josang (1972), "Special Application of Cast-in-Place Walls for Tunnels in Soft Clay in Oslo," Proceedings of the Fifth European Conference on Soil Mechanics and Foundation Engineering, Vol. 1, pp. 485-498, Madrid, 1972.

Goldstein, M. and G. Ter-Stepanian (1957), "The Long-Term Strength of Clays and Depth Creep of Slopes," Proceedings of the Fourth International Conference on Soil Mechanics and Foundation Engineering, Vol. 2, pp. 311-314, London, 1957.

Hvorslev, M. J. (1937), Uber die Festigkeitseigenschaften Gestorter Bindiger Boden, 159 pp., Copenhagen, 1937.

Kennedy, T. W. and E. S. Perry (1970), An Experimental Approach to the Study of the Creep Behavior of Plain Concrete Subjected to Triaxial Stresses and Elevated Temperatures, Research Report 2864-1, Department of Civil Engineering, University of Texas, Austin, June, 1970.

Kennedy, T. W. (1972), Long Term Creep Behavior of Concrete and the Effects of Curing, Research Report 3661-2, Department of Civil Engineering, University of Texas, Austin, June, 1972.

Marsal, R. J. and M. Mazari (1969), The Subsoil of Mexico City, 2 Volumes, Mexico City, 1969.

O'Neill, M. W. and L. C. Reese (1970), Behavior of Axially Loaded Drilled Shafts in Beaumont Clay, Research Report 89-8, Center for Highway Research, University of Texas, Austin, December, 1970.

Peck, Ralph B. (1965), "Pile and Pier Foundations," Journal of the Soil Mechanics and Foundations Division, ASCE, Vol. 91, No. SM2, March, 1965.

Schmertmann, J. M. and J. O. Osterberg (1961), "An Experimental Study of the Development of Cohesion and Friction with Axial Strain in Saturated Cohesive Soils," ASCE, Research Conference on Shear Strength of Cohesive Soils, pp. 643-694, Boulder, Colorado, 1960.

Terzaghi, K. (1925), Erdbaumechanik Auf Bodenphsikalische Grundlage, 399 pp., Leipzig, 1925.

Torstensson, B. A. (1973), Kohesionspalars Funktionssatt. Ett Faltsudium i Modellskala, Thesis, Chalmers University of Technology, Gothenberg, 1973.

Touma, F. T. and L. C. Reese (1972), Behavior of Axially Loaded Drilled Shafts in Sand, Research Report 176-1, Center for Highway Research, University of Texas, Austin, December, 1972.

Troxell, G. E., J. M. Raphael, and R. E. Davis (1958), "Long-Time Creep and Shrinkage Tests of Plain and Reinforced Concrete," Proceedings, American Society for Testing Materials, Vol. 58, pp. 1101-1120, 1958.

Vyalov, S. S. and S. R. Meschyan (1969), "Creep and Long-Term Strength of Soils Subjected to Variable Load," Proceedings of the Seventh International Conference on Soil Mechanics and Foundation Engineering, Vol. 1, pp. 411-417, Mexico City, 1969.

York, G. P., T. W. Kennedy, and E. S. Perry (1970), Experimental Investigation of Creep in Concrete Subjected to Multiaxial Compressive Stresses and Elevated Temperatures, Research Report 2864-2, Department of Civil Engineering, University of Texas, Austin, June, 1970.